Chapter 28: Electronic Spectroscopy

Calculate the bond dissociation energy of ground-state O_2.

Absorption of light can promote a molecule into an excited electronic state. Excited electronic states result from changes of the molecular orbital electron configuration. Electronic transitions are typically in the visible and ultraviolet. A molecule can also be ionized, if the light is sufficiently energetic. After photoionization, the resulting molecular ion can be in the ground or an excited electronic state. The characterization of excited states is central to the study of chemical reactivity. Electronic spectroscopy determines the energy of excited states. In high resolution spectra of gases, vibrational and rotational fine-structure are often observed that are used to determine excited state spectroscopic constants. Bond dissociation energies are commonly determined from absorption spectra. The energy of the excited state, the bond dissociation energies, and the spectroscopic constants characterize the potential energy surface of the excited state. Transition states for many reactions result from intersections of excited state potential energy surfaces. Photoionization is also used to estimate molecular orbital energies.

After absorption of light, what is the fate of the electronic excited state? The excited state energy can be lost by the emission of light as fluorescence or phosphorescence, by photochemistry, and by non-radiative transitions. Fluorescence and phosphorescence are important analytical tools and also provide information about the ground state of molecules. Photochemistry results from the channeling of the energy of the excited state into breaking and making chemical bonds. Non-radiative transitions result in heat transfer to the surroundings. Many fundamental processes in the environment are driven by photochemistry, for example ozone formation in the stratosphere, Eq. 5.2.1, and photosynthesis.

28.1 Electronic Absorption and Emission Spectroscopy

In solution, the UV-visible spectrum of SO_2 appears as two broad featureless, more or less Gaussian shaped transitions. The two transitions correspond to electronic transitions from the ground electronic state to different excited electronic states. In the gas phase, Figure 28.1.1, vibrational fine-structure is resolved in both electronic transitions.

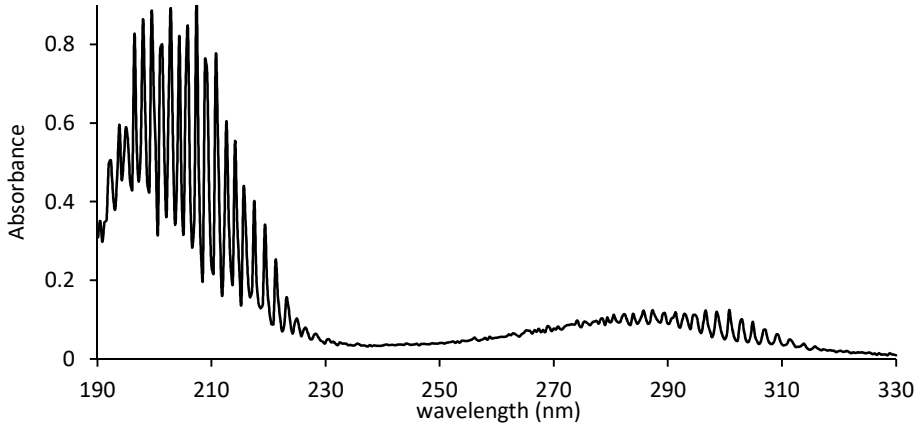

Figure 28.1.1: Electronic absorption spectrum of SO_2 gas. Vibrational fine-structure appears in both electronic transitions. An additional very weak transition occurs at 390 to 340 nm.

The vibrational fine-structure is evident as bands of closely spaced narrow lines. The vibrational fine-structure appears since the molecule can change vibrational levels along with the change in electronic state. The vibrational fine-structure is usually not observed in solution, since rapid collisions with solvent molecules shorten the lifetime of the excited state, severely broadening each vibrational transition. Referring to the molecular orbital diagrams in Figures 26.6.7-26.6.9, the redder 340 to 260 nm band of SO_2 is assigned to the electronic transition:[1]

$$(1a_2^\circ)^1(4b_2^\circ)^2(6a_1^\circ)^2(2b_1^*)^1 \leftarrow (1a_2^\circ)^2(4b_2^\circ)^2(6a_1^\circ)^2 \qquad 28.1.1$$

final upper-electronic state ← *initial lower-electronic state*

Because the electron is promoted from the $1a_2^\circ$ non-bonding orbital to the $2b_1^*$ π-anti-bonding orbital, this transition is denoted as a $\pi^* \leftarrow$n transition. Two or three electronic transitions overlap in the bluer 240 to 180 nm band. The most intense contribution is assigned to:[1]

$$(5a_1)^1(3b_2)^2(1a_2^\circ)^2(4b_2^\circ)^2(6a_1^\circ)^2(2b_1^*)^1 \leftarrow (5a_1)^2(3b_2)^2(1a_2^\circ)^2(4b_2^\circ)^2(6a_1^\circ)^2 \qquad 28.1.2$$

Because the electron is promoted from the $5a_1$ σ-bonding orbital to the $2b_1^*$ π-anti-bonding orbital, this transition is denoted as a $\pi^* \leftarrow \sigma$ transition. A wide variety of electronic transitions occur in UV-visible spectra. The transition wavelengths tell us the energies of the excited electronic states: $\Delta E = E_{excited\ state} - E_{gs} = hc/\lambda = hc\tilde{\nu}$. To simplify matters, we first turn our attention to diatomic molecules.

High Resolution Spectra Show Vibrational and Rotational Fine-structure: The vibrational fine-structure in Figure 28.1.1 shows that vibrational transitions "go along for the ride" with electronic transitions. In diatomic molecules and some polyatomics, rotational fine-structure can also be observed using high-resolution spectrographs, Figure 28.1.2. Different transitions occur as the molecule changes rotational and vibrational levels during the electronic transition.

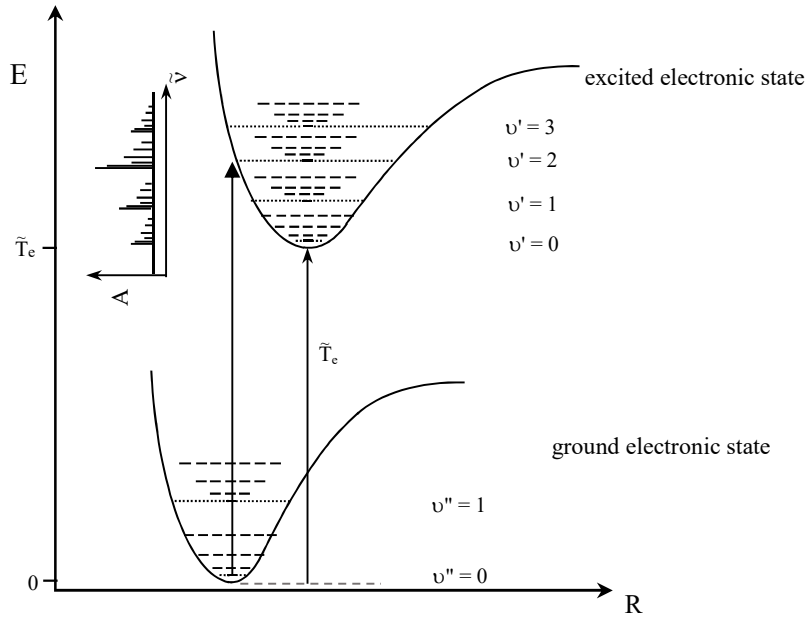

Figure 28.1.2: Molecules can change rotational and vibrational levels during electronic transitions. For most molecules the rotational selection rule is $\Delta J = \pm 1$, the molecule must "rotate faster or slower" after the electronic transition. The inset shows a schematic spectrum.

Historically, high resolution spectra were recorded using photographic film. In the photographic image, each transition corresponds to a vertical bar. Modern high resolution spectrometers use Fourier-transform interferometers or spectrographs with diode-array or charge coupled device detectors (CCD) to record the intensity as a function of wavelength. However, the old, film-type spectra are useful to visually appreciate the relationships of the vibrational and rotational components of the electronic transition bands. Many molecules have been studied by emission spectroscopy using high-voltage electric discharges in low pressure gases. The emission spectrum of N_2 shows vibrational fine-structure at moderate resolution, giving a "band-like" appearance, Figure 28.1.3a-28.1.3b. At high resolution, each vibrational band is shown to consist of many very closely spaced rotational fine-structure transitions Figure 28.1.3cd.

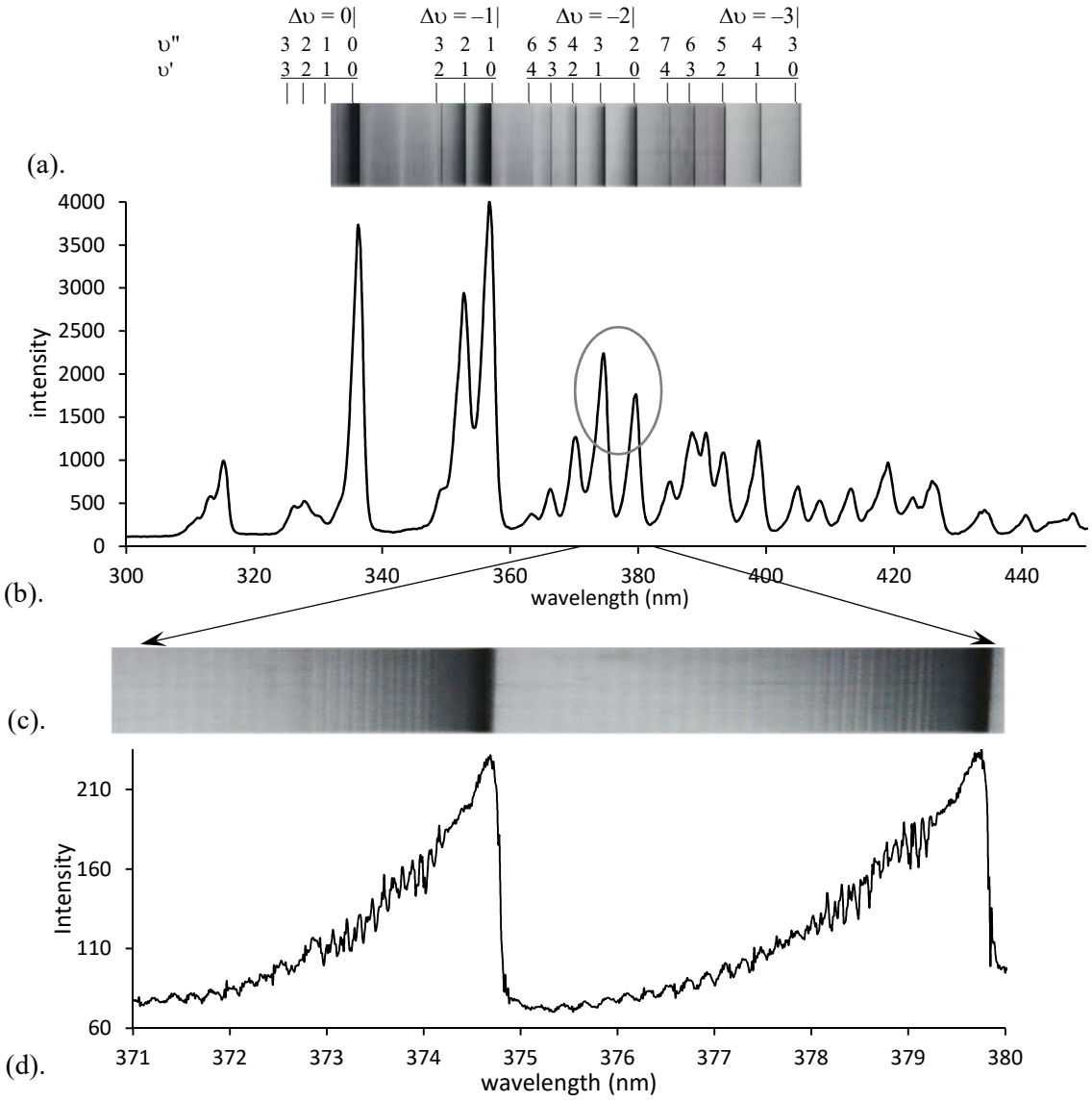

Figure 28.1.3: Emission spectrum of N_2 for the $^3\Pi_u \rightarrow {}^3\Pi_g$ electronic transition. (a). Spectrograph image. (b). Diode array spectrograph spectrum. (c-d). High resolution plots of two $\Delta\upsilon = -2$ bands showing rotational fine-structure.

For a diatomic, the total energy of electronic state i is the sum of the electronic energy with respect to the ground state $\tilde{T}_{e,i}$, the vibrational energy for vibrational quantum number υ, and the rotational energy for rotational quantum number J, using Eqs. 27.4.8 and 27.5.8:

$$\tilde{E}_{i,\upsilon,J} = \tilde{T}_{e,i} + \tilde{G}(\upsilon) + \tilde{F}(J) = \tilde{T}_{e,i} + \tilde{\nu}_{e,i}\,(\upsilon + ½) - \chi_{e,i}\,\tilde{\nu}_{e,i}\,(\upsilon + ½)^2 + \tilde{B}_{\upsilon,i}\,J(J+1) - \tilde{D}_{e,i}\,[J(J+1)]^2 \qquad 28.1.3$$

The vibrational and rotational transitions allow the fundamental vibration frequency, anharmonicity, and the rotational $\tilde{B}$-values to be determined in each corresponding state. In absorption, these spectroscopic constants are for the excited state of the molecule, and not the ground state. In emission, if the transition results in the ground state of the molecule, then spectroscopic constants can be determined for the ground state. The availability of ground-state spectroscopic constants from electronic emission spectroscopy is important if infrared or microwave absorption spectra of the molecule are not dipole allowed. For the particular example of the N_2 emission spectrum, the transitions are between two excited electronic states; the resulting spectroscopic constants are for the excited states involved in the transition.

The intensity of electronic transitions varies greatly, Figure 28.1.1. The intensity of each electronic transition is determined by the transition dipole moment of the two coupled states.

Transition Probabilities are Determined by the Transition Dipole Moment: For a diatomic molecule, the transition dipole moment between electronic states i and j, in the Born-Oppenheimer approximation, is:

$$\vec{\mu}_{tr} = <\vec{\mu}> = \int [\Psi_{el,j}\,\chi_{\upsilon'}(R)Y_{J',m_{J'}}(\theta,\phi)]^*\,\hat{\vec{\mu}}\,\Psi_{el,i}\,\chi_{\upsilon''}(R)Y_{J'',m_{J''}}(\theta,\phi)\,d\tau \qquad (j\leftarrow i) \quad (27.1.8)\ 28.1.4$$

where the initial quantum numbers for vibration and rotation are υ'' and J" and the final quantum numbers are υ' and J'. In essence, the gross selection rule is that the dipole moment of the molecule must change between electronic states. The terms in the vibrational coordinate, $\chi_\upsilon(R)$, determine the relative intensities of the different vibrational transitions within each electronic transition. The vibrational transitions in electronic spectroscopy are not restricted by symmetry or the $\Delta\upsilon = \pm 1$ selection rule that governs pure vibrational spectroscopy in the harmonic approximation (see Figure 28.1.3a for the vibrational assignments of the emission spectrum of N_2). The terms in the rotational coordinates, $Y_{J,m_J}(\theta,\phi)$, conserve total angular momentum. For a common case of transitions between singlet electronic states with no net orbital angular momentum, the rotational selection rule is $\Delta J = \pm 1$.

The symmetries of the electronic states involved in the transition determine if the transition dipole moment vanishes, resulting in no transition. The electronic state symmetries are determined by the total molecular-orbital and electron spin angular momenta. The orbital and spin angular momenta of an electronic state are summarized by a molecular term symbol.

Term Symbols are Unique Nicknames for Electronic States of Atoms and Molecules: Term symbols uniquely identify atomic and molecular electronic states. Atomic term symbols are discussed in Sec. 25.4. The symmetry of the electronic state under rotation, inversion, and reflection are necessary to define the term symbol. We consider each symmetry in turn. We will focus on diatomic molecules and use molecular oxygen, O_2, as an example. The photochemistry of O_2 is a central factor in atmospheric chemistry. Characterizing the important excited states of molecular oxygen is necessary to understand ozone production and the atmospheric absorption of

UV light in the stratosphere. First, remember that the ground state of atomic oxygen is ^3P, and the lowest energy excited state of oxygen atoms is ^1D:

ground state: $(1s)^2\,(2s)^2\,(2p)^4$: $\boxed{\uparrow\downarrow}\ \boxed{\uparrow\downarrow}\ \boxed{\uparrow}\ \boxed{\uparrow}$ (+1 0 -1) $\quad L = M_{L,max} = +1 +1 + 0 - 1 = 1 \Rightarrow {}^3P$

excited state: $(1s)^2\,(2s)^2\,(2p)^4$: $\boxed{\uparrow\downarrow}\ \boxed{\uparrow\downarrow}\ \boxed{\uparrow\downarrow}\ \boxed{\ }$ (+1 0 -1) $\quad L = M_{L,max} = +1 +1 + 0 + 0 = 2 \Rightarrow {}^1D$

We now develop a corresponding method that, for a given configuration, provides a complete and unique name for the electronic states of diatomic molecules. The rotational symmetry of a molecular electronic state is determined by the total orbital angular momentum. The orbital contribution to the angular momentum is characterized by the component along the internuclear axis. The z-axis is defined as the internuclear axis. Review the distinction that we discussed in Sec. 25.2 between p-type atomic orbitals with definite projections of the angular momentum, $m_\ell = \pm 1$, and the linear combinations that give p_x and p_y orbitals. For a diatomic molecule, in the absence of an electric field, the appropriate p-orbitals are the representations that have definite angular momentum quantum numbers. The p-atomic orbitals combine to give σ_{2pz} and π_{2p} molecular orbitals. σ-Orbitals are the result of the overlap of $2p_z$ orbitals, which have $m_\ell = 0$ and so have no angular momentum around the z-axis. π-Orbitals are the result of the overlap of Ψ_{2px} and Ψ_{2py} orbitals, or equivalently Ψ_{211} and Ψ_{21-1} orbitals, which have unit angular momentum around the z-axis. For a single-electron molecular orbital with angular wave function $\Phi(\phi)$:

$$\hat{L}_z\,\Phi(\phi) = \lambda\hbar\,\Phi(\phi) \qquad \text{with} \quad \Phi(\phi) = e^{i\lambda\phi} \qquad \lambda = 0, \pm 1 \qquad 28.1.5$$

where ϕ is the azimuthal angle around the z-axis, and $\lambda = 0$ for a σ orbital or ± 1 for a π orbital. The λ quantum number plays the same role as m_ℓ for atoms. The motion of the electron is clockwise around the z-axis for $\lambda = +1$ and counterclockwise for $\lambda = -1$, Figure 28.1.4.

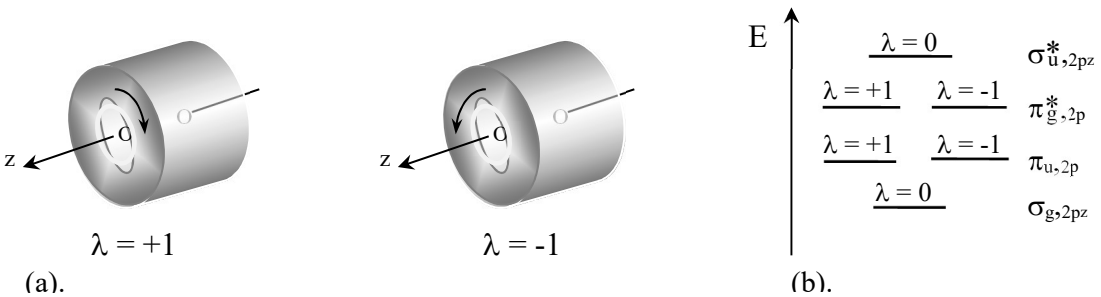

Figure 28.1.4: (a). π-orbitals have either +1 ħ or -1 ħ angular momentum around the z-axis, corresponding to clockwise or counterclockwise rotation. (b). The molecular orbitals for a homonuclear diatomic, in a field-free region of space, are characterized by the projection of the angular momentum along the z-axis.

The projection of the total orbital angular momentum around the z-axis is given by the angular momentum quantum number Λ as the absolute value:

$$\Lambda = |M_\lambda| = |\sum_{i=1}^{n} \lambda| \qquad 28.1.6$$

which is in direct analogy with the M_L quantum number for atoms. The value of Λ is represented in the molecular term symbol using the Greek letters Σ, Π, and Δ:

Λ	0	1	2
term	Σ	Π	Δ

Consider the O_2 configuration: KK $(\sigma_{g,2s})^2(\sigma^*_{u,2s})^2(\sigma_{g,2pz})^2(\pi_{u,2p})^4(\pi^*_{g,2p})^2$. This configuration can be realized with three explicit orbital assignments, Figure 28.1.5a. These orbital assignments result in three different term values. Using the conventions for assigning λ shown in Figure 28.1.4b, the value of the projection of the total angular momentum quantum number for the first assignment is given by the sum over each electron:

$$\Lambda = +1 +1 -1 -1 +1 -1 = 0 \qquad \Rightarrow {}^3\Sigma \qquad 28.1.7$$

Since the total orbital angular momentum quantum number is zero, the resulting term is Σ. Since there are two unpaired electrons, the total spin angular momentum quantum number is S = 1 giving a triplet state, $g_s = 2S + 1 = 3$. The resulting term is $^3\Sigma$. Note that closed core orbitals always give Λ = 0. So we can skip any closed shells, for example completely filled $(\sigma_{g,2pz})^2$ and $(\pi_{u,2p})^4$ shells. These diagrams are schematic because they do not take into account electron indistinguishability and orbital degeneracy. In other words, every electron can occupy every molecular orbital and degenerate states combine in symmetry adapted linear combinations to form the final complete eigenstates (see the end of this section for examples).

O_2: KK $(\sigma_{g,2s})^2(\sigma^*_{u,2s})^2(\sigma_{g,2pz})^2(\pi_{u,2p})^4(\pi^*_{g,2p})^2$

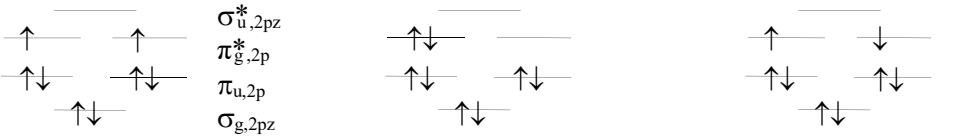

Λ= +1+1-1-1+1-1 = 0 Λ= +1+1-1-1+1+1 = 2 Λ= +1+1-1-1+1-1 = 0

(a). $^3\Sigma_g^-$ + $^1\Delta_g$ + $^1\Sigma_g^+$

O_2: KK $(\sigma_{g,2s})^2(\sigma^*_{u,2s})^2(\sigma_{g,2pz})^2(\pi_{u,2p})^3(\pi^*_{g,2p})^3$

Λ= +1+1-1+1-1-1 = 0 Λ= +1+1-1+1+1-1 = 2 Λ= +1+1-1+1-1-1 = 0 Λ= +1+1-1+1+1-1 = 2

(b). $^3\Sigma_u^+ + {}^3\Sigma_u^-$ + $^3\Delta_u$ $^1\Sigma_u^+ + {}^1\Sigma_u^-$ + $^1\Delta_u$

Figure 28.1.5: Term symbols for the ground state and several excited states of the O_2 molecule. The + and – superscripts are explained at the end of this section.

The first triplet state, $^3\Sigma_g$, Figure 28.1.5a, is the ground state. The values for Λ of the remaining two explicit assignments, derived from the same configuration, give $^1\Delta$ and $^1\Sigma$ terms.

The excited state configuration KK $(\sigma_{g,2s})^2(\sigma^*_{u,2s})^2(\sigma_{g,2pz})^2(\pi_{u,2p})^3(\pi^*_{g,2p})^3$ gives $^3\Sigma$, $^3\Delta$, $^1\Sigma$, and $^1\Delta$ terms, Figure 28.1.5b. The two $^3\Sigma$ terms from the first configuration are explained at the end of this section. The repeated $^3\Sigma$ term between the ground state and the excited states show that we need to consider other symmetry properties to meet our goal of a unique term symbol for each electronic state.

The inversion symmetry of the molecular orbitals is used to determine the overall inversion symmetry of the electronic state. For example, multiplying the g and u character for each of the electrons for the first term in Figure 28.1.5a gives the overall inversion symmetry of the ground state $^3\Sigma$ term as:

$$g\cdot g\cdot u\cdot u\cdot u\cdot u\cdot g\cdot g = g \qquad \Rightarrow \quad {}^3\Sigma_g \qquad (O_2 \text{ ground state}) \qquad 28.1.8$$

The multiplication rules are g·g = g, u·u = g, and u·g = u, in the same way as 1·1 = 1, -1·-1 = 1, and -1·1 = -1. The remaining two terms resulting from the $\ldots(\pi_{u,2p})^4(\pi^*_{g,2p})^2$ configuration are also g symmetry. The g or u symmetry is also called the parity. The terms resulting from the $\ldots(\pi_{u,2p})^3(\pi^*_{g,2p})^3$ configuration are all u.

Example 28.1.1: *Electronic State Term Symbols*

Two of the explicit orbital assignments are shown below corresponding to the O_2 configuration KK $(\sigma_{g,2s})^2(\sigma^*_{u,2s})^2(\sigma_{g,2pz})^1(\pi_{u,2p})^4(\pi^*_{g,2p})^3$. Determine the term symbols of the states.

(a). (b).

Answer: The total spin quantum number for state (a) is zero, S = 0, giving a singlet state. For state (b) the total spin quantum number is S = 1, giving a triplet state. Next note, using the convention for the λ values given in Figure 28.1.4b. Correspondingly, the projections of total orbital angular momentum and the corresponding terms are:

(a). $\Lambda = +1\ +1\ -1\ -1\ +1\ +1\ -1\ -1 = 1 \quad \Rightarrow {}^1\Pi$

(b). $\Lambda = +1\ +1\ -1\ -1\ +1\ +1\ -1 = 1 \quad \Rightarrow {}^3\Pi$

The inversion symmetries for the molecular orbtials are:

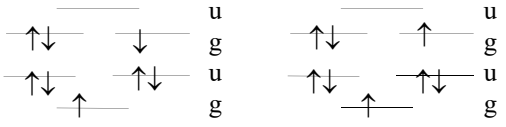

The overall inversion symmetries are the same for (a) and (b): g·u·u·u·u·g·g·g = g:

(a). $^1\Pi_g$ (b). $^3\Pi_g$

We still don't have a unique set of term symbols for the Σ terms, however. Reflection symmetry is also necessary to distinguish Σ states. States that are symmetric with respect to

reflection across a plane that includes the internuclear axis are given a + superscript and states that are anti-symmetric are given a – superscript, as listed in Figure 28.1.5. The details of assigning the reflection symmetry are discussed at the end of this section.

In summary, it is important to note that a given configuration can give rise to multiple terms. The three lowest energy configurations for O_2 result in the terms:

$$\begin{aligned} O_2\text{: KK } (\sigma_{g,2s})^2(\sigma^*_{u,2s})^2(\sigma_{g,2pz})^2(\pi_{u,2p})^4(\pi^*_{g,2p})^2 &\Rightarrow {}^3\Sigma_g^- + {}^1\Sigma_g^+ + {}^1\Delta_g \\ \text{KK } (\sigma_{g,2s})^2(\sigma^*_{u,2s})^2(\sigma_{g,2pz})^2(\pi_{u,2p})^3(\pi^*_{g,2p})^3 &\Rightarrow {}^3\Sigma_u^+ + {}^3\Sigma_u^- + {}^3\Delta_u \text{ ; } {}^1\Sigma_u^+ + {}^1\Sigma_u^- + {}^1\Delta_u \\ \text{KK } (\sigma_{g,2s})^2(\sigma^*_{u,2s})^2\,(\sigma_{g,2pz})^1(\pi_{u,2p})^4(\pi^*_{g,2p})^3 &\Rightarrow {}^1\Pi_g + {}^3\Pi_g \end{aligned} \qquad 28.1.9$$

Note that in general:

- All closed shell diatomic molecules are $^1\Sigma^+$. [Example F_2 ($^1\Sigma_g^+$): …$(\sigma_{g,2pz})^2(\pi_{u,2p})^4(\pi^*_{g,2p})^4$]
- For a single electron outside of a closed core, the term is $^2\Sigma^+$ if the unpaired electron is in a σ-orbital and $^2\Pi$ if the electron is in a π-orbital. [Example N_2^+ ($^2\Sigma_g^+$): … $(\pi_{u,2p})^4(\sigma_{g,2pz})^1$]
- Heteronuclear diatomic molecules don't have an inversion center, so g and u don't apply.

With unique "nicknames" for the different electronic states, we are now in a position to better understand the electronic absorption and emission spectra of diatomic molecules. A lot of interesting chemistry is hidden within a given configuration.

The potential energy curves for the low energy electronic states for O_2 are shown in Figure 28.1.6. The $^3\Sigma_g^-$ term is the ground state. The $^3\Sigma_u^-$ excited state dissociates to a ground state and an excited ^{1}D oxygen atoms:

$$O_2 + h\nu \rightarrow O_2\,(^3\Sigma_u^-) \rightarrow O\,(^3P) + O\,(^1D) \qquad (\lambda < 175.05 \text{ nm}) \qquad 28.1.10$$

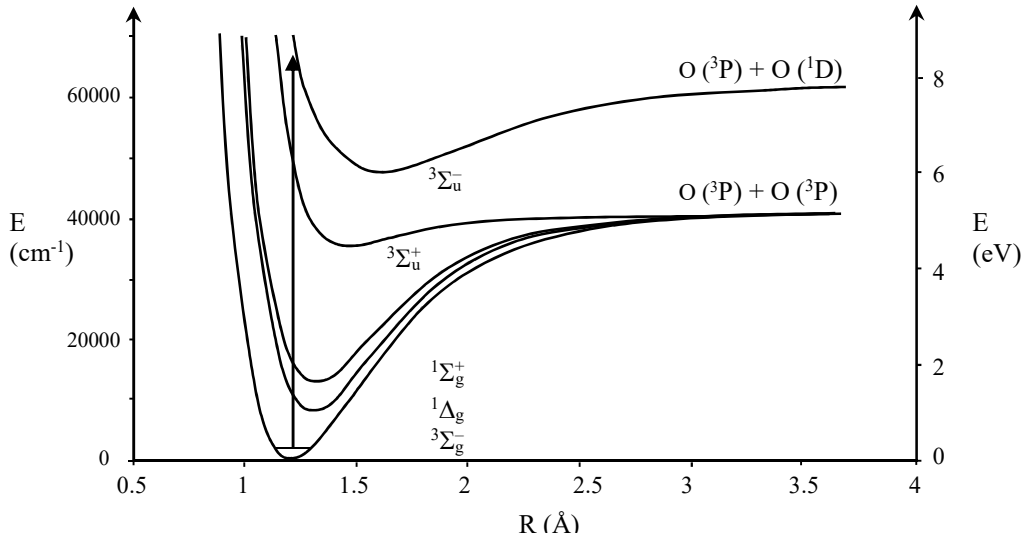

Figure 28.1.6: Potential energy curves for the ground state and low-lying electronic excited states of O_2. The indicated transition, the Schumann-Runge band, is dissociative for $\lambda < 175$ nm and results in a ^{1}D oxygen atom.

The lower excited states dissociate to two ^3P oxygen atoms. The absorption transition to the $^3\Sigma_u^-$ state is responsible for the formation of highly reactive ^1D oxygen atoms in the atmosphere, which are created by the absorption of UV light from the sun with wavelengths less than 175.05 nm. This transition is called the Schumann-Runge band of molecular oxygen. The ^1D state of atomic oxygen is thermodynamically a very good oxidizing agent and kinetic barriers for oxidation of singlet ground state molecules by ^1D oxygen atoms are typically small. The oxidation of H_2O by ^1D oxygen atoms is responsible for the formation of hydroxyl radicals in the atmosphere:

$$H_2O + O\,(^1D) \rightarrow \bullet OH + \bullet OH \qquad 28.1.11$$

$^1\Delta_g\ O_2$ is similarly a kinetically voracious oxidizing agent and gives reactions that are distinct from those of ground state $^3\Sigma_g^-\ O_2$. Unique, synthetically useful reactions of $^1\Delta_g\ O_2$ include Diels-Alder type processes, Figure 28.1.7.[2] The $^1\Delta_g\ O_2$ is easily generated photochemically under UV irradiation using a photosensitizing organic dye, such as methylene blue, to transfer energy to the ground state oxygen molecule.

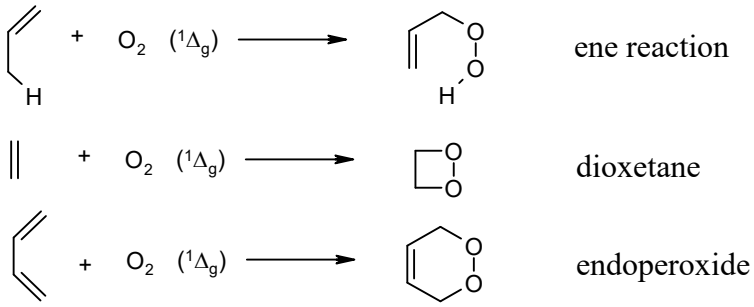

Figure 28.1.7: Synthetically useful reactions of $^1\Delta_g$ molecular O_2. Ground state $^3\Sigma_g^-\ O_2$ does not undergo these reactions. Rather, oxidation by $^3\Sigma_g^-\ O_2$ gives epoxides or ultimately CO_2.

Electronic Selection Rules: The Schumann-Runge band is not the only allowed transition for O_2. The selection rules for electronic transitions depend on changes in orbital and spin angular momentum and symmetry. The projection of the orbital angular momentum around the internuclear axis is Λ, Eq. 28.1.6. The projection of the spin angular momentum around the internuclear axis is Σ_s, which varies from –S to S in integer steps: Σ_s: –S, …, S. For molecules, Σ_s is analogous to M_S in atoms. The projection of the total angular momentum, which combines spin and orbital angular momentum, is the quantum number Ω: $\Omega = |\Lambda + \Sigma_s|$. The selection rules for electronic absorption or emission, assuming weak spin-orbit interactions, are:

$$\Delta\Lambda = 0, \pm 1 \qquad \Delta S = 0 \qquad \Delta\Omega = 0, \pm 1$$
$$g \rightarrow u \text{ or } u \rightarrow g \text{ for molecules with inversion symmetry} \qquad \text{(weak spin-orbit)} \qquad 28.1.12$$
$$+ \rightarrow + \text{ or } - \rightarrow - \text{ for } \Sigma \text{ states}$$

For example, $\Sigma \leftarrow \Sigma$, $\Sigma \leftarrow \Pi$, and $\Delta \leftarrow \Pi$ are allowed, but $\Delta \leftarrow \Sigma$ is forbidden. Considering inversion symmetry, $\Sigma_u \leftarrow \Sigma_g$ is allowed, but $\Sigma_g \leftarrow \Sigma_g$ is forbidden. Considering the spin multiplicity, $^1\Sigma \leftarrow {}^1\Sigma$ is allowed, but $^1\Sigma \leftarrow {}^3\Sigma$ is not. For reflection symmetry, $\Sigma^+ \leftarrow \Sigma^+$ and $\Sigma^- \leftarrow \Sigma^-$ are allowed, but $\Sigma^- \leftarrow \Sigma^+$ is forbidden. The Schumman-Runge transition, $^3\Sigma_u^- \leftarrow {}^3\Sigma_g^-$ is allowed following all these selection rules.

The Schumann-Runge band of molecular O_2 is also important in determining the bond dissociation energy of O_2. However, before we continue on to discuss the determination of bond dissociation energies, we should briefly discuss reflection symmetry in more detail and why two $^3\Sigma_u$ states, $^3\Sigma_u^+ + {}^3\Sigma_u^-$, result from the configuration $...(\sigma_{g,2pz})^2(\pi_{u,2p})^3(\pi^*_{g,2p})^3$. The $^3\Sigma_u^-$ term is the excited state responsible for the photo-production of ^{1}D oxygen atoms.

Reflection Symmetry (+,–) takes Orbital Degeneracy and Electron Indistinguishablity into Account: Consider an electron with angular momentum around the z-axis, Figure 28.1.8a. The viewpoint is along the internuclear axis. Reflection symmetry is determined by choosing a plane that passes through the nuclei. The plane includes the internuclear axis, which is chosen as the z-axis. Reflection across this plane, $\hat{R}_z$, reverses the sense of the rotation. Since rotation clockwise and counter-clockwise differ by the sign of the angular momentum quantum number, the effect of the reflection is to switch the sign of λ: $\lambda \rightarrow -\lambda$. Reflection has the effect of switching an electron between degenerate π-orbitals, Figure 28.1.8b. Reflection symmetry has an effect only on π and δ orbitals, because $\lambda = 0$ for a σ-orbital.

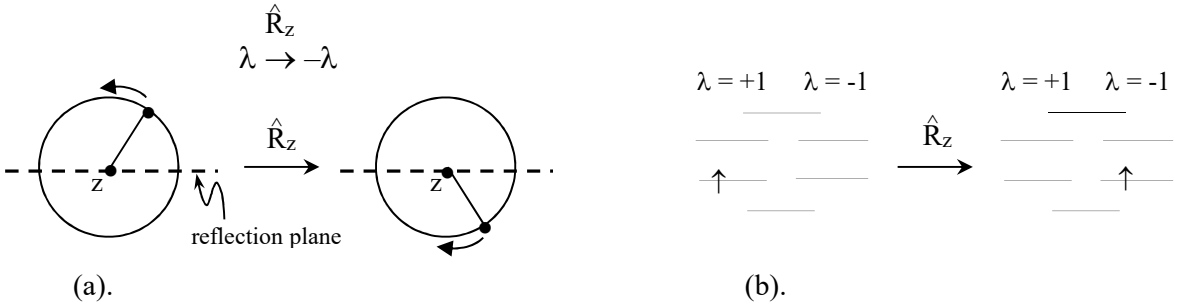

(a). (b).

Figure 28.1.8: (a). Reflection across a plane that includes the z-axis changes the sense of the rotation. The z-axis is perpendicular to the plane of the page. (b). The reflection switches the sign of λ: $\lambda \rightarrow -\lambda$. We adopt the convention of labeling the left π-MO as $\lambda = +1$.

Now consider the terms resulting from the $\ldots(\sigma_{g,2pz})^2(\pi_{u,2p})^4(\pi^*_{g,2p})^2$ configuration, Figure 28.1.5a. The $^3\Sigma_g$ ground state of O_2 is a triplet, so the spin part of the wave function must be symmetric with respect to exchange of spin labels. The spin part of the two unpaired electrons is proportional to $\alpha(1)\alpha(2)$, $\alpha(1)\beta(2) + \beta(1)\alpha(2)$, or $\beta(1)\beta(2)$. The spatial part must then be anti-symmetric to satisfy the Pauli Exclusion Principle, Figure 28.1.9a. The effect of reflection is to switch the π orbitals for the two unpaired electrons, which switches the sign of the molecular orbital after reflection. The $^3\Sigma_g$ ground state is therefore anti-symmetric with respect to reflection, and correspondingly is labeled as $^3\Sigma_g^-$. Conversely, the $^1\Sigma_g$ state, as a singlet, must have an anti-symmetric spin part and a symmetric spatial part with respect to exchange of spin labels, Figure 28.1.9b. The linear combination of four explicit arrangements is required to satisfy electron indistinguishability and reflection symmetry (see Problems 10 and 11). After reflection, the sign of this singlet state is unchanged. The $^1\Sigma_g$ state is therefore symmetric with respect to reflection, and correspondingly is labeled as $^1\Sigma_g^+$.

These diagrams are schematic in that all electrons occupy each possible molecular orbital in the full set of Slater determinants that determine the state. However, the reflection symmetry can be determined by just focusing on the two unpaired electrons.

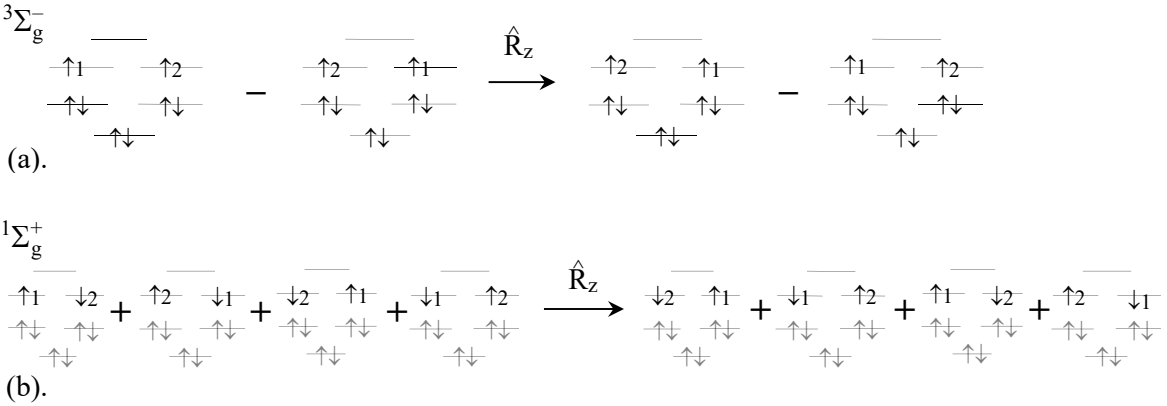

Figure 28.1.9: The effect of reflection across a plane that includes the internuclear axis for the Σ terms derived from the configuration $\ldots(\sigma_{g,2pz})^2(\pi_{u,2p})^4(\pi^*_{g,2p})^2$. (a). The sign of the $^3\Sigma_g^-$ ground state of O_2 changes upon reflection and is anti-symmetric with respect to reflection. (b). The sign of the $^1\Sigma_g^+$ term is unchanged and is symmetric with respect to reflection.

Now consider the Σ states resulting from the $\ldots(\sigma_{g,2pz})^2(\pi_{u,2p})^3(\pi^*_{g,2p})^3$ configuration. A $^3\Sigma_u$ state is a triplet, so the spin part of the wave function is symmetric with respect to exchange of spin labels. The spatial part must then be anti-symmetric with respect to the exchange of spin labels to satisfy the Pauli Exclusion Principle, Figure 28.1.10a. Following the changes in each of the four explicit assignments upon reflection shows that this $^3\Sigma_u$ term is symmetric with respect to reflection, and correspondingly is labeled as $^3\Sigma_u^+$. Note however, that there is another way to assign the signs of the four explicit assignments that also satisfies the Pauli Exclusion Principle, Figure 28.1.10b; so there are two states of $^3\Sigma_u$ symmetry. This second $^3\Sigma_u$ term is anti-symmetric with respect to reflection, however, which yields a $^3\Sigma_u^-$ term for the second state. The $^3\Sigma_u^+$ and $^3\Sigma_u^-$ states have very different energies and reactivity.

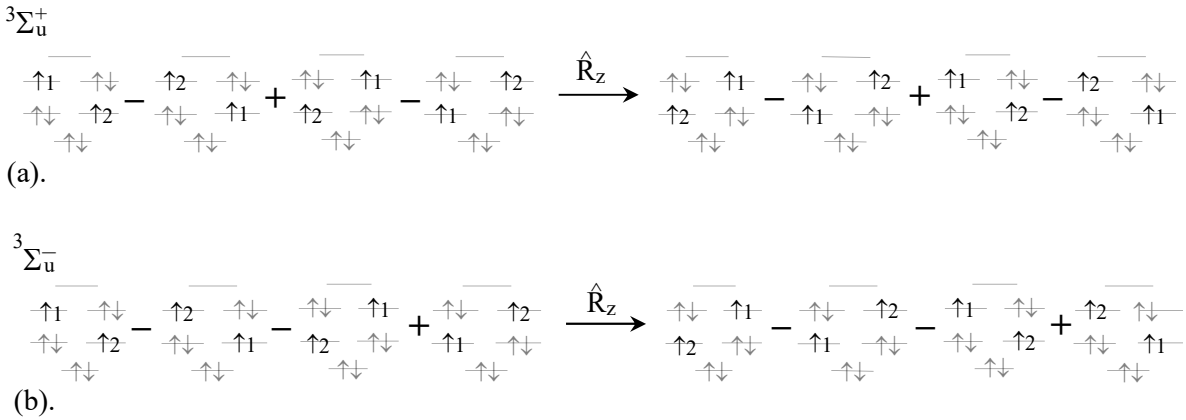

Figure 28.1.10: The $\ldots(\sigma_{g,2pz})^2(\pi_{u,2p})^3(\pi^*_{g,2p})^3$ configuration results in two $^3\Sigma_u$ terms, because there are two possible ways of assigning the signs that satisfy the Pauli Exclusion Principle and result in terms that transform as either symmetric or anti-symmetric states under reflection. (a). $^3\Sigma_u^+$ is symmetric under reflection and (b). $^3\Sigma_u^-$ is anti-symmetric.

The importance of considering the label exchange and reflection symmetry goes beyond just finding the term symbol of an electronic state. Figures 28.1.9 and 28.1.10 are examples of the general principle that degenerate states combine in symmetry adapted linear combinations to form the final eigenstates of the system. In other words, no single explicit orbital assignment can represent the final electronic state of an open shell system.

Our need to understand the reactivity of O_2 in the atmosphere has led us to an appreciation of the role that symmetry plays in controlling chemical reactions. At first, symmetry might appear to be unimportant in the everyday world, but fundamental symmetries play a central role in the underlying form of physical processes. Now that we understand more about selection rules, the next step is to discuss how electronic spectra are used to determine bond dissociation energies.

28.2 Vibrational Fine-Structure and Molecular Dissociation

The Franck–Condon Principle Predicts the Intensity of Vibrational Transitions: Electronic absorption spectra have two extreme behaviors. The spectra of many molecules have a bell-shaped appearance; the electronic transition begins with low absorbance, continues through a maximum, and ends at low absorbance, Figure 28.2.1a. At the other extreme, some molecules for some electronic transitions show a dissociation limit and absorption continuum, Figure 28.2.1b. Examples of molecules that have dissociative transitions are Br_2, I_2, and O_2. In a dissociative transition, the electronic transition begins with low absorbance and the short-wavelength region is structureless with continuous, high absorbance. Light absorption at short wavelengths causes the molecule to dissociate, for example Eq. 28.1.10. The continuum results because the energy levels above the dissociation limit are no longer quantized by vibration. Excess energy above the dissociation limit is released as translational kinetic energy of the fragment atoms.

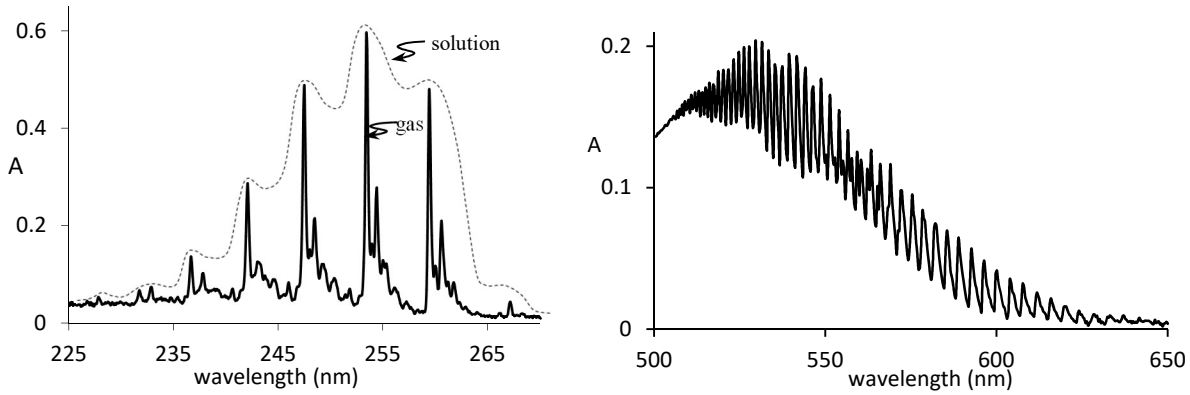

(a). Benzene (b). I_2 vapor

Figure 28.2.1: (a). The electronic absorption spectrum of benzene is typical of many molecular systems, showing low intensity at both extremes of the electronic transition. (b). I_2 vapor shows a vibrational progression ending at the dissociation limit with an absorption continuum.

The appearance of the electronic transition is determined by the intensities of the vibrational fine-structure transitions. A bell-shaped distribution of vibrational fine-structure intensities results from transitions to low-lying vibrational levels of the electronic excited state, Figure 28.2.1a. Electronic transitions ending in a high-absorbance dissociation continuum result from

transitions to highly-excited vibrational levels of the electronic excited state, Figure 28.2.1b. The differences between adjacent transition frequencies approach zero at the convergence limit, which is the onset of continuous absorption. The adjacent differences approach zero because of anharmonicity, Figure 27.5.2. The vibrational fine-structure in the absorbance spectrum corresponds to the vibrational spacing in the excited state of the molecule, not the ground state as in pure vibrational spectroscopy.

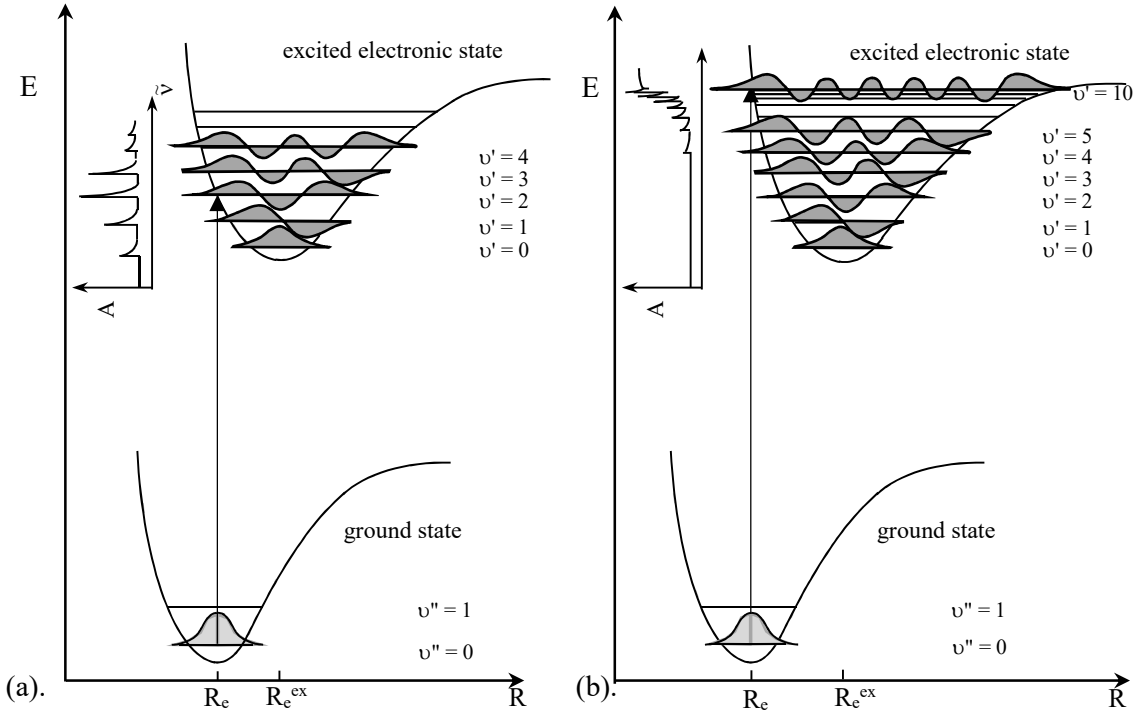

Figure 28.2.2: (a). The vibrational motion of a molecule is much slower than the time interval of an electronic transition. The nuclei essentially remain frozen during the transition, giving a vertical-transition. (b). A large difference in equilibrium internuclear distance gives a vibrational progression ending at the dissociation limit.

Franck-Condon factors determine the intensity of vibrational transitions within a given electronic transition. Most electronic spectra are taken at moderate resolution, so that rotational fine-structure is not resolved. In the Born-Oppenheimer limit, the transition dipole moment of an electronic transition of a diatomic molecule is then given by Eq 28.1.3, neglecting the rotational portion of the integrals:

$$\vec{\mu}_{tr} = <\vec{\mu}> = \int [\Psi_{el,j}\, \chi_{\upsilon'}(R)]^* \hat{\vec{\mu}}\, \Psi_{el,i}\, \chi_{\upsilon''}(R)\, d\tau_{el}\, dR \qquad (j,\upsilon' \leftarrow i,\upsilon'') \qquad 28.2.1$$

where the volume element is the product over the coordinates of the electrons, $d\tau_{el}$, and the nuclear separation, dR. The electric dipole-moment operator consists of a term dependent on the electron coordinates and a term dependent on the nuclear coordinates: $\hat{\vec{\mu}} = \hat{\vec{\mu}}_{el} + \hat{\vec{\mu}}_{nuclei}$, Eq. 27.1.5. The vibrational wave functions are only functions of the nuclear coordinate, R. Substitution of Eq. 27.1.5 into Eq. 28.2.1 gives:

$$\vec{\mu}_{tr} = \int \Psi_{el,j}^{*} \hat{\vec{\mu}}_{el} \Psi_{el,i} \, d\tau_{el} \int \chi_{\upsilon'}(R)^{*} \chi_{\upsilon''}(R) \, dR + \int \Psi_{el,j}^{*} \Psi_{el,i} \, d\tau_{el} \int \chi_{\upsilon'}(R)^{*} \hat{\vec{\mu}}_{nuclei} \chi_{\upsilon''}(R) \, dR \qquad 28.2.2$$

In the second term of the sum, the integral over the electron coordinates vanishes by orthogonality; both wave functions are eigenfunctions of the electronic Hamiltonian. In the first term, the integral over the electron coordinates is the same for every vibrational transition. Defining the integral over the electron coordinates as the electronic transition dipole, $\vec{\mu}_{tr,el}$, gives the transition intensity for the vibrational fine-structure line $\upsilon' \leftarrow \upsilon''$ as:

$$\vec{\mu}_{tr} = \vec{\mu}_{tr,el} \int \chi_{\upsilon'}(R)^{*} \chi_{\upsilon''}(R) \, dR \qquad \text{with} \quad \vec{\mu}_{tr,el} = \int \Psi_{el,j}^{*} \hat{\vec{\mu}}_{el} \Psi_{el,i} \, d\tau_{el} \qquad (j,\upsilon' \leftarrow i,\upsilon'') \qquad 28.2.3$$

The intensity of a vibrational transition is proportional to the square of the transition dipole moment:

$$q_{\upsilon' \leftarrow \upsilon''} \propto \left| \int \chi_{\upsilon'}(R)^{*} \chi_{\upsilon''}(R) \, dR \right|^{2} \qquad 28.2.4$$

where $q_{\upsilon' \leftarrow \upsilon''}$ is the **Franck-Condon factor**. The integral is the overlap of the ground-state vibrational wave function with the excited electronic state vibrational wave function. Franck-Condon factors vary from 0 to 1, Figure 28.2.3.

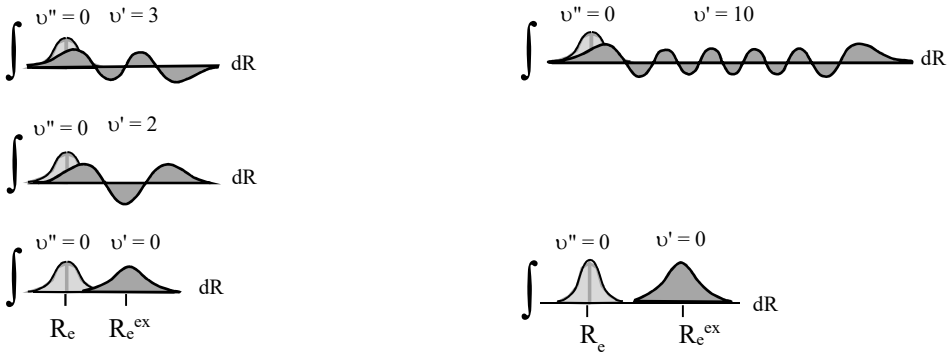

(a). $R_e^{ex} \cong R_e$ (b). $R_e^{ex} >> R_e$

Figure 28.2.3: Franck-Condon integrals based on the potential energy curves in Figure 28.2.2. (a). For a small difference in equilibrium internuclear separation between the ground-state and the excited-state, low lying vibrational transitions have high intensity. (b). For a large difference in equilibrium internuclear separation, highly excited vibrational transitions have high intensity.

Given the Boltzmann distribution at room temperature, the vast majority of molecules start in the lowest energy vibrational state, $\upsilon'' = 0$. The equilibrium internuclear separation in the excited electronic state, R_e^{ex}, is typically larger than the ground electronic state, R_e. For electronic transitions with a small change in equilibrium internuclear separation, the Franck-Condon factors are largest for low-lying vibrational levels. In Figures 28.2.12a and 28.2.13a, the overlap between vibrational wave functions is largest for $2 \leftarrow 0$ and $3 \leftarrow 0$. The remaining Franck-Condon factors are small, giving a bell-shaped distribution of vibrational fine-structure intensities. For electronic transitions with a large change in equilibrium internuclear separation, $R_e^{ex} >> R_e$, the

Franck-Condon factors are large for highly excited vibrational levels. In Figures 28.2.12b and 28.2.13b, the overlap between vibrational wave functions increases with υ', giving the largest intensities for transitions near the dissociation limit. As exemplified by the two extreme types of transitions, bell-shaped or dissociative, the vibrational progressions within each electronic transition are a sensitive indicator of the properties of the excited state.

Franck-Condon factors are easily determined if the potential energy curves of the two electronic states are known. However, a quick visual method for estimating the most intense vibrational transition is useful and instructive. The period of a vibration is orders of magnitude longer than the time interval of an electronic transition. From the perspective of the electronic transition, the nuclear positions are fixed during the electronic transition. Visually, the electronic transition is a **vertical transition**; the transition arrow is at constant nuclear separation, Figure 28.2.2. The most probable nuclear separation in the υ' = 0 vibrational state of the ground electronic state is the equilibrium internuclear separation, R_e. The vertical transition begins in the middle of the ground state vibrational potential energy well. We can estimate the vibrational quantum number of the most intense vibrational transition by noting the intersection of the vertical transition with the excited electronic state potential curve. In Figure 28.1.12a, the vertical transition intersects the excited state potential curve at the energy of the υ' = 2 vibrational level, predicting the 2←0 transition as the most intense. In Figure 28.2.2b for $R_e^{ex} >> R_e$, the vertical transition intersects the excited state potential curve near the dissociation limit, predicting transitions with large υ' as the most intense. This visual approximation works best for highly excited vibrational levels, since the largest vibrational wave function amplitude approaches the classical turning points as the vibrational quantum number increases. As a result, for large υ', the vertical transition intersection corresponds to a region with large vibrational wave function amplitude. A classical analogy is helpful at this point.

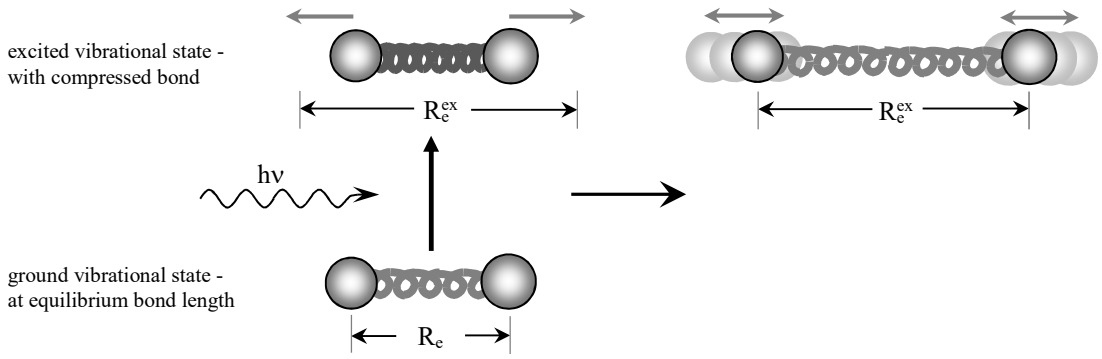

Figure 28.2.4: Before a vertical transition, a molecule is most probably at the equilibrium bond length. With $R_e^{ex} >> R_e$, after the vertical transition the bond is compressed in the new electronic state. Rebound produces a highly excited vibrational state.

The equilibrium nuclear separation in the ground state is the equilibrium bond length. A vertical transition is pictured as taking the molecule from the ground electronic state to the excited electronic state with the bond length frozen at the equilibrium separation of the ground state, Figure 28.2.4. If the excited electronic state equilibrium bond length is significantly larger than the ground state then the excited state molecule initially finds its bond compressed, smaller

than the new equilibrium bond length. This compressed bond rebounds throwing the molecule into large amplitude vibration. Large amplitude vibration corresponds to states with large quantum number, υ'. This analogy also predicts a long **vibrational progression** for transitions that have a large change in equilibrium bond length; strong rebound produces many excited vibrational levels, Figure 28.2.2b. By comparison, a small number of vibrational levels result from a small change in equilibrium bond length.

Dissociation Energies Can Be Measured Using Electronic Absorption Spectra: Assuming the initial ground-state molecule is in υ" = 0, the lowest energy transition for electronic states i and j is $\Delta E(j,0\leftarrow i,0)$. In wave numbers this lowest energy transition is $\Delta E(j,0\leftarrow i,0)/hc = \tilde{\nu}_{oo}$, Figure 28.2.5. The onset of the dissociation continuum is the convergence limit, which is the energy where the spacing between adjacent peaks is zero. The convergence limit corresponds to υ' = ∞ with transition energy $\Delta E(j,\infty\leftarrow i,0)$ or in wave numbers $\tilde{\nu}_{\infty o}$. If the complete vibrational progression is observed, the bond dissociation energy of the excited state, D_o^{ex}, is determined as:

$$D_o^{ex} = \Delta E(j,\infty\leftarrow i,0) - \Delta E(j,0\leftarrow i,0) \quad \text{in joules or} \quad \tilde{D}_o^{ex} = \tilde{\nu}_{\infty o} - \tilde{\nu}_{oo} \quad \text{in cm}^{-1} \quad \text{(excited state)} \quad 28.2.5$$

Unfortunately, the full vibrational progression is rarely observed. However, the bond dissociation energy of the ground electronic state can be determined from the convergence limit by the difference, Figure 28.2.5:

$$D_o = \Delta E(j,\infty\leftarrow i,0) - \Delta E_{atomic} \quad \text{in joules or} \quad \tilde{D}_o = \tilde{\nu}_{\infty o} - \Delta\tilde{E}_{atomic} \quad \text{in cm}^{-1} \quad \text{(ground state)} \quad 28.2.6$$

where ΔE_{atomic} is the energy necessary to produce the product atoms of the photodissociation compared to the ground state atoms. Bond dissociation energies, D_o, are listed in Table 8.8.1.

Example 28.2.1: *Determining Bond Dissociation Energies*

Calculate the bond dissociation energy of O_2. For the Schumann-Runge band of O_2, the convergence limit occurs at 57128 ± 5 cm^{-1}, which corresponds to 175.05 nm or 7.083 eV, Figure 28.2.5. Referring to Eq. 28.1.10, the atomic excitation energy for ^{1}D-oxygen is:

$$O\,(^3P) \rightarrow O\,(^1D) \qquad \Delta E_{atomic} = 15867.9\ cm^{-1} = 1.9674\ eV \qquad 28.2.7$$

Answer: Using Eq. 28.2.6 for the bond dissociation energy of the ground state gives:

$$\tilde{D}_o = \tilde{\nu}_{\infty o} - \Delta\tilde{E}_{atomic} = 57128 \pm 5\ cm^{-1} - 15867.9\ cm^{-1} = 41260 \pm 5\ cm^{-1}$$
$$D_o = \Delta E(j,\infty\leftarrow i,0) - \Delta E_{atomic} = 7.083\ eV - 1.9674\ eV = 5.116\ eV = 493.6\ kJ\ mol^{-1}$$

ΔE_{atomic} must be determined by a separate experiment; extensive tabulations are available.[3-5]

The Convergence Limit is Estimated by Birge-Sponer Extrapolation: The convergence limit is often obscured by instrumental noise. The Birge-Sponer extrapolation is designed to better estimate the wavenumber at the convergence limit; please review Section 27.5. The vibrational

fine-structure converges to a limit that is the sum of the dissociation energy of the ground state of the molecule and the atomic excitation energy, Eq. 28.2.6. Alternately, the convergence limit is the sum of the lowest energy transition and the dissociation energy of the excited state:

$$\tilde{\nu}_{\infty o} = \tilde{D}_o + \Delta\tilde{E}_{atomic} = \tilde{\nu}_{oo} + \tilde{D}_o^{ex} \qquad 28.2.8$$

The Birge-Sponer extrapolation is based on the difference in wave number between adjacent transitions, $\Delta\tilde{\nu}_\upsilon$, where the adjacent peaks correspond to the υ+1 ← 0 and the υ ← 0 transitions, Figure 28.2.5. For example, in electronic spectroscopy the first difference is: $\Delta\tilde{\nu}_o = \tilde{\nu}_{1o} - \tilde{\nu}_{oo}$.

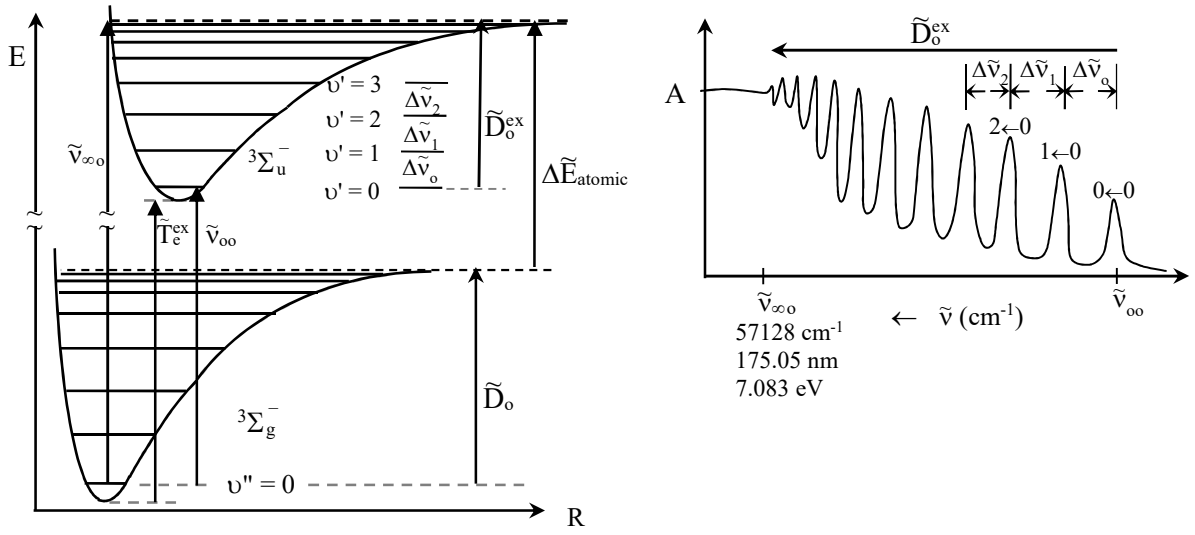

Figure 28.2.5: Molecular and atomic transition energies in electronic absorption spectroscopy. The convergence limit, where $\upsilon' \to \infty$, is the onset of dissociation continuum.

The first step is to find the relationship between the convergence limit and the excited state vibrational energy levels. By convention the symbol $\tilde{T}$ is used for electronic energy, in the same way as the rotational term is designated $\tilde{F}$ and the vibrational term is designated $\tilde{G}$. Assuming a Morse potential for the vibration, the energy of the υ' vibrational level of the excited state is:

$$\tilde{E}_{\upsilon'}^{ex} = \tilde{T}_e^{ex} + \tilde{G}(\upsilon') = \tilde{T}_e^{ex} + \tilde{\nu}_e^{ex}(\upsilon' + ½) - \chi_e^{ex}\tilde{\nu}_e^{ex}(\upsilon' + ½)^2 \qquad 28.2.9$$

where $\tilde{T}_e^{ex}$ is the energy difference from the minimum energy of the ground state potential curve to the minimum energy of the excited state potential curve. The fundamental vibration frequency, $\tilde{\nu}_e^{ex}$, and anharmonicity, $\chi_e^{ex}\tilde{\nu}_e^{ex}$, are for the excited state. The dissociation energy of the excited state corresponds to the difference in energy between the convergence limit, $\upsilon' = \upsilon_{cl}$, and the $\upsilon' = 0$ vibrational state of the excited state; using Eq. 28.2.9 gives:

$$\begin{aligned}\tilde{D}_o^{ex} &= \tilde{E}_{\upsilon cl}^{ex} - \tilde{E}_o^{ex} \\ &= [\tilde{T}_e^{ex} + \tilde{\nu}_e^{ex}(\upsilon_{cl} + ½) - \chi_e^{ex}\tilde{\nu}_e^{ex}(\upsilon_{cl} + ½)^2] - [\tilde{T}_e^{ex} + \tilde{\nu}_e^{ex}(½) - \chi_e^{ex}\tilde{\nu}_e^{ex}(½)^2]\end{aligned} \qquad 28.2.10$$

The $\tilde{T}_e^{ex}$ terms cancel and then multiplying out the factors and cancelling terms gives:

$$\tilde{D}_o^{ex} = \tilde{\nu}_e^{ex}\,\upsilon_{cl} + \tfrac{1}{2}\,\tilde{\nu}_e^{ex} - \chi_e^{ex}\,\tilde{\nu}_e^{ex}\,\upsilon_{cl}^2 - \chi_e^{ex}\,\tilde{\nu}_e^{ex}\,\upsilon_{cl} - \tfrac{1}{4}\,\chi_e^{ex}\,\tilde{\nu}_e^{ex} - \tfrac{1}{2}\,\tilde{\nu}_e^{ex} + \tfrac{1}{4}\,\chi_e^{ex}\,\tilde{\nu}_e^{ex}$$
$$= \tilde{\nu}_e^{ex}\,\upsilon_{cl} - \chi_e^{ex}\,\tilde{\nu}_e^{ex}\,\upsilon_{cl}^2 - \chi_e^{ex}\,\tilde{\nu}_e^{ex}\,\upsilon_{cl} \qquad 28.2.11$$

Factoring out the common factor of υ_{cl} gives:

$$\tilde{D}_o^{ex} = (\tilde{\nu}_e^{ex} - \chi_e^{ex}\,\tilde{\nu}_e^{ex}\,\upsilon_{cl} - \chi_e^{ex}\,\tilde{\nu}_e^{ex})\,\upsilon_{cl} \qquad 28.2.12$$

The Birge-Sponer extrapolation for pure vibrational spectroscopy is based on Eq. 27.5.20. The extrapolation for electronic spectroscopy is completely analogous, except that the adjacent peak spacing is for adjacent vibrational levels of the excited electronic state, from Eq. 27.5.20:

$$\Delta\tilde{\nu}_\upsilon = (\tilde{\nu}_e^{ex} - 2\chi_e^{ex}\,\tilde{\nu}_e^{ex}) - 2\chi_e^{ex}\,\tilde{\nu}_e^{ex}\,\upsilon \qquad 28.2.13$$

The convergence limit, υ_{cl}, corresponds to $\Delta\tilde{\nu}_{\upsilon cl} = 0$. Rearrangement of Eq. 28.2.13 then gives:

$$\chi_e^{ex}\,\tilde{\nu}_e^{ex}\,\upsilon_{cl} = \tfrac{1}{2}\,\tilde{\nu}_e^{ex} - \chi_e^{ex}\,\tilde{\nu}_e^{ex} \qquad 28.2.14$$

Substituting this result into the center term in Eq. 28.2.12 gives the excited state dissociation energy from the quantum number at the convergence limit as:

$$\tilde{D}_o^{ex} = \tfrac{1}{2}\,\tilde{\nu}_e^{ex}\,\upsilon_{cl} \qquad 28.2.15$$

Next we need to solve Eq. 28.2.13 for the quantum number at the convergence limit. The first adjacent difference, which is for $\upsilon = 0$, is:

$$\Delta\tilde{\nu}_o = \tilde{\nu}_e^{ex} - 2\chi_e^{ex}\,\tilde{\nu}_e^{ex} \qquad 28.2.16$$

Substituting this result back into Eq. 28.2.13 gives a linear equation in υ for the adjacent differences:

$$\Delta\tilde{\nu}_\upsilon = \Delta\tilde{\nu}_o - 2\chi_e^{ex}\,\tilde{\nu}_e^{ex}\,\upsilon \qquad 28.2.17$$

as the basis for the Birge-Sponer extrapolation, Figure 28.2.6. A plot of the adjacent differences versus the vibrational quantum number υ gives the slope = $-2\chi_e^{ex}\,\tilde{\nu}_e^{ex}$ and intercept = $\Delta\tilde{\nu}_o$. The quantum number at the convergence limit is found by setting Eq. 28.2.17 to zero, $\Delta\tilde{\nu}_{\upsilon cl} = 0$; then Eq. 28.2.17 rearranges to give:

$$\Delta\tilde{\nu}_o = 2\chi_e^{ex}\,\tilde{\nu}_e^{ex}\,\upsilon_{cl} \qquad\qquad \upsilon_{cl} = \frac{\Delta\tilde{\nu}_o}{2\chi_e^{ex}\,\tilde{\nu}_e^{ex}} \qquad 28.2.18$$

With the convergence limit in hand, Eq. 28.2.15 is used to find $\tilde{D}_o^{ex}$. The anharmonicity is usually small, which allows the approximation $\tilde{\nu}_e^{ex} \cong \Delta\tilde{\nu}_o$ in Eq. 28.2.15. With this approximation the dissociation energy of the excited state is approximately given by the area of the triangle with base $\Delta\tilde{\nu}_o$ and height υ_{cl}, Figure 28.2.6:

$$\tilde{D}_o^{ex} = \tfrac{1}{2}\,\tilde{\nu}_e^{ex}\,\upsilon_{cl} \cong \tfrac{1}{2}\,\Delta\tilde{\nu}_o\,\upsilon_{cl} = \text{area} \qquad 28.2.19$$

Using Eqs. 28.2.19 and 28.2.8, the transition energy at the convergence limit is:

$$\tilde{\nu}_{\infty o} = \tilde{\nu}_{oo} + \tilde{D}_o^{ex} = \tilde{\nu}_{oo} + \tfrac{1}{2}\,\tilde{\nu}_e^{ex}\,\upsilon_{cl} \cong \tilde{\nu}_{oo} + \tfrac{1}{2}\,\Delta\tilde{\nu}_o\,\upsilon_{cl} = \tilde{\nu}_{oo} + \text{area} \qquad 28.2.20$$

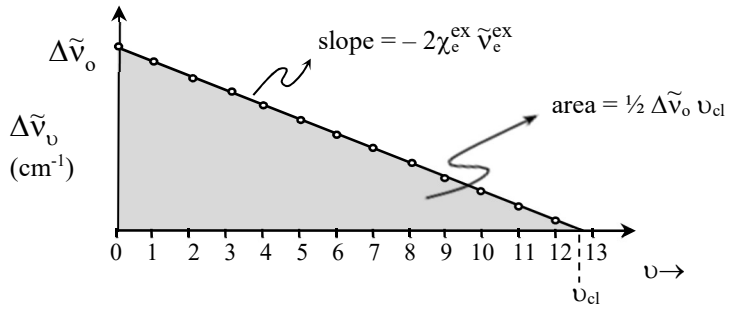

Figure 28.2.6: A Birge-Sponer plot estimates the vibrational quantum number at the convergence limit. The intercept is $\Delta\tilde{\nu}_o = \tilde{\nu}_e^{ex} - 2\chi_e^{ex}\tilde{\nu}_e^{ex}$ and the slope = $-2\chi_e^{ex}\tilde{\nu}_e^{ex}$.

Example 28.2.2: *Dissociation Energy of SO*

Calculate the bond energy of the diatomic molecule SO. The vibrational fine-structure transitions in the electronic spectrum are given in the table below.[6] The excited state dissociates into a ground state O(^{3}P) and an excited state S(^{1}D)-atom:

$$SO + h\nu \rightarrow S\ (^1D) + O\ (^3P) \qquad (\lambda < 188.7\ nm)$$

The atomic excitation energy is:[3-5]

$$S\ (^3P) \rightarrow S\ (^1D) \qquad \Delta\tilde{E}_{atomic} = 9238.61\ cm^{-1} = 1.1454\ eV$$

$\tilde{\nu}$ (cm^{-1})	50412	50621	50835	51029	51225	51420	51598	51750	51884	52041	52174	52267	52379

Answer: For diatomic molecules, the bond energies are given by the dissociation energies. The vibrational quantum numbers of the listed transitions are not known. However, the first transition can be arbitrarily assigned as $\upsilon = 0$ and Eq. 28.2.20 still applies. However, with the arbitrary assignment of the quantum number, the Birge-Sponer intercept does not give the fundamental vibration frequency of the excited state from the intercept, Eq. 28.2.17. The adjacent differences and corresponding Birge-Sponer plot are given below:

υ	0	1	2	3	4	5	6	7	8	9	10	11
$\Delta\tilde{\nu}_\upsilon$ (cm^{-1})	209	214	194	196	195	178	152	134	157	133	93	112

slope	-10.444055	221.35897	intercept
±	1.1240284	7.2989760	±
r2	0.89619	13.44142	s(y)
F	86.334380	10	df
ss_{reg}	15598.197	1806.7191	ss_{resid}

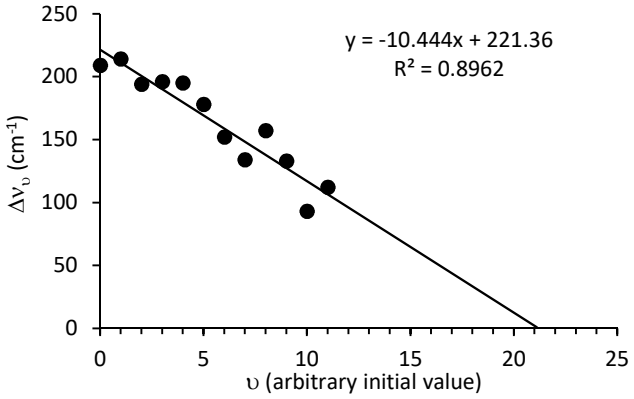

Using Eq. 28.2.17, the slope gives the anharmonicity: $\chi_e^{ex}\,\tilde{\nu}_e^{ex} = -\,½$ slope = 5.22 ± 0.51 cm^{-1}

Using Eq. 28.2.18: $\upsilon_{cl} = \dfrac{\Delta\tilde{\nu}_o}{2\chi_e^{ex}\,\tilde{\nu}_e^{ex}} = \dfrac{221.358}{10.444} = 21.195 \pm 2.4$

Using Eq. 28.2.19: area = ½ $\Delta\tilde{\nu}_o\,\upsilon_{cl}$ = ½ (221.358)(21.195) = 2345.8 ± 275.1 cm^{-1}
Using Eq. 28.2.20, the transition wave number at the convergence limit is:

$$\tilde{\nu}_{\infty o} = \tilde{\nu}_{oo} + \text{area} = 50412\ \text{cm}^{-1} + 2345.8\ \text{cm}^{-1} = 52757.8 \pm 275.1\ \text{cm}^{-1} = 6.541 \pm 0.034\ \text{eV}$$

Using Eq. 28.2.6, the bond energy of the ground state is:

in cm^{-1}: $\tilde{D}_o = \tilde{\nu}_{\infty o} - \Delta\tilde{E}_{atomic}$ = (52758 ± 275 cm^{-1}) – 9238.61 cm^{-1} = 43519 ± 275 cm^{-1}
in eV: $D_o = \Delta E(j,\infty\leftarrow i,0) - \Delta E_{atomic}$ = (6.541 ± 0.034 eV) – 1.1454 eV = 5.396 ± 0.034 eV
in kJ mol^{-1}: = 520.6 ± 3.3 kJ mol^{-1}

This bond energy is consistent with Figure 26.4.12 and the expected qualitative bond order of 2.

Photochemistry - Dissociation and Predissociation: Photochemistry can result from the excited electronic state as one of the primary reactants, as in the reactions of O_2 ($^1\Delta_g$), Figure 28.1.7. The initial mechanistic step can also occur by bond breaking directly from the excited state. There are three possibilities:
(1). The direct photo-dissociation described in Examples 28.2.1 and 28.2.2 is one type of photodissociation. Such photochemical processes result from the excited-state dissociation continuum of a bound←bound electronic transition. In other words, both the ground and excited states have potential energy surfaces with minima.
(2). Bond dissociation always results if the electronic transition is to a repulsive excited state, Figure 28.2.7. Such photochemical processes are repulsive←bound electronic transitions.

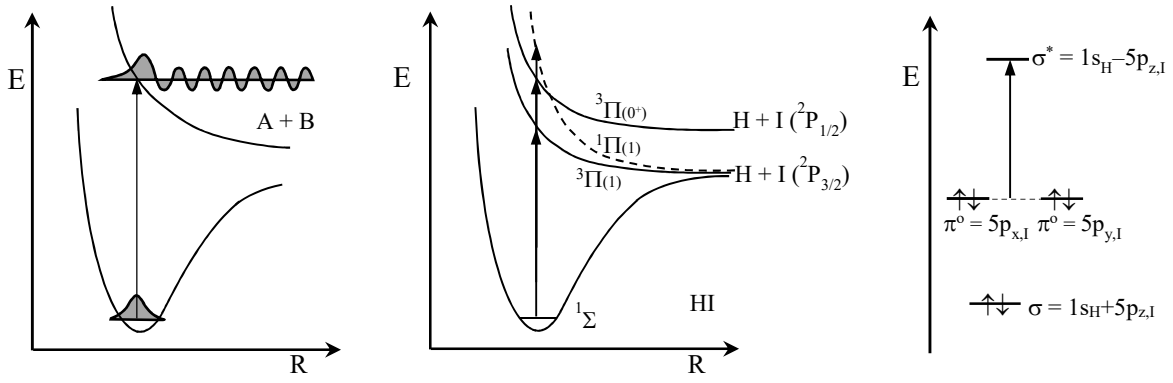

(a). (b). (c).

Figure 28.2.7: Direct photodissociation by repulsive←bound transitions.[7] The final electronic state is a continuum of translational energy levels. (a). Franck-Condon factors determine the intensity of transitions into the translational continuum. (b). Dissociation at $\lambda < 303$ nm in HI is primarily to three repulsive states, each with configuration $\sigma^2(\pi^o)^3(\sigma^*)^1$. (c). Molecular orbital diagram for the transitions in HI.

A repulsive excited state has a continuum of levels that differ by the translational kinetic energy of the dissociated atoms. The excess energy above the excited-state dissociation limit is released as translational kinetic energy of the dissociated atoms. The intensities of transitions into the repulsive continuum are predicted using Franck-Condon factors and the density of states of the translational energy levels, Figure 28.2.7a. Molecules typically have many available repulsive electronic states, so that direct repulsive←bound dissociation is a common occurrence, especially in the vacuum UV. Examples are the 33,000-53,000 cm^{-1} transitions to three low lying repulsive states of HI, Figure 28.2.7b.[7] The ground state of HI is $\sigma^2(\pi^o)^4$; the bonding σ-orbital results from the overlap of the H(1s) orbital and the I($5p_z$). The π-non-bonding orbitals are pure atomic I($5p_x$) and I($5p_y$). All three repulsive states result from the configuration $\sigma^2(\pi^o)^3(\sigma^*)^1$, with different spin and total angular momenta.

(3). **Predissociation** is a common third possibility. In predissociation the bound excited-state potential energy curve intersects with a repulsive potential energy curve, with the same symmetry, Figure 28.2.8a. The repulsive potential energy curve may have the same dissociation limit as the ground state or as another excited state. The intersection is called a **curve crossing**. At the curve crossing the two potential energy surfaces have degenerate energies. As we saw in Section 27.7, the interaction of two degenerate transitions of the same symmetry produces two closely spaced energy levels. The first electronic state takes on some of the character of the second, and the second takes on some of the character of the first; the two electronic states mix. The result is an **avoided-crossing,** Figure 28.2.8bc. The potential energy surface that is bound for small R smoothly joins to the repulsive potential surface at large R. Correspondingly, the potential energy surface that is repulsive at short R smoothly joins to the bound potential energy surface at large R. At the curve-crossing, the two excited states are so similar, in energy and angular momenta, that the molecule loses track of which excited state it is in.

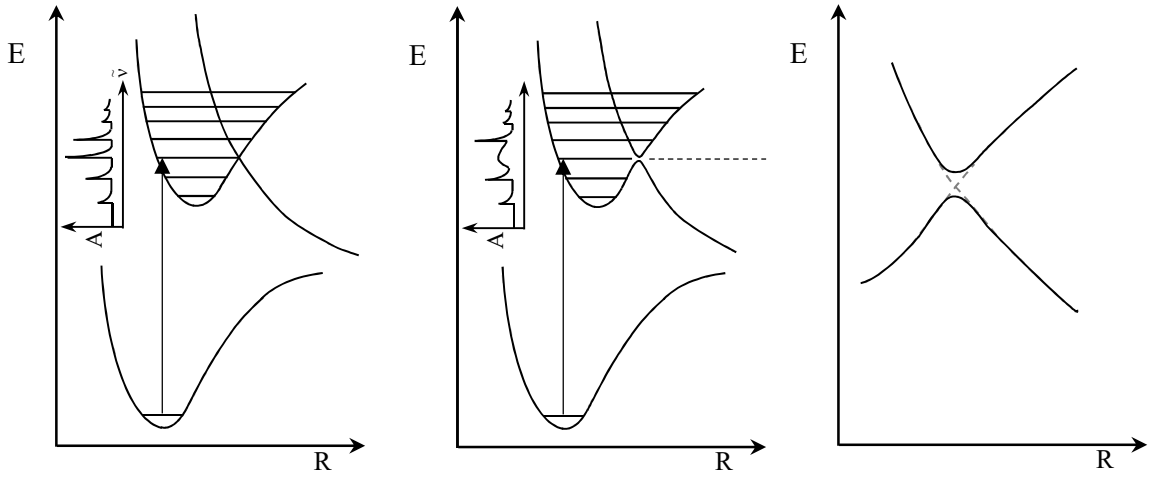

(a). No interaction (b). Strong interaction (c). Avoided curve crossing

Figure 28.2.8: (a). Predissociation results from an avoided crossing of a bound potential energy surface and a repulsive potential energy surface. (b). Vibrational fine-structure transitions near the energy of the curve crossing are lifetime broadened by bond breaking. (c). Expanded view of the potential energy surfaces near the avoided crossing.

Electronic transitions to vibrational levels near the energy of the avoided-crossing cross-over to the repulsive surface, which results in bond dissociation. The transfer to the repulsive surface, typically within 10^{-11}–10^{-10} s, requires many vibrational periods. The effect on the absorbance spectrum is that transitions near the energy of the avoided-crossing are broadened, because the lifetime of the excited state is severely shortened by bond breakage. The effect of pre-dissociation is to lower the energy required for bond fission in the excited state. The $^2\Pi \leftarrow {}^2\Pi$ transition in NO is an example of pre-dissociation that has an important impact on NO_x concentrations in the stratosphere and mesosphere (the mesosphere extends from 50-85 km).[8] Pre-dissociation produces highly reactive excited state ^{4}S nitrogen-atoms:

$$NO\ (^2\Pi) + h\nu \rightarrow NO\ (^2\Pi\ \pi(3p)^1) \rightarrow N\ (^4S) + O\ (^3P) \qquad (\lambda < 192\ nm) \qquad 28.2.21$$

The cross-over from one potential energy surface to another results from a breakdown in the Born-Oppenheimer approximation. The bond length change caused by vibration drives the switchover between the bound and repulsive electronic states.

Rydberg States Give a Series of Atomic-like Transitions: So far we have considered excited states that correspond to promotion of electrons among the valence molecular orbitals of the system, as in Figures 26.4.4, 26.6, 26.6.7, and 26.6.8. In these molecular orbitals, the electrons in the atoms have valence state quantum numbers. Rydberg excited states are produced if an electron in an atom is promoted to an atomic orbital with principal quantum number higher than the valence state. For example, a valence 2p-electron in the C-atom in C≡O can be promoted to a 3s- or 3p-orbital or higher, or a valence 5p-electron in HI can be promoted to a 6s, 6p, or 6d orbital or higher. Any atom in a molecule can be a center for Rydberg promotion, including H-atoms. All molecules have Rydberg states. Promotion of an electron decreases energy matching with atomic orbitals on adjacent atoms. As a result the promoted electron is primarily non-bonding and the orbital of the promoted electron is then similar to the isolated atom. Rydberg states are strongly localized on the atom that has been promoted. For high Rydberg excitations, n = 10, 11, 12, etc., the molecule acts like a "charged core" with a small net nuclear charge giving an atomic-like orbital with very large extent. Rydberg states form series of transitions with increasing principle quantum number that follow an atomic-like energy pattern similar to the Rydberg formula for hydrogen-atoms, Eq. 23.2.10:[9]

$$\tilde{\nu}_n = \tilde{\nu}_I - \frac{\Re_h}{(n + c)^2} \qquad 28.2.22$$

where $\tilde{\nu}_n$ is the wave number of the Rydberg transition, $\tilde{\nu}_I$ is the series limit, $\Re_h$ is the Rydberg constant, n is the principal quantum number of the promoted electron, and c is a constant specific to the series (the quantum defect). For example, a Rydberg series for O_2 is observed in the vacuum UV with transitions:[10]

$$\tilde{\nu}_n = 146548\ cm^{-1} - \frac{\Re_h}{(n + 0.32)^2} \qquad n = 3, 4, 5, \ldots, 15 \qquad 28.2.23$$

The limit $\tilde{\nu}_I$ corresponds to the ionization of the electron and the formation of the corresponding molecular ion, which is O_2^+ in the present example. Rydberg states show vibrational and rotational fine-structure and otherwise act like any other excited state. Now that we have a better understanding of diatomics, we can expand our discussion to polyatomic molecules.

28.3 Electronic Absorption and Emission Spectroscopy-Polyatomic Molecules

The absorption and emission spectra of diatomics and polyatomics follow the same fundamental principles, so in many aspects nothing differs between diatomics and larger systems. As a practical matter, the spectra of polyatomics are much more complicated than diatomics. Polyatomics often have a richer and more varied set of excited states than diatomics. Diatomics are simpler because the symmetry of a bound excited state of a diatomic molecule is necessarily the same as the ground state. However, the excited states of polyatomics often have a different symmetry than the ground state.[1] For example, the LUMO←HOMO transition in CO_2, Figure 26.6.8, corresponds to $(1\pi_g^o)^3(2\pi_u^*)^1 \leftarrow (1\pi_g^o)^4$, assuming a linear excited state. However, the excited state is bent so that the experimentally observed transition is: $(4b_2^o)^1(1a_2^o)^2(6a_1^o)^1 \leftarrow (1\pi_g^o)^4$. The 340 to 260 nm band of SO_2, Figure 28.1.1, also shows a change in symmetry.[1] Ground state formaldehyde is planar, but some formaldehyde excited states are pyramidal. Another reason that polyatomics have a more varied set of excited states is that Rydberg states are numerous.

Some generalizations can be made.[11,12] Transitions can be classified by the molecular orbitals involved, as we did for SO_2 in Sec. 28.1. Typical regions of electronic transitions of non-conjugated small organics are given in Figure 28.3.1. Conjugation moves transitions to longer wave length.

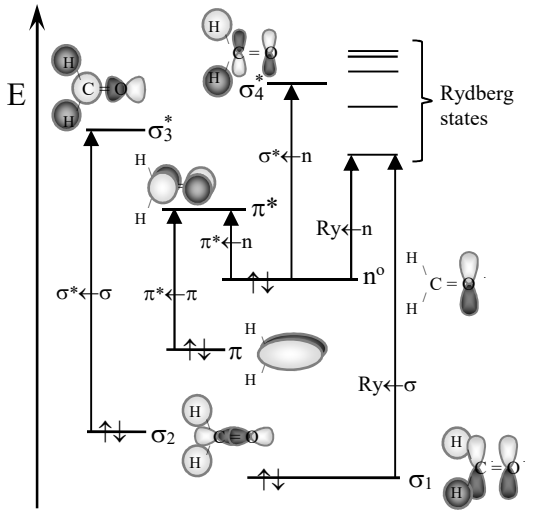

Transition	Example	λ_{max} (nm)	ε_{max} (M^{-1} cm^{-1})
$\sigma^*\leftarrow\sigma$	C-H	160	10^2-10^3/ 10^3-10^5
$\sigma^*\leftarrow$n	C-Cl, C-OH	180	10^2-10^3/ 10^3-10^5
$\pi^*\leftarrow\pi$	C=C, C=O	180	10^2-10^3/ 10^3-10^5
$\pi^*\leftarrow$n	C=O, C-Cl	300	10-100/ 100-10^3

Figure 28.3.1: Typical transitions in non-conjugated small organics. The MO diagram for formaldehyde is given as an example. Molar absorption coefficients, ε_{max}, are given in two ranges: for formally forbidden and allowed transitions. Ry←σ and Ry←n Rydberg transitions are often as intense as transitions among the valence MOs, ($f \cong 1$).

Transitions of various kinds often overlap and dissociation continua are common, making spectral assignments difficult. The complexities of polyatomic spectra require a change in perspective in the way that we think about transitions.

A Continuous Distribution of Quantum States is Characterized by the Density of States: As a result of the extra vibrational degrees of freedom for polyatomics and the three rotational degrees of freedom for non-linear molecules, the observation of well-resolved vibrational and rotational fine-structure is much less common than for diatomics. Transitions in polyatomics often overlap

due to "spectral congestion." In addition, transition line widths are usually much broader in polyatomics, due to many more possibilities for non-radiative processes, such as predissocation.[9]

The number of normal modes of a non-linear molecule is 3N – 6, which is a rapidly increasing function of the number of atoms. Even triatomics take on the characteristics of "large" systems. Bent triatomics have three normal modes. The vibrational energy level diagram for SO_2 is given in Figure 28.3.2, with the vibrational mode quantum numbers listed in the order: (symmetric stretch, bend, asymmetric stretch), (υ_1, υ_2, υ_3). Notice that the number of states per unit interval in wave number increases with energy. In other words, as energy increases, more (υ_1, υ_2, υ_3) combinations are degenerate or nearly degenerate. Figure 28.3.2 considers vibrational energy only. Remember that vibrational manifolds of this type are superimposed on the ground and each excited electronic state. Spectroscopic transitions to or from these levels become quite numerous. Figure 28.1.1 shows that transitions to low lying vibrational levels of the excited state for SO_2 are well resolved, but spectral congestion for transitions to more highly excited vibrational levels overlap sufficiently that the spectrum takes on a smooth continuous appearance.

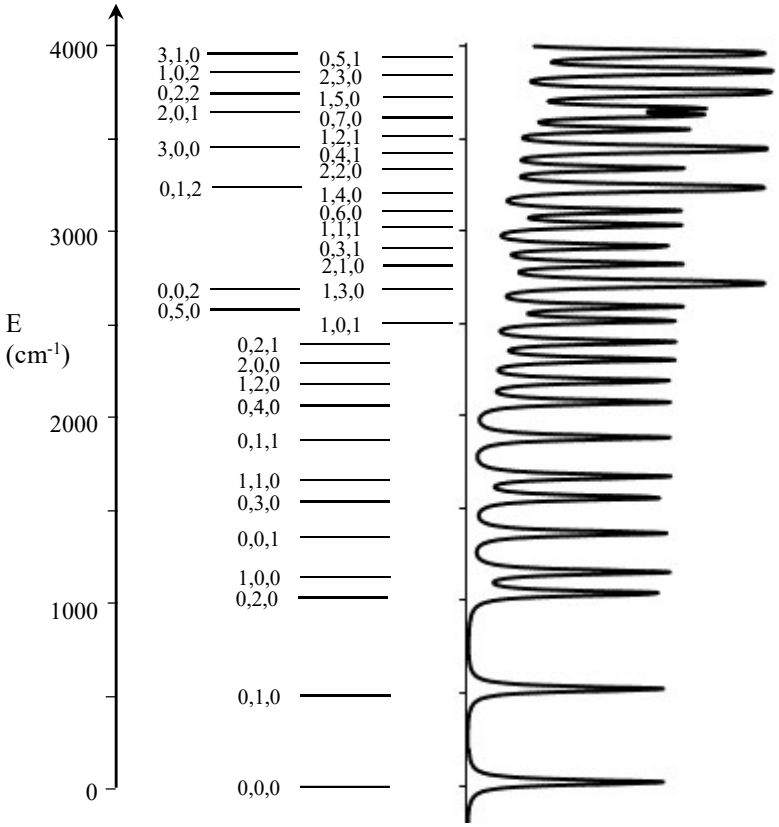

Figure 28.3.2: SO_2 vibrational energy levels. The tracing shows the energy levels as broadened by collisions. The quantum numbers are in the order: symmetric stretch, bend, and asymmetric stretch with fundamentals 1151 cm^{-1}, 518 cm^{-1}, and 1362 cm^{-1}, respectively.

The width of each transition is increased by lifetime broadening. The effect of collisional broadening for gas phase spectra is simulated for the SO_2 energy level diagram, Figure 28.3.2 at right. In condensed media, collisional broadening is sufficient to obscure most all vibrational

fine-structure. For large numbers of normal modes, highly excited vibrational levels, and collisional broadening, the vibrational levels become essentially a continuum of levels. In other words, the spacing between the levels is << kT so that electronic transitions involving the continuous band of states are a smooth continuous distribution. Beyond obscuring fine-structure, vibrational continua also have important effects on non-radiative energy transfer processes and chemical reactions, Sections 28.4, 28.6, and 32.5.

The number of quantum states per unit interval in energy or wave number is called the **density of states**. For a simple illustrative example, consider electronic transitions in a diatomic molecule for a continuum of highly excited vibrational levels of an excited electronic state. For continuous ranges of energy levels, summations can be replaced by integrals. Narrow regions of the spectrum of such a continuous band of states cover many different vibrational fine-structure transitions. The total integrated intensity of transitions in a spectrum from vibrational quantum number υ'_1 to υ'_2 is proportional to the integral over the corresponding transition dipole moments:

$$I \propto \int_{\upsilon'_1}^{\upsilon'_2} \mu_{tr}\, d\upsilon \qquad 28.3.1$$

However, spectra are recorded as a function of energy and not quantum number. A change in variables is required in the last equation to integrate over the transition energy and not the quantum number:

$$I \propto \int_{\varepsilon_1}^{\varepsilon_2} \mu_{tr} \left(\frac{d\upsilon}{d\varepsilon}\right) d\varepsilon \qquad 28.3.2$$

where υ'_1 and υ'_2 correspond to energies ε_1 and ε_2, respectively. The change in variables requires the derivative $(d\upsilon/d\varepsilon)$, which is defined as the density of states, $\rho(\varepsilon)$:

$$\rho(\varepsilon) \equiv \frac{d\upsilon}{d\varepsilon} \qquad \text{with} \qquad I \propto \int_{\varepsilon_1}^{\varepsilon_2} \mu_{tr}\, \rho(\varepsilon)\, d\varepsilon \qquad 28.3.3$$

The density of states converts from a given energy, ε, to the number of quantum states near that energy. The density of states in wave numbers for a harmonic oscillator with frequency $\tilde{\nu}_o$ is evaluated from the harmonic oscillator energy, $\tilde{\varepsilon}_\upsilon = \tilde{\nu}_o\,(\upsilon + ½)$, as:

$$\rho(\tilde{\varepsilon}_\upsilon) = \left(\frac{d\upsilon}{d\tilde{\varepsilon}_\upsilon}\right) = \left(\frac{d\tilde{\varepsilon}_\upsilon}{d\upsilon}\right)^{-1} = \left(\frac{d[\tilde{\nu}_o(\upsilon + ½)]}{d\upsilon}\right)^{-1} = \left(\tilde{\nu}_o\right)^{-1} = \frac{1}{\tilde{\nu}_o} \qquad \text{(harmonic oscillator)} \quad 28.3.4$$

In other words, there is one vibrational state every $\tilde{\nu}_o$ cm^{-1}. As an example of the application of the density of states, the integral $\int_{\varepsilon_1}^{\varepsilon_2} \rho(\varepsilon)\, d\varepsilon$ counts the number of states in the energy range from ε_1 to ε_2. The density of states is a fundamental construct that we will use repeatedly in many different chemically useful circumstances. The large density of states for vibrations of polyatomic molecules gives significant spectral crowding in electronic spectra.

Aromatics in condensed media are an intermediate case. The spectrum of benzene in ethanol shows some vibrational fine-structure, which is assigned to a symmetric ring-breathing C-C stretch, but vibrational-fine structure for other modes in benzene is obscured by spectral crowding, Figure 28.1.12a. Usually no vibrational fine-structure is observed in condensed media. Aromatics are unique in other ways. Many aromatic molecules fluoresce or phosphoresce. At this point we turn our attention to molecular emission spectroscopy.

28.4 Fluorescence and Phosphorescence

Where-Oh-Where Has My Energy Gone? What is the fate of the electronic excited state? Spontaneous emission from an excited state results in fluorescence or phosphorescence, Section 2.4. Fluorescence transitions occur between states with the same spin multiplicity, while phosphoresce occurs between states with differing multiplicity. For example, since the vast majority of molecules have singlet ground states, spin-allowed absorption produces excited singlet states, Figure 28.4.1. Fluorescence from a singlet excited state back to the singlet ground state conserves spin multiplicity and usually occurs with a short lifetime, ~5 ns - 10 us. Phosphorescence from a triplet excited state back to the singlet ground state is spin forbidden and therefore usually occurs with millisecond or longer lifetimes. The formation of the triplet state from an excited singlet state requires an electron spin flip, which is again spin forbidden. The non-radiative process of conversion of a state with one spin multiplicity into another spin multiplicity is called **intersystem crossing**, ISC. Intersystem crossing is mediated by spin-orbit coupling, which mixes singlet and triplet electronic state character. Most molecules have ground singlet states; intersystem crossing correspondingly converts the lowest energy excited singlet state to an excited triplet state, from which phosphorescence can occur. Heavy atoms increase spin-orbit coupling and hence intersystem crossing.

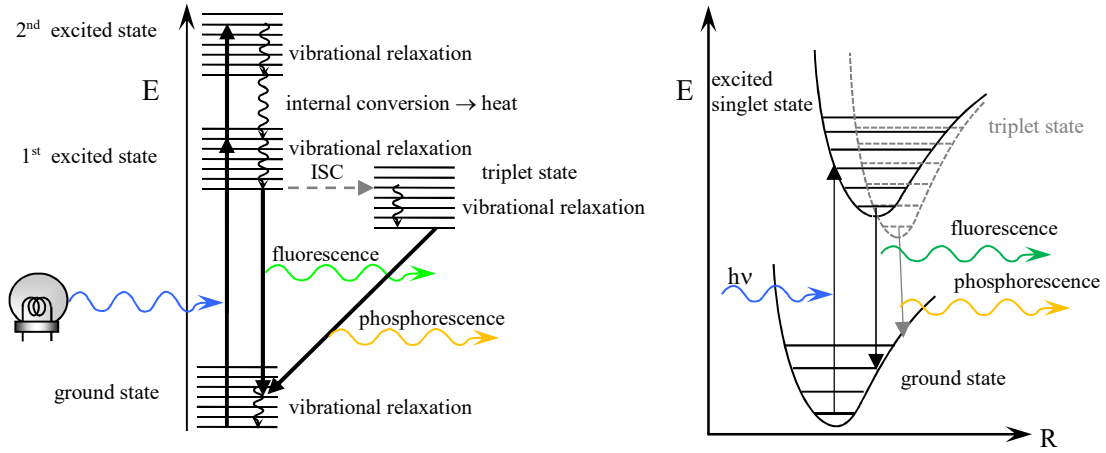

(a). Jablonski diagram (b). Potential energy surfaces

Figure 28.4.1: (a). Jablonski diagram for fluorescence and phosphorescence beginning from a singlet ground state. Intersystem crossing, ISC, converts the first-excited singlet state into a triplet state. (b). The potential energy curve for the triplet state is shown in dotted gray to make the excited singlet and triplet states easier to distinguish.

Fluorescence and phosphorescence are rare. Rather, most molecules lose the excess energy of the excited state by **non-radiative** processes, returning to the ground state without emission of light. Non-radiative processes include internal conversion, intersystem crossing, chemical reactions, and intermolecular energy transfer. In **internal conversion**, an excited state is converted into a highly excited vibrational level of a lower energy electronic state. In intersystem crossing, the energy of the excited sate is transferred to a state of different spin multiplicity. In chemical reactions, the excited state energy is lost through bond breaking and making processes. In

intermolecular energy transfer, the energy of the excited state is transferred to another molecule. Internal conversion, intersystem crossing, excited state chemical reactions, and intermolecular energy transfer compete with fluorescence. Fluorescence usually loses.

The properties of fluorescence and phosphorescence spectra of organic molecules in condensed media are summarized by:

1. Kasha's Rule: fluorescence always originates from the first excited state.
2. Fluorescence is redder than the corresponding absorption spectrum.
3. Phosphorescence is redder than the corresponding fluorescence.

Rule 1: If absorption is to the second or higher excited states, internal conversion rapidly degrades the excess energy leaving the molecule in the first, lowest energy excited state with the same multiplicity. In other words, starting from a singlet ground state, no matter how blue the excitation, fluorescence always originates from the lowest excited singlet state. Phosphorescence occurs from the lowest excited triplet state. Conversely, starting from a triplet ground state, fluorescence originates from the lowest energy excited triplet and phosphorescence from the lowest energy excited singlet. Given a set of singlets of increasing energy, S_o, S_1, S_2…. and triplets of increasing energy T_1, T_2…. internal conversion gives $S_2 \rightarrow S_1$ and $T_2 \rightarrow T_1$. Internal conversion from the first excited state, $S_1 \rightarrow S_o$, diminishes fluorescence and internal conversion from the first triplet state, $T_1 \rightarrow S_o$, diminishes phosphorescence. Kasha's Rule is sometimes violated. In fluorescence $S_2 \rightarrow S_o$ and $T_2 \rightarrow T_o$ occur. One cause is a large energy gap between S_2 and S_1, so that $S_2 \rightarrow S_1$ internal conversion is slow while $S_1 \rightarrow S_o$ internal conversion is fast.

Rule 2: After direct absorption or internal conversion into the first excited state, excess vibrational energy is degraded by **vibrational relaxation** leaving the molecule in the lowest vibrational level of the first excited state. Vibrational relaxation is caused by collisions, which result in the transfer of heat to the surroundings. Starting from a singlet ground state, no matter how blue the excitation, fluorescence always originates from the $\upsilon' = 0$ vibrational level of the lowest excited singlet state. For phosphorescence, after intersystem crossing vibrational relaxation also rapidly converts the molecule into the $\upsilon' = 0$ vibrational level. Phosphorescence occurs from the $\upsilon' = 0$ vibrational level of the lowest excited triplet state. In summary, fluorescence is a multi-step process; for example assuming a ground singlet state and excitation into the second excited singlet state:

$$\underset{}{S_o + h\nu \rightarrow} \underset{\textit{absorption}}{S_2(\upsilon' \geq 0)} \underset{}{\rightarrow} \underset{\textit{internal conversion}}{S_1(\upsilon' \geq 0)} \underset{}{\rightarrow} \underset{\textit{vibrational relaxation}}{S_1(\upsilon'=0)} \underset{}{\rightarrow} \underset{\textit{fluorescence}}{S_o(\upsilon'' \geq 0) + h\nu} \quad (2.4.10)\ 28.4.1$$

Phosphorescence is a multistep process; for example assuming a ground singlet state and excitation into the second excited singlet state:

$$\underset{}{S_o + h\nu \rightarrow} \underset{\textit{absorption}}{S_2(\upsilon' \geq 0)} \underset{}{\rightarrow} \underset{\textit{internal conversion}}{S_1(\upsilon' \geq 0)} \underset{}{\rightarrow} \underset{\textit{intersystem crossing}}{T_1((\upsilon' \geq 0)} \underset{}{\rightarrow} \underset{\textit{vibrational relaxation}}{T_1(\upsilon'=0)} \underset{}{\rightarrow} \underset{\textit{phosphorescence}}{S_o(\upsilon'' \geq 0) + h\nu} \quad 28.4.2$$

Absorption usually occurs from the $\upsilon'' = 0$ vibrational level of the ground state and ends in the υ' state of the excited state: $\upsilon' \leftarrow \upsilon'' = \upsilon' \leftarrow 0$, Figure 28.4.1b. Fluorescence occurs from the $\upsilon' = 0$ vibrational level of the excited state and ends in the υ'' state of the ground state: $0 \rightarrow \upsilon''$. The lowest energy, reddest, absorption is $0 \leftarrow 0$. The largest energy, bluest fluorescence is $0 \rightarrow 0$. The $0 \leftarrow 0$ and $0 \rightarrow 0$ absorption and fluorescence transitions are at the same wavelength, and so

overlap. More likely however, absorption is to an excited vibrational level of the excited state, υ' > 0, and fluorescence is more likely to an excited vibrational level of the ground state, υ" > 0. Accordingly, the most likely absorption transitions are bluer than 0←0 and the most likely emission transitions are redder than 0→0. The most likely transitions are determined by Franck-Condon factors.

Rule 3: Given the same electron configuration, a triplet state has a lower energy than the corresponding singlet state. The lower energy of the triplet results from decreased electron-electron repulsion through quantum mechanical avoidance, as summarized by Hund's First Rule. As a result, the triplet state to ground state transitions are at lower energy, redder, than the corresponding singlet state, for the same υ' → υ".

In molecules with heavy atoms, spin-orbit coupling blurs the distinction between singlet and triplet, fluorescence and phosphorescence. Taken together, fluorescence and phosphorescence is then termed luminescence. All forms of luminescence spectroscopy play an important role in analytical chemistry. The advantage in analytical determinations is the specificity allowed because both the absorption and emission frequencies can be tailored to a particular analyte. In gas phase species, the use of lasers as excitation sources in **laser induced fluorescence**, LIF, allows specific vibrational and rotational levels to be excited. LIF is a key technique in monitoring reactive atmospheric contaminants. In condensed media, LIF is also a key technique in single molecule biomolecular microscopy. One additional advantage of fluorescence and phosphorescence is that spectroscopic constants for the ground state of the molecule can be determined if vibrational fine-structure is resolved.

The Franck–Condon Principle Predicts the Intensity of Vibrational Transitions: The intensity profile of both υ'← 0 absorption and 0→ υ" fluorescence transitions is predicted using Franck-Condon factors. Remember that in absorption spectroscopy the intersection of a vertical transition from the initial state with the potential energy curve of the final state is a rough prediction of the highest intensity vibrational transition. The same principle applies to fluorescence emission, taking into account that the vertical transition begins in the middle of the potential well of the first excited state, Figure 28.4.2. In emission, the typical increase in equilibrium bond length between the ground state and excited state gives vertical transitions that peak for excited vibrational levels within the ground electronic state. The result is that absorbance and fluorescence spectra appear roughly as mirror images with overlap only for the 0←0 and 0→0 transitions. The vibrational spacing in absorbance is for the excited state and the vibrational spacing in fluorescence is for the ground state. The availability of the ground state spectroscopic constants in fluorescence is particularly useful for molecules that are electric-dipole forbidden in infrared and microwave absorption. Luminescence is also useful for studies of reactive species, such as unstable ions, which are difficult to study in absorption.

Fluorescence and Phosphorescence Lifetime Measurements: Fluorescence and phosphorescence emission are first-order kinetic processes. The kinetics of emission are discussed in Section 5.1. The rate constants for fluorescence, intersystem crossing, non-radiative processes, photochemical reactions, and quenching are related to the fluorescence quantum yield and lifetime using Eqs. 5.1.27-5.1.33. The non-radiative term is often dominated by internal conversion. In solutions that contain two different photoactive molecules, the energy of the primary photoexcited state can be lost by transfer to another molecule. These **intermolecular energy transfer** processes compete with fluorescence and phosphorescence and can alternately be included in the non-radiative kinetic term or as a particular type of quenching.

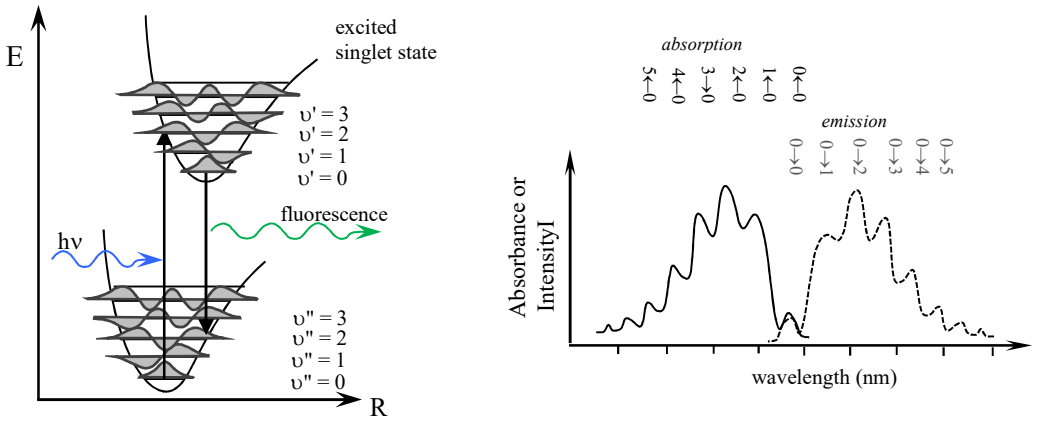

Figure 28.4.2: Franck-Condon factors determine the intensity of vibrational fine-structure transitions in absorbance and emission. Only the 0←0 and 0→0 transitions overlap.

Electronic Energy Transfer: The general form of electronic energy transfer between the primary electronically excited donor, D^{ex}, and a ground state acceptor, A, is:

$$D^{ex} + A \xrightarrow{k_{DA}} D + A^{ex} \qquad 28.4.3$$

In general, the lowest energy vibrational level of the acceptor must be less than the lowest energy vibrational level of the donor, $E_{oA} < E_{oD}$. After energy transfer, the acceptor can fluoresce or phosphoresce. However, internal conversion can spoil the party by converting the acceptor excited state to the ground state without emission of a photon. The experimental consequence of energy transfer is that the absorption spectrum of the mixture is characteristic of the donor while the emission spectrum is characteristic of the acceptor. The mechanism of intermolecular energy transfer is primarily characterized by the distance between the donor and acceptor. For donor-acceptor distances greater than the wavelength of light, $\gtrsim$ 500 nm, energy transfer is radiative. The excited donor emits a photon and the acceptor absorbs the photon. The rate of radiative intermolecular transfer is proportional to the degree of overlap of the fluorescence emission spectrum of the donor, $F_D(\tilde{\nu})$, and the absorption spectrum of the acceptor, $\varepsilon_A(\tilde{\nu})$, Figure 28.4.3:[13]

$$k_{DA} \propto \int_o^\infty F_D(\tilde{\nu})\, \varepsilon_A(\tilde{\nu})\, d\tilde{\nu} \qquad 28.4.4$$

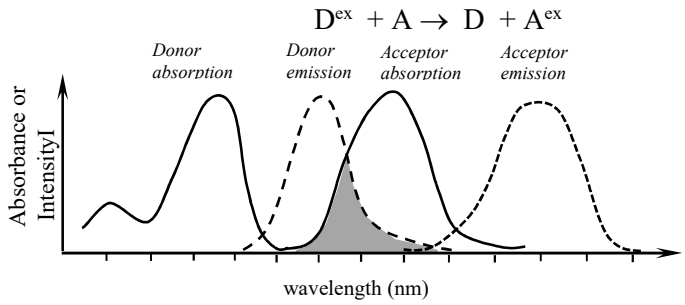

Figure 28.4.3: Intermolecular energy transfer is proportional to the overlap, in gray, between the fluorescence emission of the donor with the absorption spectrum of the acceptor.

Simply, the acceptor must be able to absorb at the same wave number that the donor emits. For donor-acceptor distances less than the wavelength of light, energy transfer is non-radiative. The Coulomb interaction between the transition dipole moments of the donor and acceptor mediates the energy transfer. The excited state donor and ground state acceptor transitions must be isoenergetic to allow the energy transfer to have a significant rate. For short distances, $\lesssim 1$ nm, direct overlap of the donor and acceptor molecular orbitals results in energy transfer mediated by the exchange interaction. In dilute solution, intermolecular energy transfer through the Coulomb interaction is most applicable and is the basis of commonly used biochemical assays.

Förster Resonance Energy Transfer Can Determine Distances, FRET: For distances less than the wavelength of light, **Förster Resonance Energy Transfer**, **FRET**, is the mechanism of intermolecular energy transfer that is mediated by weak Coulomb interactions. FRET is often used as a "molecular ruler." The fluorescence intensity of the acceptor is proportional to the rate of intermolecular energy transfer, k'_{DA}, which is a sensitive measure of the distance between the donor and acceptor:[13]

$$k'_{DA} = \frac{1}{\tau_D}\left(\frac{R_o}{r}\right)^6 \qquad 28.4.5$$

where τ_D is the fluorescence lifetime of the donor in the absence of the acceptor, r is the distance between the donor and acceptor, and R_o is the **critical transfer distance**. The critical transfer distance is the distance for which the rate of intermolecular energy transfer is equal to the rate of donor deactivation by fluorescence and internal conversion, $k'_{DA} = k_f + k_{nr}$. R_o is related to the extent of overlap of the fluorescence emission spectrum of the donor and the absorption spectrum of the acceptor:[13]

$$R_o^6 = \frac{(9000 \ln 10)\kappa^2}{128\pi^5 n^4 N_A}\int_o^\infty \frac{F_D(\tilde{\nu})\,\varepsilon_A(\tilde{\nu})}{\tilde{\nu}^4}\,d\tilde{\nu} \qquad 28.4.6$$

where n is the index of refraction of the solvent, N_A is Avogadro's number, and κ is an orientation factor. In solution for rapidly tumbling donor and acceptor, the orientation average gives $\langle\kappa^2\rangle = {}^2/_3$. For example, 8-anilinonaphthalene-1-sulfonic acid, ANS, is a commonly used fluorescent dye in biochemical studies. R_o for tryptophan and ANS is 2.3 nm. The small value of R_o and the r^6 distance dependence makes FRET a useful molecular ruler for dimensions on the order of the sizes of proteins and oligonucleotides. In viscous solution, FRET follows Stern-Volmer kinetics for the donor fluorescence, Eqs. 5.1.26-5.1.28 with $k_q = k'_{DA}$. In Section 28.6 we discuss in greater detail the fundamental interactions that underlie the Förster mechanism.

We have now characterized absorption of energy from light and the subsequent fate of the excited electronic state, through radiative and non-radiative processes. To this point we have considered the case of light absorption that results in an excited state of the molecule. If the excitation is in the far ultraviolet or vacuum ultraviolet, $\lambda < 190$ nm, absorption may also produce a molecular ion. The resulting process is photoionization.

28.5 Photoelectron Spectroscopy

Absorption of light of sufficient energy may produce a molecular ion. In photoionization, an electron is removed from the molecule:

$$A + h\nu \rightarrow A^+(\upsilon') + e^- \qquad \upsilon' = 0, 1, 2, 3, \ldots\ldots \qquad 28.5.1$$

The resulting ion may be produced in the ground vibrational level, $\upsilon' = 0$, or an excited vibrational level, $\upsilon' > 0$. The molecular ion can be produced in the ground electronic state or an excited electronic state. Photoionization is an energetic process that usually requires excitation in the vacuum UV. A common light source for photoionization studies is a helium discharge lamp, which provides a fixed excitation energy of 21.22 eV, $\lambda = 58.4$ nm. Electrons in molecular orbitals with energy higher than -21.22 eV are ionized using a helium discharge lamp. In **photoelectron spectroscopy, PES**, the kinetic energy distribution of the ejected photoelectrons is determined. With excitation in the UV, the technique is often called **Ultraviolet Photoelectron Spectroscopy**, **UPS**. Samples can be solid, low vapor pressure liquid, or gas. UPS studies of surface absorbed species allow the characterization of the perturbation by the surface upon the electronic structure of the absorbed molecule. Low pressure gas samples allow the determination of vibrational fine-structure. The photoionization process is governed by the Einstein photoelectric effect equation, Eq. 23.2.4. However, the work function of the metal is replaced by the gas phase ionization energy of the molecule with the production of the molecular ion in vibrational level υ', $I_1(\upsilon')$. Energy in excess of the ionization energy is released as kinetic energy of the photoelectron, E_k:

$$E = h\nu = E_k + I_1(\upsilon') = \tfrac{1}{2} m_e v^2 + I_1(\upsilon') \qquad \upsilon' = 0, 1, 2, 3, \ldots\ldots \qquad 28.5.2$$

fixed

where ν is the exciting light frequency, m_e is the mass of an electron and v is the velocity of the electron. A UPS spectrum is a plot of electron current or ion `count rate as a function of electron kinetic energy, Figure 28.5.1. The ionization energy is determined by difference, $I_1(\upsilon') = h\nu - E_k$. The horizontal axis of a photoelectron spectrum is often plotted with electron kinetic energy increasing to the right and the corresponding ionization potential increasing to the left.

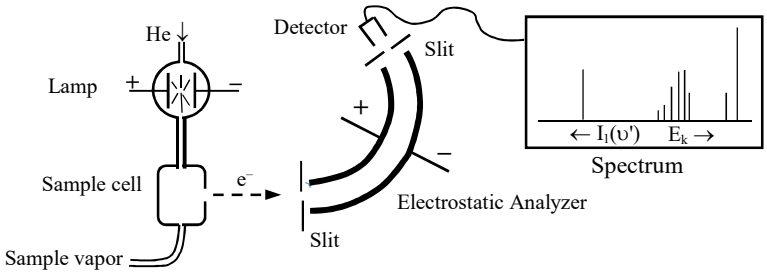

Figure 28.5.1: A photoelectron spectrometer determines the kinetic energy distribution of the emitted electrons. The entire spectrometer is under vacuum. To maintain high vacuum, the excitation light and sample vapor are introduced into the sample cell through capillaries.

The UPS spectrum of H_2 at 21.22 eV produces the ground state of the H_2^+ ion, Figure 28.5.2. The peaks correspond to vibrational fine-structure; the lowest ionization energy peak is the $0 \leftarrow 0$ transition:

$$H_2\,(^1\Sigma_g^+, \upsilon''= 0) + h\nu \rightarrow H_2^+\,(^2\Sigma_g^+, \upsilon') + e^- \qquad \upsilon' = 0, 1, 2, 3, \ldots\ldots \qquad 28.5.3$$

The full vibrational progression that ends in a dissociation continuum is observed.[14] The first vibrational spacing is $\tilde{\nu}_o$ for the molecular ion at 2189 cm^{-1}, which is much less than neutral H_2 at 4158.5 cm^{-1}. In other words, the bond in H_2^+ is much weaker than in neutral H_2, as predicted by the qualitative molecular orbital bond order of ½ and one respectively. The energy difference

between the convergence limit and the 0 ← 0 transition is the dissociation energy of the H_2^+ ion. The dissociation energy of H_2^+ is important in the development of molecular orbital theory, Table 26.2.1. The convergence limit is at 18.07 eV and the 0 ← 0 transition is at 15.43 eV, giving the dissociation energy of the molecular ion as D_o^{ion} = 18.07 eV – 15.43 eV = 2.64 eV.

The intensity of the vibrational fine-structure lines is predicted using Franck-Condon factors. The vertical transitions end in an intersection with the potential energy curve of the molecular ion. For H_2^+ a large change in equilibrium bond length between the ground state of the molecule and the molecular ion produces a long vibrational progression, terminating in a dissociation continuum, Figures 28.2.3-28.2.4.

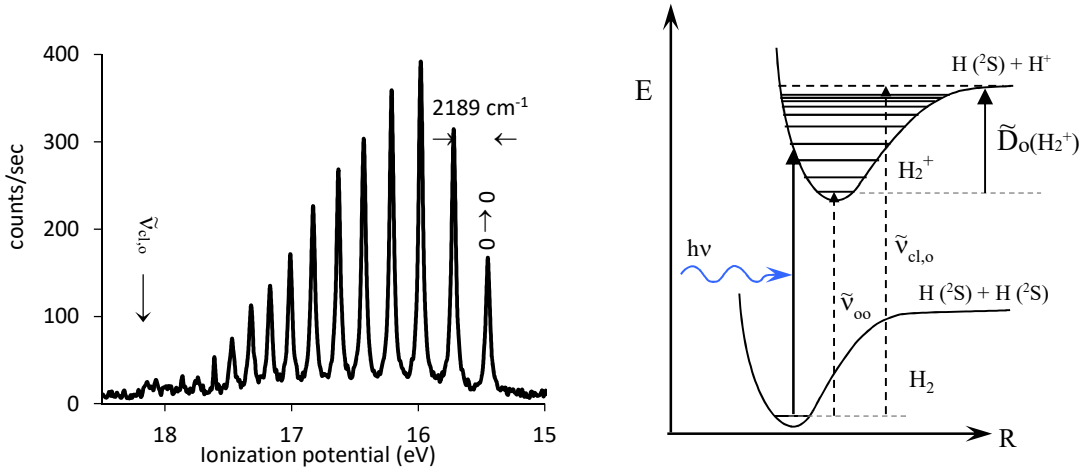

Figure 28.5.2: UPS of H_2 excited at 21.22 eV. The convergence limit for the H_2^+ molecular ion is 18.07 eV.[14] The fundamental vibration frequency of H_2 is 4158.5 cm^{-1}.

Photoelectron Spectroscopy Estimates Molecular Orbital Energies: The UPS spectrum of N_2 shows three transitions with vibrational fine-structure that correspond to the removal of an electron from three different molecular orbitals of the neutral molecule, Figure 28.5.3. Subject to several approximations, the ionization potentials at the 0 ← 0 transitions are direct experimental measures of the energies of the molecular orbitals from which the electrons are ionized. These approximations are that the orbital approximation is valid, the molecule does not change shape upon ionization, and the correlation energies of the ground state molecule and the molecular ion are similar. These approximations, called **Koopmans' Theorem**, are valid to ~1-3 eV. Under Koopmans' Theorem, UPS ionization potentials are comparable to Hartree-Fock molecular orbital calculations, which do not account for correlation energies. For example, consider the ionization process labeled b, Figure 28.5.3, which is the ionization of a $\pi_u(2p)$ electron:

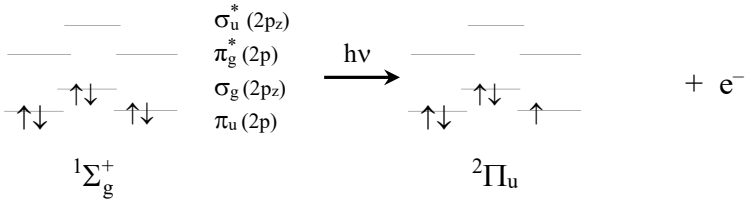

28.5.4

The $\pi_u(2p)$ molecular orbital energy is the equal to the negative of the ionization energy, assuming that the molecular orbital energies are unchanged in the molecular ion. The lack of

change in molecular orbital energies is called the **frozen orbital approximation**. In reality, the molecular orbitals do change, or relax, as the molecule adjusts to the loss of one electron. The correlation energy in the molecular ion is changed relative to the neutral molecule because there are fewer electrons in the ion. If Koopmans' Theorem is not valid, the UPS ionization energies are not equal to the molecular orbital energies. Correlation of the experimental ionization energies with careful CI calculations is then necessary to infer molecular orbital energies.

We are now ready to ask an important question: what is the molecular orbital ordering in neutral N_2? Careful molecular orbital calculations place the $\sigma_g(2p_z)$-orbital above the doubly degenerate $\pi_u(2p)$-orbitals, Figures 26.4.8-26.4.11.

In N_2 and CO, $\sigma_g(2p_z)$ is above $\pi_u(2p)$: The assignment of the transitions to specific molecular orbitals is based primarily on the vibrational fine-structure. In Figure 28.5.3, the a-transition shows only three peaks. This short vibrational progression corresponds to a small change in equilibrium bond length. This observation is consistent with ionization from the $\sigma_g(2p_z)$-orbital, which is close in energy to the separated atom atomic–2p orbitals. The $\sigma_g(2p_z)$ is weakly bonding. On the other hand, the b-transition has a long vibrational progression, which results from a large change in equilibrium bond length. This observation is consistent with the π_u (2p) orbital, which is more strongly bonding than the $\sigma_g(2p_z)$. Removing a $\pi_u(2p)$ electron makes a big change in bond strength.

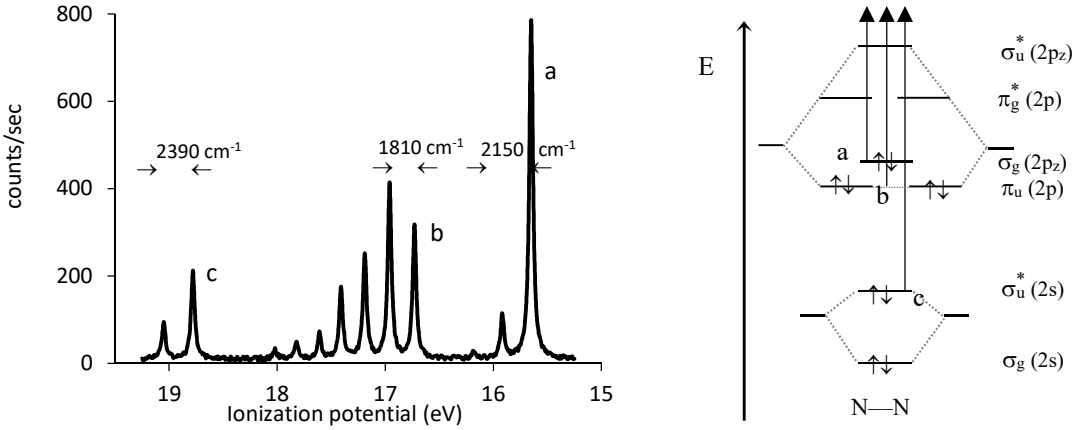

(a). N_2 UPS (b). N_2 molecular orbital transitions

Figure 28.5.3: (a). Photoelectron spectrum of N_2 gas excited at 21.22 eV.[14-16] (b). Corresponding molecular orbital ionization processes. The HOMO requires the smallest energy for ionization, process a, giving the smallest ionization potential.

Finally, the c-transition has a short vibrational progression, which is consistent with the removal of a σ_u^*-anti-bonding electron. The removal of an anti-bonding electron strengthens the bond giving a shorter equilibrium bond length for the ion compared to the neutral molecule. These assignments can be verified by observing the vibrational spacing of each transition. The fundamental stretch of neutral N_2 is at 2345 cm^{-1}. The a-transition is at 2150 cm^{-1}, corresponding to a slightly weaker bond for the ion than the neutral N_2. The a-transition ionizes a weakly bonding electron from $\sigma_g(2p_z)$. The b-transition is at 1810 cm^{-1}, corresponding to a much weaker bond for the ion than the neutral molecule. The b-transition ionizes a strongly bonding electron

from the $\pi_u(2p)$-bonding orbital. The c-transition is at 2390 cm^{-1}, corresponding to a stronger bond for the ion than the ground state. The c-transition ionizes an anti-bonding electron from the $\sigma_u^*(2p_z)$, strengthening the bond. These results validate the molecular orbital treatment of homonuclear diatomic molecules. We can now extend these studies to heteronuclear diatomics. The orbital ordering for heteronuclear diatomics can be tricky to predict.

The UPS spectrum of CO shows a similar pattern as that for N_2, Figure 28.5.4a. The fundamental vibration frequency for neutral CO is 2170 cm^{-1}. The lowest ionization energy bands has a slightly smaller fundamental vibration frequency than the neutral molecule and a short vibrational progression, indicating removal of a weakly bonding electron. The evidence is consistent with ionization of the $\sigma_g(2p_z)$-orbital. The band with the origin at 16.54 eV is more strongly bonding as evidenced by the small fundamental vibration frequency and the long vibrational progression, consistent with the doubly degenerate $\pi_u(2p)$-orbital being at lower energy.

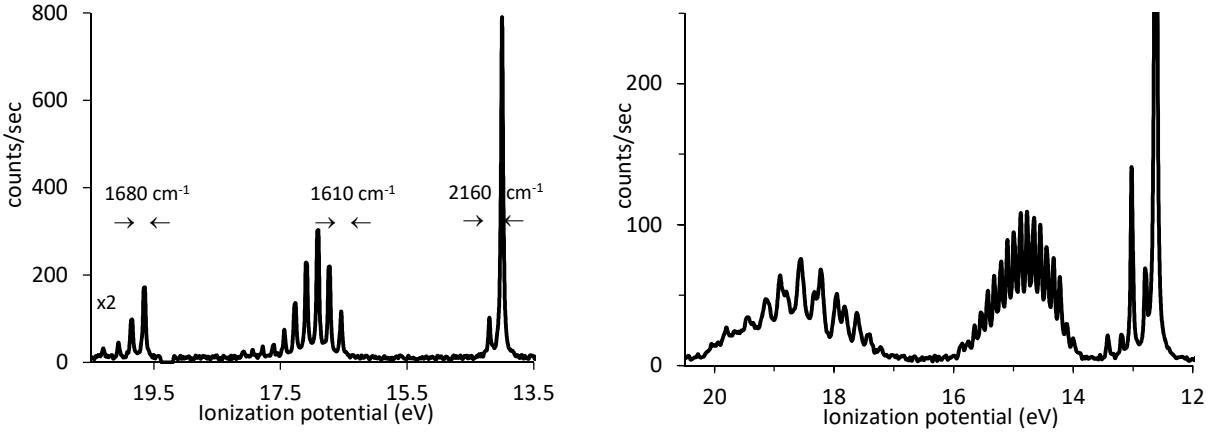

(a). CO (b). H_2O

Figure 28.5.4: Gas phase photoelectron spectra at 21.22 eV (a). CO.[15] (b). H_2O, the first transition at 12.62 eV is truncated to allow an expanded vertical scale.[17,18]

UPS is routinely applied to polyatomic molecules. The spectrum of H_2O shows three vibrational bands, Figure 28.5.4b. The lowest ionization energy band has a short vibrational progression with fine-structure lines that give the asymmetric stretch in the molecular ion at 3220 cm^{-1} and the bending vibration at 1370 cm^{-1}. The corresponding frequencies in neutral H_2O are 3756 cm^{-1} and 1595 cm^{-1}. The small changes are consistent with ionization of a non-bonding orbital, which has little effect on the bond strengths. Figures 26.6.4 and 26.6.6 place the HOMO as the $^1b_1$ non-bonding atomic 2p-orbital. This agreement validates the molecular orbital perspective. The UPS band starting at 14 eV shows a long vibrational progression and a vibrational spacing consistent with a bending vibration at 887 cm^{-1}. The large decrease from the bending fundamental in neutral H_2O suggests that ionization of this orbital has a large influence on the bond strength. The $2a_1$ molecular orbital is a strongly bonding σ-orbital. The H-atom 1s-orbitals in $2a_1$ have the same phase, suggesting that the orbital may have a large effect on the equilibrium bond angle.[1] Ionization of an electron in $2a_1$ decreases the influence of the orbital that favors bending, Figure 26.6.4. Careful CI electronic structure calculations give the molecular ion that forms from the loss of a $2a_1$ electron as almost linear. These observations validate the

molecular orbital diagram in Figure 26.6.4. The third band, starting at 17 eV shows both stretching and bending vibrational fine-structure with stretching frequency 2990 cm^{-1} and bending vibration 1610 cm^{-1}. The change in stretching frequency is consistent with the strong σ-bonding character of the $1b_2$ molecular orbital. The small increase in the bending fundamental is consistent with the angle dependence in the Walsh diagram, which is dependent on the opposite phases of the H-atom 1s-orbitals in $^1b_2$. In the analysis of the H_2O spectrum, we see an example of a continuing theme. The analytical power of spectroscopy is magnified by comparisons to careful electronic structure calculations; the two go hand-in-hand. Spectroscopy determines molecular structure. Spectroscopy is also a critical tool in determining the flow of energy in chemical systems.

28.6 Fermi's Golden Rule and Non-radiative Energy Transfer

Most molecules don't fluoresce, and even fewer show phosphorescence. As a result we can conclude that internal conversion is typically quite efficient. Why is that so? Our understanding of internal conversion is based on Fermi's Golden Rule.[19-21]

Energy Transfer is Proportional to the Density of States: The transfer of energy between two states is most probable for states with the same energy. The probability of energy transfer decreases rapidly with increasing energy mismatch. In systems with closely spaced energy levels, the probability of energy transfer is proportional to the density of states that match the required energy. Internal conversion and intersystem crossing are good examples. After absorption of light, internal conversion between the first excited state and the ground state competes with fluorescence emission. Internal conversion, IC, results in transfer of the excited state energy into highly excited vibrational levels of the ground state, Figure 28.6.1.

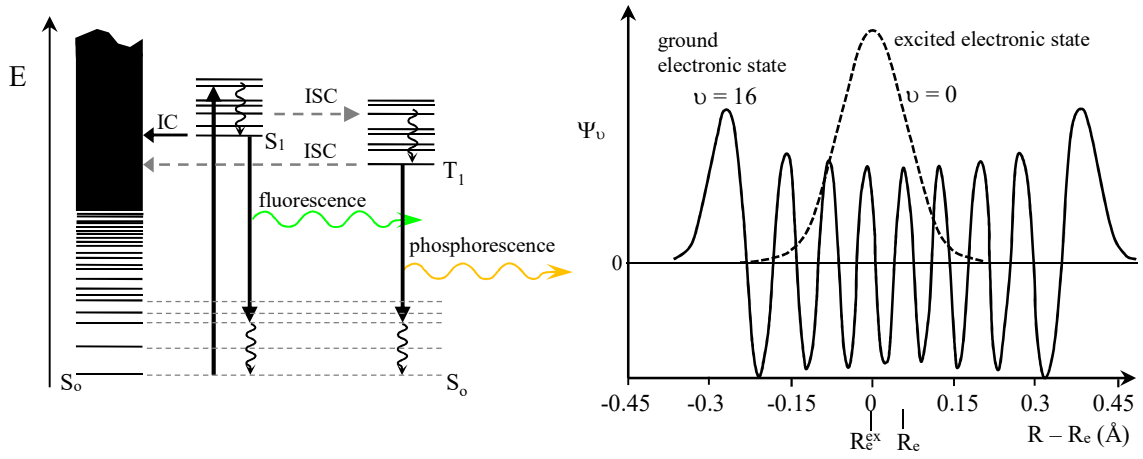

(a). (b).

Figure 28.6.1: Internal conversion from S_1 to the ground state vibrational continuum competes with fluorescence. Intersystem crossing from T_1 to the ground state continuum competes with phosphorescence. (a). Internal conversion, IC, and intersystem crossing, ISC, are horizontal processes. Radiative processes are vertical. (Highly excited vibrational levels of S_1 and T_1 not shown.) (b). Franck-Condon factors to highly excited vibrational levels in the continuum are typically small, assuming a small change in equilibrium bond length.

The energy transfer is intramolecular, that is within the same molecule. The $\upsilon' = 0$ vibrational level of the first excited electronic state, S_1, is the initial state, while a highly excited vibrational level of the ground electronic state, S_o, is the final state. The highly excited vibrational levels of the ground state are closely spaced, because of spectral crowding of the normal modes of the molecule, Figure 28.3.2. Because the vibrational levels approach a continuum of available states, the density of states is the appropriate measure of the availability of the final levels, Figure 28.6.1a. The rate of energy loss of the excited state is proportional to the density of vibrational levels of the ground state at the same energy.

The rate of non-radiative energy transfer, k^{nr}, is given by **Fermi's Golden Rule**. The Golden Rule results from first-order perturbation theory and is the extension of the electric transition dipole moment to cases for non-radiative interaction with a continuum of final levels:[19]

$$k^{nr} = \frac{4\pi^2}{h^2} \rho_E |H_{ji}|^2 \qquad 28.6.1$$

where ρ_E is the density of states at or near energy E, the initial wave function is Ψ_i, the final wave function at energy E is $\Psi_j(E)$, and the interaction integral H_{ji} is:

$$H_{ji} = \int \Psi_j^*(E)\, \hat{J}_N\, \Psi_i \, d\tau \qquad 28.6.2$$

For internal conversion, the energy E is the vibrational energy of the ground state. The integral, is negligible unless $E \cong E_{jo} - E_{io}$, where E_{jo} and E_{io} are the energies of the $\upsilon = 0$ levels of the final and initial states, respectively. In other words, the energy transfer is **isoenergetic**; the initial and final states are at the same energy, electronic and vibrational. But how close in energy is close enough? The density of states provides the criterion for energy matching, that being within $\pm 1/(2\rho_E)$.[19] In the interaction integral, Eq. 28.6.2, $\hat{J}_N$ is the kinetic energy operator of the nuclear motion. For a diatomic molecule $\hat{J}_N = (1/2\mu)(\partial^2/\partial R^2)$, with μ the reduced mass. The nuclear kinetic energy operator takes the place of the electric dipole operator in the transition dipole moment for radiative processes. As such, the energy transfer results from a breakdown of the Born-Oppenheimer approximation, just as in predissociation. The transfer of energy is driven by the motion of the nuclei. The states are said to be **vibronically coupled**. At a first level of approximation, using first-order perturbation theory, we can assume the wave functions in Eq. 28.6.2 are products of an electronic wave function with fixed nuclear coordinates and a vibrational wave function. For internal conversion, the vibrational wave functions are adequately approximated by harmonic oscillator wave functions. In a parallel manner to Eq. 28.1.44, the interaction integral, Eq. 28.6.2, can then be separated into an electronic term, J_{ji}, and a Franck-Condon integral:[20,21]

$$H_{ji} = J_{ji} \int \chi_{\upsilon''}(R)^* \chi_{\upsilon'}(R)\, dR \qquad (j,\upsilon' \rightarrow i,\upsilon'') \qquad \text{(diatomic)} \qquad 28.6.3$$

The electronic integral J_{ji} takes into account the effect of the motion of the nuclei on the transition between electronic states. The Franck-Condon factor, $q_{\upsilon' \rightarrow \upsilon''}$, shows that non-radiative energy transfer is sensitive to the vibrational levels, in the same fashion as radiative absorbance. Substituting Eqs. 28.6.3 and 28.6.2 into Eq. 28.6.1 gives the rate of non-radiative energy transfer from vibrational level υ' in the excited electronic state to vibrational level υ'' of the ground electronic state as:

$$k^{nr} = \frac{4\pi^2}{h^2} \rho_E J_{ji}^2 q_{\upsilon' \rightarrow \upsilon''} \qquad (j,\upsilon' \rightarrow i,\upsilon'') \quad \text{(diatomic)} \quad 28.6.4$$

Remember that the two vibrational wave functions are on the same molecule at the same internuclear separations; one vibrational wave function is for the excited electronic state and the other is for the ground electronic state. With equal total energies and high probabilities of being at the same internuclear separation in the excited and ground electronic states, the molecule forgets which electronic state it is in. For internal conversion, Eq. 28.6.4 is applied to each vibrational level of the ground state molecule that is isoenergetic to the energy of the first excited state. The density of states, ρ_E, is for each vibrational state. The result is the overall non-radiative rate is proportional to the density of states of all the vibrational levels of the ground state with the required energy, $\pm 1/(2\rho_E)$. For diatomics in the harmonic approximation, the density of states is constant. The addition of anharmonic corrections gives an increase in density of states for highly excited vibrational states. For polyatomic molecules, the overall density of states increases with energy, Figure 28.6.1a, suggesting increased non-radiative transfer with increasing energy gap between the excited and ground electronic states. However, internal conversion is experimentally observed to decrease with increasing energy gap. Why?

The Franck-Condon overlap of the two interacting states is a strong decreasing function of the quantum number of the ground state vibrational wave function. For many molecules, there is typically a small difference in internuclear separation between the first excited singlet state and the ground state, Figure 28.6.1b. The excited state begins in the $\upsilon' = 0$ vibrational level. Energy matching requires that the ground state be highly vibrationally excited, giving a large value for υ''. The ground electronic state vibrational wave function then has a large number of nodes. Given $\upsilon' = 0$ for the excited state vibrational level, the Franck-Condon overlap integral samples only the central portion of the ground state vibrational wave function. As the vibrational quantum number increases, the relative amplitude of the central portion of the vibrational wave function decreases in favor of increased amplitude near the classical turning points. This decrease in amplitude near the center with increasing υ'' decreases the Franck-Condon integral. In addition, the highly vibrationally excited ground state wave function has many lobes of positive and negative phase. After multiplication of the two vibrational wave functions, the positive and negative lobes tend to cancel upon integration. Summarizing then, internal conversion results from the transfer of energy into a continuum of vibrational levels isoenergetic with the first excited state. Even though the density of states is constant or increases with an increasing energy gap between the ground and first excited state, the rate of energy transfer decreases because of poor Franck-Condon overlap.

Our treatment so far has assumed a diatomic molecule. Polyatomic molecules have multiple normal modes and hence a greater overall density of states, making internal conversion more efficient. For illustration purposes, assume that the molecule has three normal modes, as in SO_2, with vibrational quantum numbers (υ_1, υ_2, υ_3), Figure 28.3.2. In the harmonic approximation, the vibrational wave function is a product of the three normal mode harmonic oscillator wave functions: $\chi_{1,\upsilon 1}(q_1)\ \chi_{2,\upsilon 2}(q_2)\ \chi_{3,\upsilon 3}(q_3)$, where the q_i are the normal mode coordinates. The energy of the vibrational level is the sum of the normal mode energies:
$E(\upsilon_1, \upsilon_2, \upsilon_3) = E_1(\upsilon_1) + E_2(\upsilon_2) + E_3(\upsilon_3)$. Given the non-radiative transition $(\upsilon_1', \upsilon_2', \upsilon_3') \rightarrow (\upsilon_1'', \upsilon_2'', \upsilon_3'')$, the Franck-Condon factor is correspondingly a product of three terms, one for each mode:[20-21]

$$q_{(\upsilon 1',\upsilon 2',\upsilon 3')\rightarrow(\upsilon 1'',\upsilon 2'',\upsilon 3'')} = \int \chi_{1,\upsilon 1''}(q_1)^* \chi_{1,\upsilon 1'}(q_1)\, dq_1 \int \chi_{2,\upsilon 2''}(q_2)^* \chi_{2,\upsilon 2'}(q_2)\, dq_2 \int \chi_{3,\upsilon 3''}(q_3)^* \chi_{3,\upsilon 3'}(q_3)\, dq_3 \qquad 28.6.4$$

These Franck-Condon factors are summed for all combinations of (υ_1", υ_2", υ_3") that give the total energy of the ground state nearly equal to the energy of the excited state in vibrational level (υ_1', υ_2', υ_3').[20-21] This sum over all isoenergetic vibrational levels is the total Franck-Condon factor, $F = \Sigma\, q_{(\upsilon 1',\upsilon 2',\upsilon 3')\rightarrow(\upsilon 1'',\upsilon 2'',\upsilon 3'')}$:

$$k^{nr} = \frac{4\pi^2}{h^2} \rho_E\, J_{ji}^2\, F \qquad \text{(all isoenergetic vibrational levels)} \qquad 28.6.4$$

The number of such isoenergetic combinations is typically large, which increases the total density of states. Greater density of states enhances the internal conversion rate. For example, benzene has 3N – 6 = 30 normal modes, giving a richly dense vibrational continuum at high E.

The same analysis holds for internal conversion between higher excited singlet states and the first excited singlet state, providing the justification for Kasha's first rule. The same analysis holds for non-radiative energy loss from the first excited triplet state to the ground state, which competes with phosphorescence. Since this non-radiative process involves a change in spin multiplicity, the process is called intersystem crossing, rather than internal conversion. Similar involvement of the density of a continuum of states also plays a role in direct photodissociation to repulsive excited states and in pre-dissociation.

28.7 Fermi's Golden Rule and Förster Resonance Energy Transfer

Förster Resonance Energy Transfer, FRET, is Proportional to the Density of States: The rate of non-radiative intermolecular energy transfer, k'_{DA}, Eq. 28.4.5, is also derived from **Fermi's Golden Rule**. The Förster mechanism applies to donor-acceptor intermolecular distances less than the wavelength of light in the limit of very weak coupling. The Förster mechanism for intermolecular energy transfer differs in two keys aspects from internal conversion. First, the conditions for isoenergetic matching involve electronic states of two molecules. For internal conversion, the isoenergetic levels are two electronic states of the same molecule. Second, the interaction is the Coulombic interaction between the transition dipoles of the donor and acceptor. For internal conversion the interaction is vibronic. We consider the conditions for isoenergetic transfer first. For isoenergetic matching in intermolecular energy transfer, the non-radiative transition of the donor from the excited state to the ground state must be at the same energy as the non-radiative transition of the acceptor from the ground state to the excited state, within $\pm\, 1/(2\rho_E)$, Figure 28.7.1. Such isoenergetic transitions are said to be in resonance.

The transfer probability is proportional to the density of states of isoenergetic transitions of the donor and acceptor as given by Fermi's Golden Rule:[13,22,23]

$$k'_{DA} = \frac{4\pi^2}{h^2} \rho_E\ \beta_{el}^2\, F \qquad 28.7.1$$

where ρ_E is the density of states for a single vibrational level, β_{el} is the electronic interaction integral, and F is the Franck-Condon factor of the transfer (compare to Eq. 28.6.4). Because two molecules are involved, the Franck-Condon factors are given by the product of a Franck-Condon integral for the donor and a Franck-Condon integral for the acceptor. The Franck-Condon overlaps of the donor vertical-transition and the acceptor vertical-transition must both be large.

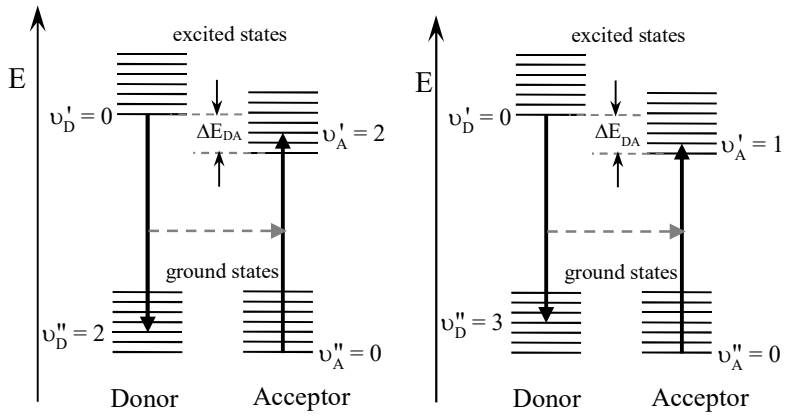

Figure 28.7.1: Two example isoenergetic transitions of the donor and acceptor; the transitions are said to be in resonance with each other. Energy transfer requires isoenergetic transitions that have high density of states. Only one vibrational mode is shown for the donor and acceptor. In general, all normal modes contribute to the density of states.

Taking the example of a single vibrational mode on each of the donor and acceptor, in analogy with Eqs. 28.1.45 and 28.6.3, the Franck-Condon factor is:[22]

$$F = \left| \int \chi_{D,\upsilon_D''} (R_D)^* \, \chi_{D^{ex},\upsilon_D'} (R_D) \, dR_D \int \chi_{A^{ex},\upsilon_A'} (R_A)^* \, \chi_{A,\upsilon_A''} (R_A) \, dR_A \right|^2 \quad \text{(single modes)} \quad 28.7.2$$

$$D^{ex}(\upsilon_D') \rightarrow D(\upsilon_D'') \qquad\qquad A^{ex}(\upsilon_A') \leftarrow A(\upsilon_A'')$$

where the initial and final vibrational wave functions of the donor are $\chi_{D^*,\upsilon_D'}$ and $\chi_{D,\upsilon_D''}$, respectively and the initial and final vibrational wave functions of the acceptor are $\chi_{A,\upsilon_A''}$ and $\chi_{A^*,\upsilon_A'}$, respectively. The internuclear separation of the donor is R_D and of the acceptor is R_A. The total density of states is given by ρ_E F because, as in the case of internal conversion, F is summed over all isoenergetic transitions considering all possible normal mode combinations. Even though a bit complicated, the point is that the total density of states of the vibrational levels is the important factor in the transition rate.

The experimental determination of the total Franck-Condon factor and density of states is achieved by measuring the extent of overlap of the fluorescence emission spectrum of the donor and the absorption spectrum of the acceptor, as given by the integral in Eq. 28.4.6. The density of isoenergetic states is directly related to the degree of overlap of the fluorescence emission of the donor and the absorption spectrum of the acceptor. The bigger the overlap the better.

The electronic interaction integral, β_{el}, is a measure of the Coulomb interaction of the donor transition electric dipole moment, $\vec{\mu}_{D,el}$, and the acceptor electric transition dipole moment, $\vec{\mu}_{A,el}$, which are given by Eq. 28.1.44 for the corresponding donor and acceptor states. The classical view of energy transfer is that the oscillating electric field caused by the donor transition $D^* \rightarrow D$ induces an oscillating electric field that promotes the acceptor $A \rightarrow A^*$. The interaction between the donor transition dipole moment and the acceptor transition dipole moment is dependent on the distance between the transition dipoles, r, and the relative orientation of the transition dipoles, Figure 28.7.2:[13]

$$\beta_{el} = \frac{|\vec{\mu}_{D,el}|\,|\vec{\mu}_{A,el}|}{r^3}(\cos\theta_{DA} - 3\cos\theta_D\cos\theta_A) \qquad 28.7.3$$

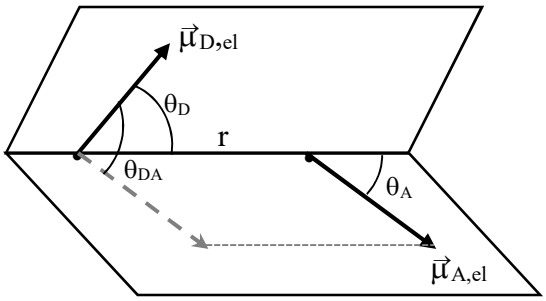

Figure 28.7.2: Coulomb interaction of the donor and acceptor transition electric dipole moments (dark black).[13] The angles θ_D and θ_A are with respect to the line joining the two dipoles. To find the angle between the two dipoles, θ_{DA}, $\vec{\mu}_{A,el}$ is translated so that the two dipoles have the same origin.

The interaction is maximal when the transition dipoles point in the same direction ($\rightarrow\rightarrow$). Substitution of Eqs. 28.7.2 and 28.7.3 into Fermi's Golden Rule, Eq. 28.6.4, with the introduction of practical units gives Eqs. 28.4.5-28.4.6. When β_{el} is squared, the final distance dependence is $1/r^6$ and the orientation factor, κ, results from the angular dependence of the dipole-dipole interaction. In summary, non-radiative intermolecular energy transfer, as modeled by the Förster Resonance Energy Transfer mechanism, results from isoenergetic exchange of energy through the Coulombic coupling of the transition electric dipole moments of the donor and acceptor. The exchange process is enhanced by the density of states of the continuum of isoelectronic transitions.

28.8 Symmetry and Electronic Transition Intensity[24,25]

The prediction of the allowed and forbidden character of electronic transitions is analogous to the procedure for vibrational normal modes. First the symmetry of the ground and excited states involved in the transition are determined from the irreducible representations of the point group. For a transition dipole moment to be non-zero, the direct product of the ground and excited electronic state wave functions and the dipole moment operator must contain the totally symmetric irreducible representation of the point group. As a common special case, if the ground state is totally symmetric, the excited state must transform according to the irreducible representation of one of the x, y, or z-components of the electric dipole operator, just as for vibrational absorption. We have already discussed the symmetries of diatomic molecules and the resulting selection rules. We now wish to extend our treatment to polyatomics and to explain the reasoning behind the selection rules. The first step is to determine the irreducible representations of the electronic states of polyatomics.

The symmetry of an electronic state is most easily handled by considering several cases. These cases, while not exhaustive, cover the vast majority of electronic states.[24]

Case 1: If all molecular orbitals are doubly occupied the state transforms as the totally symmetric irreducible representation of the group, such as $^1\Sigma_g^+$ or $^1A_1$, with singlet spin multiplicity. The totally symmetric irreducible representation has all characters as 1. Most ground states of even-electron stable molecules fall into this category. This case is analogous to the Σ-term for closed shell atoms, Chapt. 25.6. Any closed-shell core of molecular orbitals is totally symmetric, so we only need to consider the unpaired electrons for other symmetries.

Case 2: For odd-electron species with one singly occupied orbital, the electronic state transforms according to the symmetry of the singly occupied molecular orbital. For example, in the ground state of NO_2, the SOMO is a non-bonding orbital that transforms as a_1, Figure 26.6.9. The electronic state is a doublet, since there is one unpaired electron, giving the ground state of NO_2 as $^2A_1$. If the electron is promoted into the LUMO, which has symmetry b_1, the resulting excited electronic state is $^2B_1$.

Case 3: If there are two singly occupied non-degenerate orbitals, the electronic state is given by the direct product of the irreducible representations of the two singly occupied orbitals. The direct product, signified by "⊗" is the class-by-class multiplication of the characters of the two irreducible representations. The spin multiplicity with two unpaired electrons is either a singlet or a triplet. For example, consider O_3 with ground state configuration $(4b_2^o)^2(1a_2^o)^2(6a_1^o)^2$, Figure 26.6.9. The $\pi^*\leftarrow$n promotion of a non-bonding $6a_1^o$ electron into the π^*-orbital $2b_1^*$ gives the excited electronic state as either $^1B_1$ or $^3B_1$ under C_2v symmetry, Figure 28.8.1.

C_{2v}	E	C_2	σ_v	σ'_v	
A_1	1	1	1	1	
B_1	1	-1	1	-1	
$A_1 \otimes B_1 =$	1	-1	1	-1	$= B_1$

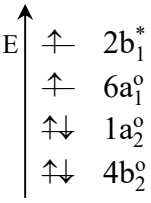

Figure 28.8.1: The $^1B_1$, $^3B_1$ ozone excited state with configuration $(4b_2^o)^2(1a_2^o)^2(6a_1^o)^1(2b_1^*)^1$. The direct product is the class-by-class multiplication of the characters of the irreducible representations. The y-component of the electric dipole moment transforms as B_1 giving an allowed electronic absorption transition for the excited singlet.

Case 4: If there are two electrons in a doubly degenerate orbital, the Pauli Exclusion Principle must be taken into account. We will use ground state O_2 as our example of this case. The O_2 ground state configuration $(\sigma_{g,2s})^2(\sigma^*_{u,2s})^2(\sigma_{g,2pz})^2(\pi_{u,2p})^4(\pi^*_{g,2p})^2$ results in the terms $^3\Sigma_g^- + {}^1\Delta_g + {}^1\Sigma_g^+$, each of which satisfies the Pauli Exclusion Principle and has a definite reflection symmetry.

In determining if an electronic transition is dipole allowed or forbidden we need focus only on the electronic portion of the transition dipole moment, Eq. 28.1.44. The transition electric dipole moment is the product of three functions, the excited state wave function, a component of the electric dipole moment operator, and the ground state wave function. The components of the transition electric dipole operator transform as x, y, and z.:

$$\vec{\mu}_{tr,x} = \int \Psi_{el}^{ex*}\, \hat{\vec{\mu}}_{el,x}\, \Psi_{el}^{gs}\, d\tau_{el} \qquad \vec{\mu}_{tr,y} = \int \Psi_{el}^{ex*}\, \hat{\vec{\mu}}_{el,y}\, \Psi_{el}^{gs}\, d\tau_{el} \qquad \vec{\mu}_{tr,z} = \int \Psi_{el}^{ex*}\, \hat{\vec{\mu}}_{el,z}\, \Psi_{el}^{gs}\, d\tau_{el} \tag{28.8.1}$$

where Ψ_{el}^{ex} is the excited state wave function and Ψ_{el}^{gs} is the ground state wave function. The integrals are over all space, so that the integrals vanish for odd integrands. As a consequence the product of the three functions must be overall even for the transition moment integrals to be non-zero. To guarantee that a transition dipole moment is non-zero, the direct product of the electronic state wave functions and the dipole moment operator must contain ($\supset$) the totally symmetric irreducible representation of the point group:

$$\Gamma(\Psi_{el}^{ex}) \otimes \begin{pmatrix} \Gamma(x) \\ \Gamma(y) \\ \Gamma(z) \end{pmatrix} \otimes \Gamma(\Psi_{el}^{gs}) \supset (\Sigma_g^+, A_1, \text{ or } A_{1g}) \qquad \text{(electric dipole)} \qquad 28.8.2$$

where $\Gamma(\Psi_{el}^{ex})$ and $\Gamma(\Psi_{el}^{gs})$ are the irreducible representations of the excited and ground electronic states and $\Gamma(x)$, $\Gamma(y)$, or $\Gamma(z)$ are alternate choices for the irreducible representation of the component of the electric dipole moment operator. This requirement is often paraphrased as "the dipole moment of the molecule must change in the electronic transition," Secs. 27.1 and 28.1. We are now ready for some examples.

For symmetric diatomic molecules g↔u transitions are allowed while g↔g and u↔u transitions are forbidden, Eqs. 28.1.12. The reason is given by Eq. 28.8.2 since the symmetry of the x, y, or z components of the dipole moment operator are u-character under inversion. The possibilities for a non-vanishing the triple direct product are uug = g and guu = g, both giving the symmetric result. However, gug = u and uuu = u are overall odd causing the transition moment integral to vanish.

Three observations on the properties of direct products are useful at this point:

1. The direct product of a given irreducible representation and the totally symmetric representation is the same as the given irreducible representation. For example $B_2 \otimes A_1 = B_2$, since the characters of A_1 are all 1.
2. The direct product of any irreducible representation with itself contains the totally symmetric representation. For example, $B_2 \otimes B_2 = A_1$, since all the terms with characters of -1 give the square (-1)(-1) = 1.
3. The direct product of two different irreducible representations is not totally symmetric. For examples, the direct products for the C_{4v} point group are given in Table 28.8.1.

Table 28.8.1: Direct Products of the Irreducible Representations of C_{4v}.

C_{4v}	A_1	A_2	B_1	B_2	E
A_1	A_1	A_2	B_1	B_2	E
A_2	A_2	A_1	B_2	B_1	E
B_1	B_1	B_2	A_1	A_2	E
B_2	B_2	B_1	A_2	A_1	E
E	E	E	E	E	$(A_1+A_2+B_1+B_2)$

These three observations simplify matters considerably, especially for the common case of totally symmetric ground states. The symmetry of any doubly filled molecular orbital is A_1, since both electrons have the same orbital symmetry. Furthermore, any set of doubly filled orbitals is totally symmetric. The consequence is that the ground states of most molecules are totally symmetric. The direct product with a totally symmetric ground state is the same symmetry as the direct product of just the excited state with the x, y, or z component of the dipole moment

operator. For example for the z-component: $\Gamma(\Psi_{el}^{ex}) \otimes \Gamma(z) \otimes \Gamma(A_1) = \Gamma(\Psi_{el}^{ex}) \otimes \Gamma(z)$. To have a non-vanishing transition electric dipole moment, the excited state must then transform according to the irreducible representation of one of the x, y, or z-components of the electric dipole operator. For example, for the $\pi^* \leftarrow$n promotion of ozone in *Case 3*, the excited state transforms as B_1. The y-component of the electric dipole moment also transforms as B_1, Table 27.8.2, giving an allowed electronic absorption transition.

If the ground state is not totally symmetric, then the full triple product is necessary to determine if the transition is allowed or forbidden. The electronic selection rule based on orbital symmetry is not as strong as the selection rule based on spin multiplicity. Except for cases with strong spin-orbit coupling, singlet↔triplet transitions are not observed in absorption. On the other hand, forbidden electronic transitions can gain intensity by coupling with unsymmetrical vibrations to give weak transitions. As a consequence formally forbidden electronic transitions can occur, but the electronic selection rule is a good guide to the relative intensity of the formally allowed and forbidden transitions.

Example 28.8.1: *Electronic selection rules*

The ground state of ethylene, C_2H_4, is $(1a_g)^2(1b_{3u})^2(1b_{2u})^2(2a_g)^2(1b_{1g})^2(1b_{1u})^2$. Because ethylene has an inversion center, the molecular orbitals are characterized as g or u. The $1b_{1g}$ HOMO-1 is a bonding σ(C-H) orbital, the $1b_{1u}$ HOMO is a bonding π, and the $1b_{2g}$ LUMO is an anti-bonding π^*. Use electronic selection rules to determine if the low energy $\pi^* \leftarrow \sigma$ and $\pi^* \leftarrow \pi$ transitions are allowed or forbidden. The corresponding molecular orbital diagram including only the $1b_{1g}$, $1b_{1u}$, and $1b_{2g}$ levels is given in Figure 28.8.2.[24]

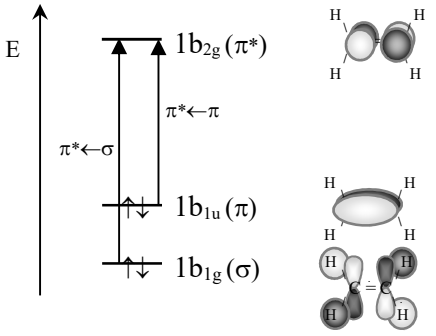

Figure 28.8.2: HOMO-1, HOMO, and LUMO for ethylene.

Answer: Ethylene is in point group D_{2h}. The character table is given below.

D_{2h}	E	$C_2(z)$	$C_2(y)$	$C_2(x)$	*i*	σ(xy)	σ(xz)	σ(yz)		
A_g	1	1	1	1	1	1	1	1	x^2,y^2,z^2	
B_{1g}	1	1	-1	-1	1	1	-1	-1	xy	R_z
B_{2g}	1	-1	1	-1	1	-1	1	-1	xz	R_y
B_{3g}	1	-1	-1	1	1	-1	-1	1	yz	R_x
A_u	1	1	1	1	-1	-1	-1	-1		
B_{1u}	1	1	-1	-1	-1	-1	1	1	z	
B_{2u}	1	-1	1	-1	-1	1	-1	1	y	
B_{3u}	1	-1	-1	1	-1	1	1	-1	x	

The ground state has all doubly occupied orbitals, giving the symmetry as ^1A_g. The LUMO←HOMO transition gives the configuration …$(1b_{1g})^2(1b_{1u})^1(1b_{2g})^1$ which gives the direct product $B_{1u} \otimes B_{2g} = B_{3u}$ as shown below:

D_{2h}	E	$C_2(z)$	$C_2(y)$	$C_2(x)$	i	$\sigma(xy)$	$\sigma(xz)$	$\sigma(yz)$
B_{1u}	1	1	-1	-1	-1	-1	1	1
B_{2g}	1	-1	1	-1	1	-1	1	-1
$B_{1u} \otimes B_{2g}$	1	-1	-1	1	-1	1	1	-1 = B_{3u}

The excited state has two unpaired electrons, which results in a singlet and triplet. The spin allowed transition is singlet←singlet. From the character table, the x-component of the transition dipole transforms according to B_3u, which matches the excited state symmetry. Correspondingly, the LUMO(π^*)←HOMO(π) transition, $^1B_{3u}\leftarrow{}^1A_g$, is allowed.

The LUMO←HOMO-1 transition gives the configuration …$(1b_{1g})^1(1b_{1u})^2(1b_{2g})^1$ which gives the direct product $B_{1g} \otimes B_{2g} = B_{3g}$:

D_{2h}	E	$C_2(z)$	$C_2(y)$	$C_2(x)$	i	$\sigma(xy)$	$\sigma(xz)$	$\sigma(yz)$
B_{1g}	1	1	-1	-1	1	1	-1	-1
B_{2g}	1	-1	1	-1	1	-1	1	-1
$B_{1g} \otimes B_{2g}$	1	-1	-1	1	1	-1	-1	1 = B_{3g}

From the character table, no component of the transition dipole transforms according to B_3g. Correspondingly, the LUMO(π^*)←HOMO-1(σ) transition, $^1B_{3g}\not\leftarrow{}^1A_g$, is not allowed. We could have saved ourselves some work by just focusing on the inversion symmetry. The components of the electric dipole operator are all u, so the excited state must also be u. The configuration …$(1b_{1g})^1(1b_{1u})^2(1b_{2g})^1$ is overall gg = g, which does not match the electric dipole symmetry, giving a forbidden transition. This result is another example of the g↔u selection rule for centro-symmetric molecules, which include diatomics.

28.9 Summary – Looking Ahead

The goal of electronic spectroscopy is to characterize energy transfer processes that are initiated by the absorption of light. The creation and fate of electronic excited states play a central role in photochemical reactions and the characterization of intermolecular interactions. Infrared absorption and Raman scattering allow the determination of the potential energy surface of the ground state. Electronic absorption and emission spectroscopy allow the characterization of the potential energy surfaces of excited states in absorption and the ground state in emission. The potential energy surfaces of the bound states of O_2, Figure 28.1.6, and the repulsive states of HI, Figure 28.1.21, are important examples of the centrality of spectroscopy in providing the information necessary for the determination of thermodynamic properties and reaction dynamics.

Infrared absorption and Raman scattering sample the low lying rotational-vibrational levels in the ground state. Electronic absorption and emission are often capable of sampling high-energy rotational-vibrational states, often near the dissociation limit. Bond breaking results from vertical excitations above the dissociation limit of bound states and from vertical excitations into repulsive states. Pre-dissociation lowers the energy necessary within the excited state for bond

dissociation. Photoionization results from vertical excitations into the ground and excited states of the molecular ion. The intensities of vibrational fine-structure transitions are determined by Franck-Condon factors. The intensities of excitations into repulsive states are determined by Franck-Condon factors into a continuum of translational levels.

We began this chapter by considering radiative transitions to discrete, well-separated stationary molecular states. Such well-resolved processes support rotational and vibrational fine-structure, which allow the characterization of the potential energy surfaces. For large molecules in condensed media the well resolved states of the gas phase become so severely congested and overlapped that a continuum of states results. Internal conversion results from the transfer of excited state energy into the vibrational continuum of a lower electronic state in the same molecule. The coupling between the excited state and the continuum is vibronic. In other words, the system crosses from one Born-Oppenheimer potential surface to another under the influence of nuclear motion. The probability of energy transfer to the continuum is proportional to the density of states. The summations which are appropriate for discrete, well-separated stationary states can be replaced by integrals over a continuous band of states. However, the states that form the continuum, while classical in terms of energy spacing, retain their quantum behavior. In particular, Franck-Condon factors, which depend on the full quantum nature of the vibrational levels, determine transition probabilities to the individual states in the continuum. Intermolecular energy transfer results from isoenergetic transfers from the vibrational continuum of an excited state of the donor molecule into the vibrational continuum of the ground state of the acceptor molecule as determined by Franck-Condon factors and the density of states. The quantum nature of states imbedded in a continuum is a guiding principle in many areas of chemical kinetics as well as spectroscopy.

Nonadiabatic Processes Result from a Breakdown of the Born-Oppenheimer Approximation:[26]
Adiabatic processes occur upon a single potential energy surface, which is generated using the Born-Oppenheimer approximation. The Born-Oppenheimer approximation assumes nuclear motion occurs over a much longer time scale than the motion of the electrons. In other words, the motion of the nuclei is uncoupled from the motion of the electrons. The Born-Oppenheimer potential energy surface is constructed by calculating molecular orbitals at fixed nuclear positions. The vibration of the molecule then takes place on this potential energy surface, Section 26.1. Direct photodissociation by a bound←bound or repulsive←bound transition is an adiabatic process within the excited state, Figures 28.1.19 and 28.1.21. Predissociation, however, is a **nonadiabatic process**. The interaction that causes the avoided crossing results from the coupling of the nuclear and electronic degrees of freedom. The nuclear motion drives the switchover between the electronic states. Similarly, internal conversion and intersystem crossing are vibronically coupled non-adiabatic processes. We will discuss nonadiabatic processes in more detail in the Molecular Dynamics chapter. We can anticipate that many, if not most, bond breaking and making processes are inherently nonadiabatic. We need to go beyond the Born-Oppenheimer approximation to understand many spectroscopic and chemical processes.

Looking Ahead: What effects do the excited state energies, fundamental vibration frequencies, anharmonicities, rotational constants, and bond dissociation energies of a molecule have on chemical reactivity? In other words, what is the relationship between molecular structure and chemical function? The principal way that we characterize chemical reactivity is through equilibrium constants and kinetic rate constants. Do knowing the spectroscopic potential energy surfaces of a molecule help us determine equilibrium and rate constants? Statistical mechanics,

which we discuss next, acts as a bridge between the world of single isolated molecules and macroscopic thermodynamic systems. The molecular information necessary to determine thermodynamic and kinetic properties is derived from spectroscopy.

Let's end with a final visual analogy. Picture a mountain range system, such as the Swiss Alps, the Rocky Mountains, or the Ozarks. As we roam through the many peaks and valleys of the mountain range we sample different environments. Our destination depends on the path that we choose. We often choose minimum energy paths by crossing over saddle points, rather than mountain peaks. We often follow valleys. The potential energy surfaces of the ground and excited states of a molecule are the energy landscape that determines the destination, or chemical outcome, of processes. The energy landscape of molecules is richly complex with bound and repulsive surfaces that have multiple intersections. For diatomic molecules, neglecting rotation, the potential energy surfaces are functions of only one spatial coordinate, the internuclear separation. For bent triatomics, the potential energy surfaces are three dimensional, corresponding to the symmetric, asymmetric, and bending vibrations. For benzene with 30 normal modes, the potential energy surface is 30-dimensional, but we can still use a mountain range as a useful visual analogy. Chemistry is a meander on the energy landscape that results from the Coulomb interactions among the electrons and nuclei.

Chapter Summary

1. At high resolution in the gas-phase, vibrational and rotational fine-structure occur with electronic transitions, which allow the fundamental vibration frequency, anharmonicity, rotational constants, and bond dissociation energy to be determined for the final state.
2. For a diatomic molecule, the total energy of electronic state i is the sum of the electronic energy with respect to the ground state $\tilde{T}_{e,i}$, the vibrational energy for vibrational quantum number υ, and the rotational energy for rotational quantum number J:

$$\tilde{E}_{i,\upsilon,J} = \tilde{T}_{e,i} + \tilde{G}(\upsilon) + \tilde{F}(J) = \tilde{T}_{e,i} + \tilde{\nu}_{e,i}\,(\upsilon + ½) - \chi_e^{ex}\,\tilde{\nu}_e^{ex}\,(\upsilon + ½)^2 + \tilde{B}_{e,i}\,J(J+1) - \tilde{D}_{e,i}\,[J(J+1)]^2$$

3. Collisional broadening in solution obscures vibrational fine-structure.
4. For diatomics, the transition electric dipole moment between electronic states i and j, in the Born-Oppenheimer approximation, is:

$$\vec{\mu}_{tr} = \langle\vec{\mu}\rangle = \int [\Psi_{el,j}\,\chi_{\upsilon'}(R)Y_{J',m_{J'}}(\theta,\phi)]^*\,\hat{\vec{\mu}}\,\Psi_{el,i}\,\chi_{\upsilon''}(R)Y_{J'',m_{J''}}(\theta,\phi)\,d\tau \qquad (j,\upsilon',J' \leftarrow i,\upsilon'',J'')$$

5. The gross electronic selection rule is that the dipole moment of the molecule must change between electronic states. The vibrational transitions in electronic spectroscopy are not restricted by symmetry or to $\Delta\upsilon = \pm 1$. For transitions between singlet electronic states with no net orbital angular momentum, the rotational selection rule is $\Delta J = \pm 1$.
6. For diatomics, the total projection of the orbital angular momentum around the z-axis is given by the angular momentum quantum number Λ, which determines the term:

$$M_\lambda = \sum_{i=1}^{n} \lambda \qquad \Lambda = M_{\lambda,max}$$

Λ	0	1	2
term	Σ	Π	Δ

The electron motion is clockwise around the z-axis for $\lambda = +1$ and counterclockwise for $\lambda = -1$.

7. For centrosymmetric molecules, the inversion symmetry is determined from the molecular orbitals using multiplication rules g·g = g, u·u = g, and u·g = u.

8. For diatomics, all closed shell diatomic molecules are $^1\Sigma^+$. For a single electron outside a closed core, the term is $^2\Sigma^+$ if the unpaired electron is in a σ orbital and $^2\Pi$ if the electron is in a π orbital.
9. $O_2(^1\Delta_g)$ is a kinetically voracious oxidizing agent with Diels-Alder type reactions that are distinct from those of ground state $O_2(^3\Sigma_g^-)$.
10. For diatomics, the selection rules for electronic absorption or emission, with weak spin-orbit interactions, are: $\Delta\Lambda = 0, \pm1$, $\Delta S = 0$, $\Delta\Omega = 0, \pm1$, $g \rightarrow u$ or $u \rightarrow g$ (centrosymmetric) and $+ \rightarrow +$ or $- \rightarrow -$ (Σ states). The total angular momentum quantum number is: $\Omega = \Lambda + S$.
11. Reflection symmetry across a plane that passes through the nuclei reverses the sense of rotation about the z-axis, $\lambda \rightarrow -\lambda$. Reflection switches an electron between degenerate π-orbitals. Σ-states must satisfy electron indistinguishability and reflection symmetry.
12. Franck-Condon integrals are vibrational overlap integrals that determine the intensity of vibrational transitions within a given electronic transition. The Franck-Condon factor is:

$$q_{\upsilon'\leftarrow\upsilon''} \propto \left|\int \chi_{\upsilon'}(R)^* \chi_{\upsilon''}(R)\, dR\right|^2 \qquad (\upsilon'\leftarrow\upsilon'')$$

13. A vibrational period is orders of magnitude longer than the time of an electronic transition. The nuclear positions are frozen during the electronic transition giving a vertical transition. Beginning in the middle of the ground state vibrational potential, the most intense vibrational transition is predicted as the vibrational level nearest the intersection of the vertical transition with the excited state potential curve.
14. A long vibrational progression results from transitions that have a large change in equilibrium bond length; strong rebound produces many excited vibrational levels. A small number of vibrational levels result from a small change in equilibrium bond length.
15. The bond dissociation energy of the excited state is $D_o^{ex} = \Delta E(j,\infty\leftarrow i,0) - \Delta E(j,0\leftarrow i,0)$ in joules or $\tilde{D}_o^{ex} = \tilde{\nu}_{\infty o} - \tilde{\nu}_{oo}$ in cm^{-1}, where $\Delta E(j,\infty\leftarrow i,0)$ or $\tilde{\nu}_{\infty o}$ is the convergence limit, which is the energy where the spacing between adjacent vibrational fine-structure peaks is zero.
16. The ground electronic state bond dissociation energy is $D_o = \Delta E(j,\infty\leftarrow i,0) - \Delta E_{atomic}$ in joules or $\tilde{D}_o = \tilde{\nu}_{\infty o} - \Delta\tilde{E}_{atomic}$ in cm^{-1}, where ΔE_{atomic} is the energy of the product atoms of the photodissociation compared to the ground state atoms.
17. The electronic transition convergence limit is the sum of the lowest energy $0\leftarrow0$ transition and the dissociation energy of the excited state, $\tilde{\nu}_{\infty o} = \tilde{D}_o + \Delta\tilde{E}_{atomic} = \tilde{\nu}_{oo} + \tilde{D}_o^{ex}$.
18. The Birge-Sponer extrapolation is given by a plot of the adjacent differences of the vibrational fine-structure transitions versus the vibrational quantum number υ:

$$\Delta\tilde{\nu}_\upsilon = \Delta\tilde{\nu}_o - 2\chi_e^{ex}\tilde{\nu}_e^{ex}\,\upsilon \quad \text{with the first adjacent difference:} \quad \Delta\tilde{\nu}_o = \tilde{\nu}_e^{ex} - 2\chi_e^{ex}\tilde{\nu}_e^{ex}$$

19. In the excited state $\tilde{D}_o^{ex} = \frac{1}{2}\tilde{\nu}_e^{ex}\upsilon_{cl}$ with convergence limit $\upsilon_{cl} = \Delta\tilde{\nu}_o/(2\chi_e^{ex}\tilde{\nu}_e^{ex})$.
20. For small anharmonicity, $\tilde{\nu}_e^{ex} \cong \Delta\tilde{\nu}_o$ and $\tilde{D}_o^{ex}$ is approximately the area of the triangle with base $\Delta\tilde{\nu}_o$ and height υ_{cl} in the Birge-Sponer plot, $\tilde{D}_o^{ex} \cong \frac{1}{2}\Delta\tilde{\nu}_o\upsilon_{cl}$ = area.
21. With small anharmonicity, the electronic transition energy at the convergence limit is $\tilde{\nu}_{\infty o} = \tilde{\nu}_{oo} + \frac{1}{2}\Delta\tilde{\nu}_o\upsilon_{cl} = \tilde{\nu}_{oo}$ + area, which holds even if an arbitrary transition is assigned as $\tilde{\nu}_{oo}$.
22. Photochemistry can result by the excited electronic state acting as one of the primary reactants or from bond dissociation (a) by a direct bound$\leftarrow$bound electronic transition above the dissociation limit, or (b) by a direct repulsive$\leftarrow$bound electronic transition into the translational continuum. (c) In predissociation a bound excited-state potential energy curve

intersects with a repulsive potential energy curve, with the same symmetry, giving an avoided curve-crossing. Electronic transitions to vibrational levels near the energy of the avoided-crossing are lifetime broadened by cross-over to the translational continuum of the repulsive curve giving bond dissociation.

23. Rydberg states are produced if an electron in an atom is promoted to an atomic orbital with principal quantum number higher than the valence state (e.g. C 3s or 3p). Any atom can be a center for Rydberg promotion, all molecules have Rydberg states, the excited atom orbital is primarily non-bonding, and Rydberg states are strongly localized on the promoted atom.

24. Rydberg states form series of transitions, $\tilde{\nu}_n$, that follow an atomic-like energy pattern:

$$\tilde{\nu}_n = \tilde{\nu}_I - \frac{\Re_h}{(n+c)^2}$$

where $\tilde{\nu}_I$ is the series limit, $\Re_h$ is the Rydberg constant, n is the principal quantum number of the promoted electron, and c is a constant specific to the series (the quantum defect).

25. Excited states of polyatomics often have a different symmetry than the ground state.

26. Electronic transitions can be characterized by the MOs involved. Typical transitions in order of increasing energy are: $\pi^* \leftarrow n$, $\pi^* \leftarrow \pi$, $\sigma^* \leftarrow n$, $\pi^* \leftarrow \sigma$, $\sigma^* \leftarrow \sigma$. Rydberg transitions include $Ry \leftarrow n$, $Ry \leftarrow \pi$, $Ry \leftarrow \sigma$.

27. A continuous distribution of quantum states is characterized by the density of states. Transitions to repulsive excited states result in a continuum of translational levels. In polyatomics, vibrational continua result from spectral congestion of transitions to different normal modes. In condensed phases, vibrational continua result from collisional broadening.

28. The density of states is the number of quantum states per unit interval in energy or wave number, which converts from a given energy to the number of quantum states near that energy, $\rho(\varepsilon) \equiv d\upsilon/d\varepsilon$. The density of states of a harmonic vibration is: $\rho(\tilde{\varepsilon}_\upsilon) = 1/\tilde{\nu}_o$ in cm^{-1}.

29. Spontaneous emission from excited states is fluorescence if transitions occur between states with the same spin multiplicity and phosphoresce if between states with differing multiplicity.

30. Fluorescence conserves spin multiplicity giving ~20 ns lifetimes. Phosphorescence is spin forbidden giving ~ 10^{-3} s lifetimes. The non-radiative conversion of the spin multiplicity of a state is intersystem crossing. ISC is mediated by spin-orbit coupling.

31. Most molecules lose the excess energy of the excited state by non-radiative processes, which compete with fluorescence: internal conversion, intersystem crossing, chemical reactions, and intermolecular energy transfer. In internal conversion, IC, an excited state is converted into a highly excited vibrational level of a lower energy electronic state.

32. For organic molecules in condensed media internal conversion, vibrational relaxation, and exchange interactions have the results:
    1. Kasha's Rule: Fluorescence always originates from the first excited state. (IC)
    2. Fluorescence is redder than the corresponding absorption spectrum. (VR)
    3. Phosphorescence is redder than the corresponding fluorescence. (exchange)

33. Electronic energy transfer between an excited donor, D^{ex}, and a ground state acceptor, A, is: $D^{ex} + A \rightarrow D + A^{ex}$ with rate constant k_{DA}. For donor-acceptor distances greater than the wavelength of light radiative transfer dominates and is proportional to the degree of overlap of the fluorescence emission spectrum of the donor, $F_D(\tilde{\nu})$, and the absorption spectrum of the acceptor, $\varepsilon_A(\tilde{\nu})$: $k_{DA} \propto \int_o^\infty F_D(\tilde{\nu})\, \varepsilon_A(\tilde{\nu})\, d\tilde{\nu}$.

34. For distances less than the wavelength of light and weak interaction, Förster Resonance Energy Transfer, FRET, is mediated by non-radiative Coulombic interaction between the transition dipole moments of the donor and acceptor, giving a sensitive measure of the distance between the donor and acceptor, r:

$$k'_{DA} = \frac{1}{\tau_D}\left(\frac{R_o}{r}\right)^6$$

where τ_D is the fluorescence lifetime of the donor in the absence of the acceptor, and R_o is the critical transfer distance that gives $k'_{DA} = k_f + k_{nr}$.

35. The Förster critical transfer distance R_o is related to the extent of overlap of the fluorescence emission spectrum of the donor and the absorption spectrum of the acceptor:

$$R_o^6 = \frac{(9000 \ln 10)\kappa^2}{128\pi^5 n^4 N_A}\int_o^\infty \frac{F_D(\tilde{\nu})\,\varepsilon_A(\tilde{\nu})}{\tilde{\nu}^4}\,d\tilde{\nu}$$

where n is the index of refraction of the solvent, N_A is Avogadro's number, and κ is an orientation factor. In solution the orientation average is $\langle\kappa^2\rangle = 2/3$.

36. In photoionization, $A + h\nu \rightarrow A^+(\upsilon') + e^-$, the molecular ion is produced in the ground or excited electronic state, in vibrational level υ'. Energy in excess of the ionization energy is released as kinetic energy of the photoelectron: $E = h\nu = E_k + I_1(\upsilon')$, where ν is the exciting light frequency and $I_1(\upsilon')$ is the ionization energy of the molecular ion in vibrational level υ'.

37. The intensity of vibrational fine-structure in UPS is determined by Franck-Condon factors. Vertical transitions end in intersection with the potential energy curve of the molecular ion. A large change in equilibrium bond length produces a long vibrational progression.

38. UPS ionization potentials approximate the molecular orbital energies of the ionized electrons. The equivalence is justified by Koopmans' Theorem: the orbital approximation is valid, the molecule does not change shape upon ionization, and the correlation energies of the ground state molecule and molecular ion are similar, which is the frozen orbital approximation.

39. Transition rates into the continuum are proportional to the density of states and Franck-Condon factors between the initial and final vibrational or translational states.

40. For internal conversion, for a single normal mode, Fermi's Golden Rule gives the non-radiative transfer rate as proportional to the density of vibrational states in the continuum, ρ_E:

$$k^{nr} = \frac{4\pi^2}{h^2}\rho_E\,|H_{ji}|^2 = \frac{4\pi^2}{h^2}\rho_E\,J_{ji}^2\,q_{\upsilon'\rightarrow\upsilon''}$$

where H_{ji} is the interaction integral between the excited state and ground state vibronic levels. H_{ji} factors into an electronic integral that depends on motion of the nuclei, J_{ji}, and the corresponding Franck-Condon factor, $q_{\upsilon'\rightarrow\upsilon''}$. The energy transfer is isoenergetic; the initial and final states are at the same energy, electronic and vibrational, within $\pm\, 1/(2\rho_E)$.

41. In internal conversion, even though the density of states is constant or increases with an increasing energy gap between the ground and first excited state, the rate of energy transfer typically decreases because of poor Franck-Condon overlap.

42. For internal conversion in large molecules, a sum is taken over all isoenergetic vibrational levels, taking into account all normal modes, to give the total Franck-Condon factor, F:

$$k^{nr} = \frac{4\pi^2}{h^2}\rho_E\,J_{ji}^2\,F$$

43. For isoenergetic matching in the Förster mechanism, the non-radiative transition of the donor from the excited state to the ground state must be at the same energy as the non-radiative transition of the acceptor from the ground state to the excited state, within $\pm 1/(2\rho_E)$.

44. Förster intermolecular transfer is proportional to the density of states of isoenergetic transitions of the excited donor and ground state acceptor by Fermi's Golden Rule:

$$k'_{DA} = \frac{4\pi^2}{h^2} \rho_E \ \beta_{el}^2 F$$

where β_{el} is the electronic interaction integral, and F is the total Franck-Condon factor.

45. In the Förster mechanism, the dipole-dipole interaction between the transition dipole moments of the donor, $\vec{\mu}_{D,el,}$ and acceptor, $\vec{\mu}_{A,el}$, depends on the distance between the transition dipoles, r, and the relative orientation of the transition dipoles, Figure 28.7.2:

$$\beta_{el} = \frac{|\vec{\mu}_{D,el}| \, |\vec{\mu}_{A,el}|}{r^3} (\cos \theta_{DA} - 3 \cos \theta_D \cos \theta_A)$$

46. The irreducible representation of an electronic state is easily assigned in cases:
Case 1: All doubly occupied molecular orbitals: the state transforms as the totally symmetric irreducible representation. Ground states of most even-electron stable molecules are totally symmetric.
Case 2: One singly occupied orbital: the electronic state transforms according to the symmetry of the singly occupied molecular orbital.
Case 3: Two singly occupied non-degenerate orbitals: the electronic state is given by the direct product of the irreducible representations of the two singly occupied orbitals.
Case 4: If there are two electrons in a doubly degenerate orbital, several terms result.

47. The components of the transition electric dipole operator transform as x, y, and z.

48. A non-zero transition electric dipole moment requires:

$$\Gamma(\Psi_{el}^{ex}) \otimes \begin{pmatrix} \Gamma(x) \\ \Gamma(y) \\ \Gamma(z) \end{pmatrix} \otimes \Gamma(\Psi_{el}^{gs}) \ \supset \ (\Sigma_g^+, A_1, \text{ or } A_{1g})$$

where $\Gamma(\Psi_{el}^{ex})$ and $\Gamma(\Psi_{el}^{gs})$ are the irreducible representations of the excited and ground electronic states and $\Gamma(x)$, $\Gamma(y)$, or $\Gamma(z)$ are alternate choices for the irreducible representation of the component of the electric dipole moment operator.

49. The direct product, "⊗", is the class-by-class multiplication of the characters of the two irreducible representations:
1. The direct product of a given irreducible representation and the totally symmetric representation is the same as the given irreducible representation, e.g. $B_2 \otimes A_1 = B_2$.
2. The direct product of any irreducible representation with itself contains the totally symmetric representation, e.g. $B_2 \otimes B_2 = A_1$.
3. The direct product of two different irreducible representations is not totally symmetric.

50. For a totally symmetric ground state to have a non-vanishing transition electric dipole moment, the excited state must transform according to the irreducible representation of one of the x, y, or z-components of the electric dipole operator (analogous to IR transitions).

51. An adiabatic process occurs upon a single Born-Oppenheimer potential energy surface. A nonadiabatic process crosses from one potential energy surface to another under the coupling

of nuclear motion with the electronic states. Predissociation is a vibronically coupled nonadiabatic process, as are most chemical reactions.

Literature Cited

1. A. D. Walsh, "The Electronic Orbitals, Shapes, and Spectra of Polyatomic Molecules, Part II. AB_2 and BAC Molecules," *J. Chem. Soc.*, **1953**, 2266-2289.
2. A. Gilbert, J. Baggott, *Essentials of Molecular Photochemistry*, CRC, Boca Raton, FL, 1991, p. 512
3. C. E. Moore, "Atomic Energy Levels," National Standard Reference Data System-NBS 35, Superintendent of Documents, US GPO, Washington, D. C., 1971.
4. J. E. Sansonetti, W. C. Martin, Handbook of Basic Atomic Spectroscopic Data, *J. Phys. Chem. Ref. Data*, **2005**, *34(4)*, 1560-2259: http://www.nist.gov/data/PDFfiles/jpcrd690.pdf (last accessed 1/2015)
5. A. Kramida, Y. Ralchenko, J. Reader, "NIST Atomic Spectra Database," http://www.nist.gov/pml/data/asd.cfm (last accessed 1/2015)
6. W. D. McGrath, J. J. McGarvey, "Absorption Spectrum and Dissociation Energy of the SO Radical," *J. Chem. Phys*., **1962**, *37*,1574-1575.
7. S. R. Langford, P. M. Regan, A. J. Orr-Ewing, M. N. R. Ashford, "On the UV photodissociation dynamics of hydrogen iodide," *Chem. Phys.,* **1998**, *231*, 245-260.
8. J. E. Frederick, R. D. Hudson, "Predissociation of Nitric Oxide in the Mesosphere and the Straosphere," *J. Atmospheric Sciences*, **1979**, *36*, 737-745.
9. K. S. Pitzer, *Quantum Chemistry*, Prentice-Hall, Englewood Cliffs, NJ, 1953, pp. 257-259.
10. K. P. Huber and G. Herzberg, *Constants of diatomic molecules*, (data prepared by J. W. Gallagher and R. D. Johnson, III) in NIST Chemistry WebBook, NIST Standard Reference Database Number 69, Eds. P. J. Linstrom and W. G. Mallard, National Institute of Standards and Technology, Gaithersburg MD, http://webbook.nist.gov/chemistry, (last accessed 3/2015).
11. C. Sandorfy, *Electronic Spectra and Quantum Chemistry*, Prentice-Hall, Englewood Cliffs, NJ, 1964.
12. H. H. Jaffé, M. Orchin, *Theory and Applications of Ultraviolet Spectroscopy*, Wiley, New York, NY, 1962.
13. B. Valeur, M. N. Berberan-Santos, *Molecular Fluorescence: Principles and Applications, 2nd Ed*. Wiley-VCH, Weinheim, DE, 2012, Chap. 8.
14. D. W. Turner, D. P. May, "Franck-Condon Factors in Ionization: Experimental Measurement Using Molecular Photoelectron Spectroscopy," *J. Chem. Phys*., **1966**, *45*(2), 471-476. (spectra simulated based on numerical data)
15. M. I. Al-Joboury, D. P. May, D. W. Turner, "*Molecular Photoelectron Spectroscopy. Part III: The Ionization Potentials of Oxygen*, *Carbon Monoxide, Nitric Oxide, and Acetylene*," *J. Chem. Soc.*, **1965**, 616-622. (spectra simulated based on numerical data)
16. A. D. Baker, "Photoelectron Spectroscopy," *Acc. Chem. Res.*, **1970**,
17. C. R. Brundle, D. W. Turner, "High resolution molecular photoelectron spectroscopy", *Proc. Roy. Soc. A.*, **1968**, *307*, 27-36. (spectra simulated based on numerical data)
18. A. W. Potts, W. C. Price, "Photoelectron spectra and valence shell orbital structures of groups V and VI hydrides," *Proc. Roy. Soc. London A*, **1972**, *326*, 181-197.
19. L. I. Schiff, *Quantum Mechanics, 3rd Ed.*, McGraw-Hill, New York, NY, 1968. Section 35.
20. J. B. Birks, *Photophysics of aromatic molecules*, Wiley-Interscience, London, England, 1970, pp 149-155.

21. W. Siebrand, “Radiationless Transitions in Polyatomic Molecules. I. Calculation of Franck-Condon Factors,” *J. Chem. Phys*., **1967**, *46(2)*, 440-447.

22. J. B. Birks, *Photophysics of aromatic molecules*, Wiley-Interscience, London, England, 1970, pp. 567-569.

23. G. W. Robinson, R. P. Frosch, “Electronic Excitation Transfer and Relaxation,” J. Chem. Phys., 1963, 38(5), 1187-1202.

24. D. C. Harris, M. D. Bertolucci, *Symmetry and Spectroscopy: An Introduction to Vibrational and Electronic Spectroscopy*, Oxford, New York, NY, 1978. Chapt. 5

25. S. F. A. Kettle, *Symmetry and Structure*, Wiley, Chichester, England, 1985. Chapt. 10.

26. M. Baer, *Beyond Born-Oppenheimer: Electronic Nonadiabatic Coupling Terms and Conical Intersections*, Wiley, New York, 2006.

Further Reading

General Theory

P. F. Bernath, *Spectra of Atoms and Molecules, 2nd Ed*., Oxford University Press, New York, NY, 2005.

G. Herzberg, *Molecular Spectra and Molecular Structure: Spectra of Diatomic Molecules, 2nd. Ed.*, Van Nostrand Reinhold, New York, NY, 1950.

G. Herzberg, *Molecular Spectra and Molecular Structure: Electronic Spectra of Polyatomic Molecules, 2nd. Ed.*, Van Nostrand Reinhold, New York, NY, 1966.

J. I. Steinfeld, *Molecules and Radiation, 2nd Ed.*, MIT Press, Cambridge, MA, 1985.

Rydberg States

C. Sándorfy, Ed., *The Role of Rydberg States in Spectrscopy and Photochemistry: Low and High Rydberg States*, Kluwer, Dordrecht, Netherlands, 1999.

Energy Transfer and Fluorescence

J. B. Birks, *Photophysics of aromatic molecules*, Wiley-Interscience, London, England, 1970.

B. Valeur, M. N. Berberan-Santos, *Molecular Fluorescence: Principles and Applications, 2nd Ed*. Wiley-VCH, Weinheim, DE, 2012.

Group Theory

D. C. Harris, M. D. Bertolucci, *Symmetry and Spectroscopy: An Introduction to Vibrational and Electronic Spectroscopy*, Oxford, New York, NY, 1978.

S. F. A. Kettle, *Symmetry and Structure*, Wiley, Chichester, England, 1985.

Non-adiabatic Chemical Processes

K. Takatsuka, T. Yonehara, K. Hanasaki, Y. Arasaki, *Chemical Theory beyond the Born-Oppenheimer Paradigm: Nonadiabatic Electronic and Nuclear Dynamics in Chemical Reactions*, World Scientific Publishing, Singapore, 2015.

M. Baer, *Beyond Born-Oppenheimer: Electronic Nonadiabatic Coupling Terms and Conical Intersections*, Wiley, New York, 2006.

J. C. Tully, “Perspective: Nonadiabatic dynamics theory,” *J. Chem. Phys*., **2012**, *137*, *22A301*, 1-7.

Chapter 28: Electronic Spectroscopy Problems

1. Why all the interest in diatomic molecules?

2. Calculate the transition wave number for the ground electronic state to first excited singlet state transition in carbon monoxide. Assume the ground state vibrational-rotational and quantum numbers are $\upsilon'' = 0$, $J'' = 3$ and the excited state quantum numbers are $\upsilon' = 3$, $J' = 4$. The spectroscopic constants are given below.[1,2]

State	$\tilde{T}_e$ (cm^{-1})	$\tilde{\nu}_e$ (cm^{-1})	$\chi_e\tilde{\nu}_e$ (cm^{-1})	$\tilde{B}_e$ (cm^{-1})	$\tilde{\alpha}_e$ (cm^{-1})	$\tilde{D}_e$ (cm^{-1})
$A\ ^1\Pi$	65075.7	1518.2	19.4	1.6115	0.02325	7.33×10^{-6}
$X\ ^1\Sigma^+$	0	2169.814	13.288	1.93128	0.017504	6.12×10^{-6}

3. In rotation-vibration absorption, with $\tilde{B}' < \tilde{B}''$, each line moves to lower wave number in proportion to the J''^2 value, Eqs. 27.6.8-27.6.9. The R-branch lines get closer together and the P-branch lines get further apart. Please review Problem 27.30. In electronic absorption, the rotational constant in the upper electronic states often differs markedly from the ground electronic state. Write a spreadsheet to simulate the electronic absorption spectrum of carbon monoxide for the $\upsilon'' = 0$ to $\upsilon' = 1$ vibrational transition. The spectroscopic constants are listed in the previous problem. Neglect centrifugal distortion. [Hints: Refer to the hint for Problem 27.30, however this time your plot will be clearer if you choose a scatter plot with marker symbols and a connecting line. Include transitions for $J'' = 0$ to 10 for the R- and P-branches. To start with, to make the plot clearer you may want to use $\tilde{B}_e = 1.93128\ cm^{-1}$ for both electronic states. Then switch to $\tilde{B}_e = 1.6115\ cm^{-1}$ for the excited state.]

4. Predict the intensities of the different vibrational transitions in the electronic absorption spectrum of the following system. Show at least four peaks. Label each transition in the energy level diagram with the vibrational quantum numbers for the transition and each corresponding peak in the spectrum (e.g. 4←0).

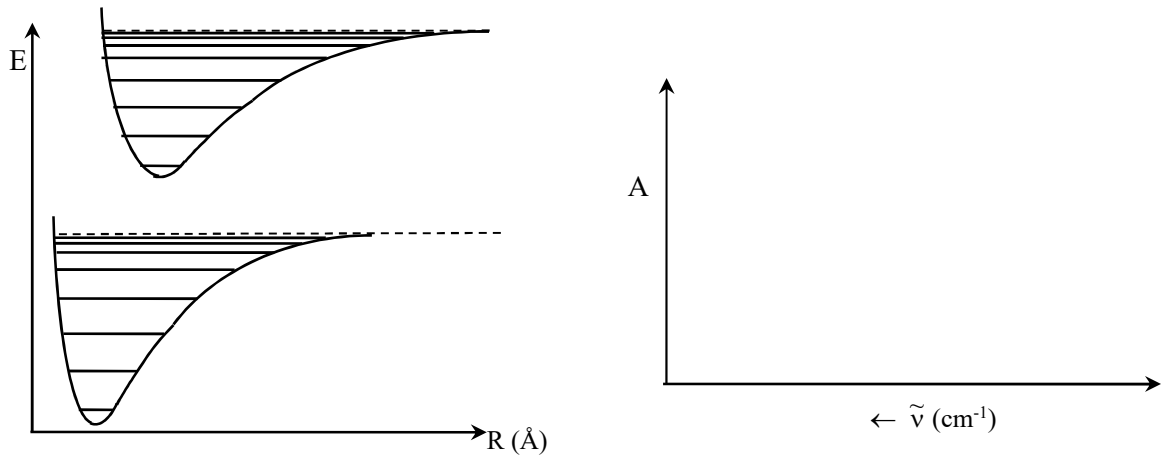

5. Show the relationship between the ground state and excited state potential energy curves for an electronic transition that has a maximum probability for the 2←0 vibrational fine-structure

transition. Draw the corresponding absorption spectrum. Label each transition in the energy level diagram with the vibrational quantum numbers for the transition and each corresponding peak in the spectrum (e.g. 4←0). (Use the potential energy curves shown in the previous question for the style of your sketch).

6. (a). In Figure 28.1.9b we needed to take the linear combination of four specific assignments to generate a state that satisfies both the Pauli Exclusion Principle and reflection symmetry. Why four states instead of two? Show that the following state does not properly account for electron indistinguishability and reflection symmetry:

$^3\Sigma_u$??

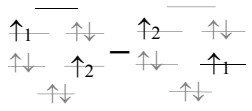

7. In Figure 28.1.10 we needed to take the linear combination of four specific assignments to generate a state that satisfies both the Pauli Exclusion Principle and reflection symmetry. However, there are eight possible combinations of the coefficients that give equal weight to each assignment: (++++), (++ – –), (+ – + –), (+ – – +), (+++ –), (+ – – –), (+ – ++), (++ – +). Show that only the two linear combinations listed in Figure 28.1.10 properly account for electron indistinguishability and reflection symmetry for the Σ_u triplet terms and two more for the singlet terms.

8. In Chapter 25, we determined the complete set of atomic terms for a given electronic configuration by exhaustively enumerating all the possible explicit orbital assignments. In this chapter we took a bit of a short-cut. However, it is still informative to determine all possible molecular terms by exhaustive enumeration. Luckily, diatomic electronic states are simpler, because the π levels are only doubly degenerate. For example, the p^1 atomic configuration gives a ^{2}P term with $M_L = \{1,0,-1\}$. However, the $(\sigma_{g,2pz})^2 (\pi_{u,2p})^1$ molecular configuration corresponds to only $M_\lambda = \{1,-1\}$, because there are only two degenerate π-molecular orbitals:

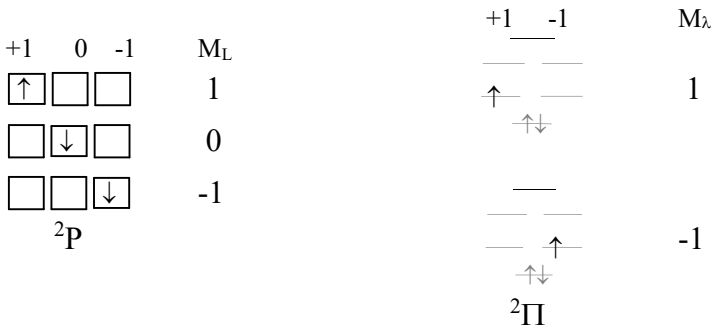

(a). atomic (b). diatomic molecular

Figure P28.8.1: (a). The p^1 atomic configuration is triply degenerate with $M_L = \{1,0,-1\}$. (b). The $(\sigma_{g,2pz})^2 (\pi_{u,2p})^1$ molecular configuration corresponds to only $M_\lambda = \{1,-1\}$, since the π orbitals are doubly degenerate.

Similarly, a Δ term is also doubly degenerate, $M_\lambda = \{2,-2\}$. Show that the molecular terms for the configuration KK $(\sigma_{g,2s})^2(\sigma^*_{u,2s})^2(\sigma_{g,2pz})^2(\pi_{u,2p})^4(\pi^*_{g,2p})^2$ are $^3\Sigma_g + {}^1\Delta_g + {}^1\Sigma_g$, by exhaustive enumeration of explicit molecular orbital assignments. Include the parity, g or u (you don't need to find the reflection symmetry).

9. Find the molecular terms for the configuration KK $(\sigma_{g,2s})^2(\sigma^*_{u,2s})^2(\sigma_{g,2pz})^2(\pi_{u,2p})^3(\pi^*_{g,2p})^3$ by exhaustive enumeration of explicit molecular orbital assignments. Include the parity, g or u (you don't need to find the reflection symmetry).

10. For a homonuclear diatomic molecule, determine which of the following transitions is allowed or forbidden, assuming weakly coupled spin and orbital angular momenta.[3] [Note: identical term symbols can result from two different configurations; term symbols are unique within a given configuration.]

$^2\Sigma_g^- \leftarrow {}^2\Pi_u$ $\quad$ $^1\Sigma_g^- \leftarrow {}^1\Sigma_g^-$ $\quad$ $^1\Delta_g \leftarrow {}^1\Pi_u$ $\quad$ $^1\Delta_u \leftarrow {}^1\Sigma_g^+$ $\quad$ $^1\Sigma_g^- \leftarrow {}^3\Sigma_u^-$ $\quad$ $^3\Sigma_u^- \leftarrow {}^3\Sigma_g^-$

11. (a). Determine the possible values of the projection of the total angular momentum, $\Omega = |\Lambda + \Sigma_s|$, for a $^3\Delta$ term. (b). Determine if the transition to each of these $^3\Delta$ terms from a $^3\Pi_o$ state is allowed or forbidden.

12. In Problem 25.31 we illustrated an angular momentum component diagram to help explain the occurrence of multiple total angular momentum states, given the projections of the orbital and spin angular momenta. Give the corresponding molecular diagram showing that the projections of the total angular momentum resolve $^3\Delta$ terms into three states: $^3\Delta_1$, $^3\Delta_2$, and $^3\Delta_3$. [Hint: simply replace M_L, M_S , and M_J with Λ, Σ_s , and Ω. Note that Λ is always positive. Use the S and Λ values corresponding to a $^3\Delta$ term.]

13. Describe in words the purpose of the Birge-Sponer extrapolation in the analysis of electronic absorption spectra.

14. Describe in words the meaning and purpose of the Franck-Condon factors in the interpretation of electronic absorption spectra.

15. The Schumann-Runge band for molecular oxygen is in the UV-region of the spectrum. The wave numbers for the $^3\Sigma_u^- \leftarrow {}^3\Sigma_g^-$ transitions are given in the table below. The corresponding vibrational quantum numbers are not known. The ground state dissociates into two ground state ^{3}P oxygen atoms, and the $^3\Sigma_u^-$ excited state dissociates into a ^{3}P and a ^{1}D oxygen atom. Calculate (a) the dissociation energy of the ground state (the bond strength). (b). Estimate the dissociation energy of the excited state by assuming the first observed transition is for $\upsilon \cong 0$. The atomic excitation energy, $^3P \rightarrow {}^1D$ is 1.9674 eV, 15867.9 cm^{-1}, or 189.82 kJ/mol.

$\tilde{\nu}$ (cm^{-1})	50062.6	50725.4	51369.0	51988.6	52579.0	53143.4	53679.6	54177.0
continued	54641.8	55078.2	55460.0	55803.1	56107.3	56360.3	56570.6	

16. For SiS the wave numbers for the $E^1\Sigma^+ \leftarrow X^1\Sigma^+$ transitions are given in the table below.[5] The ground state is labeled as the X-state and this excited state, which has the same symmetry, is the

E-state. Assume that the corresponding vibrational quantum numbers are not known. The ground and excited states dissociate into two ground-state ^3P atoms. Calculate the dissociation energy of the ground state (the bond strength).

$\tilde{\nu}$ (cm^{-1})	44482.8	44857.6	45227.0	45592.2	45952.8	46308.3	46657.7	47001.0	47337.9	47664.0

17. Vibrational potential functions commonly deviate from Morse behavior. One possibility is the appearance of a maximum, Figure P28.17.1a. One cause of a maximum is a strong Van der Waals repulsion at large distances, but strong bonding interactions at short distances.[4] Referring to Figure 26.2.4, strong electron-electron repulsion increases the potential energy at large R, possibly giving a maximum. A second cause, especially for excited states, is an avoided crossing between a bound-state potential energy curve and a repulsive state, Figure P28.17.1b. An example is a state of an alkali halide that tends to dissociate to ions, but because of the curve crossing dissociates to atoms instead.[4] Discuss the effect of a potential maximum on the spectroscopic determination of the dissociation energy of the bound state.

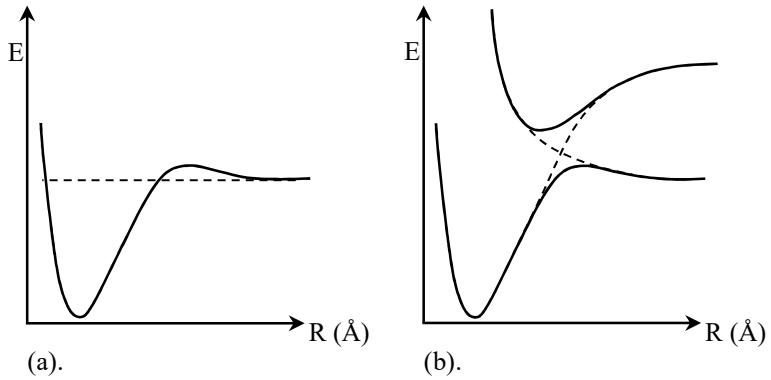

Figure P28.17.1: (a). Some vibrational potential energy curves have a maximum. (b). One cause is an avoided crossing.

18. The electronic absorption spectrum of water has a Rydberg series that start with the configuration $\ldots(3a_1)^2(1b_1°)^1(3p)^1$ for a 3p-orbital on the O-atom. See Figure 26.6.4 for the molecular orbital diagram. Is the Rydberg series consistent with the ultraviolet photoelectron spectrum, UPS, of water shown in Figure 28.5.4b? The series has transitions:

$$\tilde{\nu}_n = 101786\ cm^{-1} - \frac{\Re_H}{(n - 0.7)^2} \qquad n = 3, 4, 5, \ldots\ldots$$

19. The diatomic molecule Na_2 has a Rydberg series in the electronic absorption spectrum. The ionization limit gives the ground state of the molecular ion, Na_2^+. The ionization limit from the Rydberg series and the ionization potential measured using UPS should be identical for the specific excited state of the molecular ion. The quantum numbers of the Rydberg transitions and the wave numbers are given in the table below. Determine the ionization potential to form Na_2^+. Compare the value to the ionization potential determined using UPS, which is 4.90 eV (see Problem 37 for the reference to the literature value).

n	4	5	6	7
$\tilde{\nu}_n$	20320.02	29382	33486.8	35557

20. Using the potential energy curves shown below, predict the most intense vibrational fine-structure transitions in the absorption and fluorescence spectra. Draw the corresponding absorption and fluorescence spectra. Show four of the intense transitions in each of the spectra. Label each transition in the energy level diagram with the vibrational quantum numbers for the transition and each corresponding peak in the spectrum (e.g. 4←0).

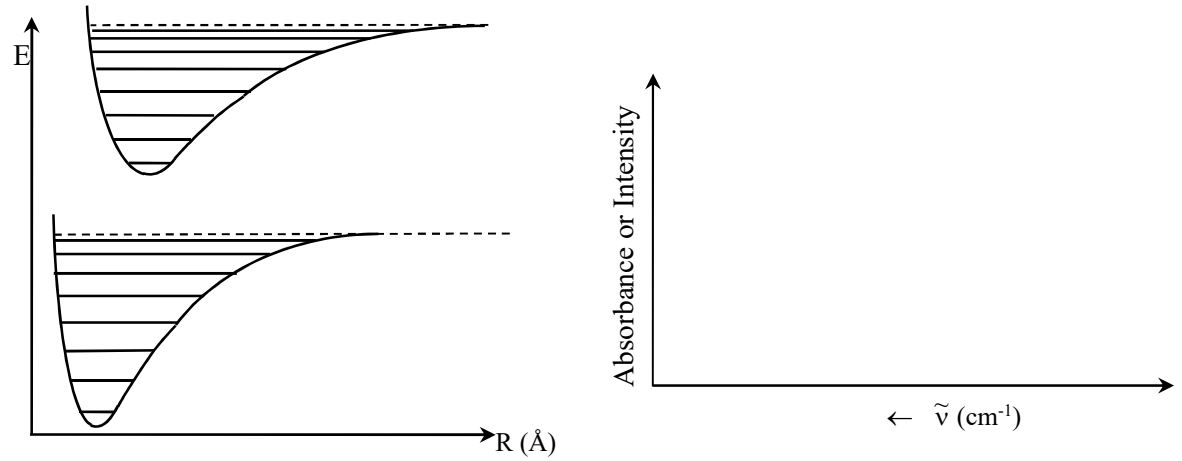

21. We took a short cut in the derivation of Eq. 28.2.13 by working in analogy with Eq. 27.5.12. In this problem we derive Eq. 28.2.13 directly from the term values of the adjacent transitions. The energy of the υ" = 0 level of the ground electronic state is $\tilde{E}_o$. The energy difference from the minimum energy of the ground state potential energy curve to the minimum energy of the excited state potential energy curve, that is the energy without vibration, is $\tilde{T}_e^{ex}$. The energy of the υ' vibrational level of the excited state is $\tilde{E}_{\upsilon'}^{ex}$, neglecting rotation:

$$\tilde{E}_{\upsilon'}^{ex} = \tilde{T}_e^{ex} + \tilde{\nu}_e^{ex}(\upsilon' + ½) - \chi_e^{ex}\tilde{\nu}_e^{ex}(\upsilon' + ½)^2 \qquad \text{P28.14.1}$$

The energy of an electronic transition from the υ" = 0 level of the ground electronic state to the υ' vibrational level of the excited state is:

$$\Delta\tilde{E}(j,\upsilon'\leftarrow i,0) = \tilde{E}_{\upsilon'}^{ex} - \tilde{E}_o = \tilde{T}_e^{ex} + \tilde{\nu}_e^{ex}(\upsilon' + ½) - \chi_e^{ex}\tilde{\nu}_e^{ex}(\upsilon' + ½)^2 - \tilde{E}_o \qquad \text{P28.14.2}$$

where the fundamental vibration frequency $\tilde{\nu}_e^{ex}$ and anharmonicity $\chi_e^{ex}\tilde{\nu}_e^{ex}$ are for the excited state. Consider two adjacent transitions: j,υ +1←i,0 and j,υ ←i,0. The adjacent energy difference is:

$$\Delta\tilde{\nu}_\upsilon = \Delta\tilde{E}(j,\upsilon+1\leftarrow i,0) - \Delta\tilde{E}(j,\upsilon\leftarrow i,0) \qquad \text{P28.14.3}$$

(a). Prove that: $\Delta\tilde{\nu}_\upsilon = = \tilde{\nu}_e^{ex} - \chi_e^{ex}\tilde{\nu}_e^{ex}[(\upsilon + ½) +1)]^2 + \chi_e^{ex}\tilde{\nu}_e^{ex}(\upsilon + ½)^2$ P28.14.4

(b). Using $((\upsilon+½)+1)^2 = (\upsilon+½)^2 + 2(\upsilon+½) + 1$, starting with Eq. P28.14.4 prove that:

$$\Delta\tilde{\nu}_\upsilon = (h\tilde{\nu}_e^{ex} - 2\chi_e^{ex}\tilde{\nu}_e^{ex}) - 2\chi_e^{ex}\tilde{\nu}_e^{ex}\upsilon \qquad (28.2.13)$$

(c). Label $\tilde{E}_o$, $\tilde{E}_\upsilon^{ex}$, $\tilde{T}_e^{ex}$, $\Delta\tilde{E}(j,\upsilon+1\leftarrow i,0)$, $\Delta\tilde{E}(j,\upsilon\leftarrow i,0)$, and $\Delta\tilde{\nu}_\upsilon$ on a plot of the ground and excited state potential energy curves. Pick a convenient arbitrary υ for your plot.

22. The next three problems discuss errors in the Birge-Sponer extrapolation procedure and why different authors chose different variables to plot along the horizontal axis, υ, υ + ½, or υ + 1.

The vibrational fine-structure in an electronic absorption spectrum converges to a limit that is the sum of the dissociation energy of the ground state of the molecule and the atomic excitation energy. The convergence limit is equivalent to the sum of $\tilde{\nu}_{oo}$ and the excited state dissociation energy, Eq. 28.2.8. Reference to Figure 28.2.5 shows that the excited state dissociation energy is the sum of all the adjacent wave number differences up to the convergence limit:

$$\Delta\tilde{E}(j,\infty\leftarrow i,0) = \tilde{D}_o + \Delta\tilde{E}_{atomic} = \tilde{\nu}_{oo} + \tilde{D}_o^{ex} = \tilde{\nu}_{oo} + \sum_{\upsilon=0}^{\infty}\Delta\tilde{\nu}_\upsilon \qquad \text{P28.22.1}$$

Based on the sum of adjacent differences, the Birge-Sponer extrapolation may be viewed from a different perspective. A graphical interpretation of Figure 28.1.20 allows a convenient calculation of the sum in Eq. P28.22.1. Consider a rectangle of unit width drawn at each data point, Figure P28.22.1.

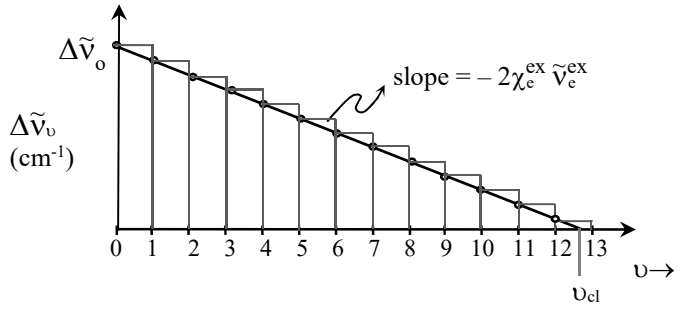

width of each rectangle = 1

height of each rectangle = $\Delta\tilde{\nu}_\upsilon$

area of each rectangle = $\Delta\tilde{\nu}_\upsilon$

area = ½ base height

Figure P28.22.1: The excited state dissociation energy $\tilde{D}_o^{ex}$ is given by the sum of adjacent energy differences, which is conveniently calculated as the triangular area under the plot of $\Delta\tilde{\nu}_\upsilon$ versus υ.

The area of each rectangle is the height multiplied by the width. The sum of all the successive differences is then equal to the total area of all the rectangles. The total area is approximated as the triangle with the area given by ½ base ·height:

$$\sum_{\upsilon=0}^{\infty}\Delta\tilde{\nu}_\upsilon = \text{area} = \tfrac{1}{2}\,\Delta\tilde{\nu}_o\;\upsilon_{cl} \qquad (28.2.19)$$

Compare this approximate result, which we also gave as Eq. 28.2.19, to the exact result using Eq. 28.2.15. Express your answer in terms of the anharmonicity, $\chi_e^{ex}\tilde{\nu}_e^{ex}$.

23. Birge-Sponer extrapolations are plotted as a function of the vibrational quantum number υ based on the following the linear forms:

$$\Delta\tilde{\nu}_\upsilon = (\tilde{\nu}_e^{ex} - 2\chi_e^{ex}\tilde{\nu}_e^{ex}) - 2\chi_e^{ex}\tilde{\nu}_e^{ex}\,\upsilon \qquad (28.2.13)$$

or equivalently $\Delta\tilde{\nu}_\upsilon = \Delta\tilde{\nu}_o - 2\chi_e^{ex}\tilde{\nu}_e^{ex}\,\upsilon$ (28.2.17)

In the previous problem we discuss a graphical interpretation that leads to the use of the triangular area under the Birge-Sponer curve to estimate the dissociation energy of the excited state. This graphical interpretation in Figure P28.22.1 shows a problem in associating the area of each rectangle with the overall area; each rectangle has a small portion above the curve-fit line. Some authors suggest doing the curve fit versus υ+½ to limit the error in this area calculation, Figure P28.23.1.

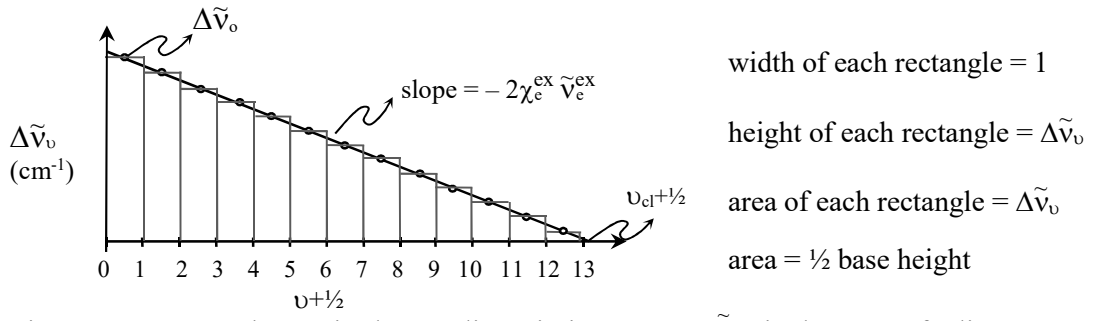

Figure P28.23.1: The excited state dissociation energy $\tilde{D}_o^{ex}$ is the sum of adjacent energy differences, which is calculated as the triangular area under the plot of $\Delta\tilde{\nu}_\upsilon$ versus υ+½.

The dissociation energy of the excited state is given approximately by area $\tilde{D}_o^{ex} = ½\,\Delta\tilde{\nu}_o\,\upsilon_{cl}$, where $\Delta\tilde{\nu}_o$ is taken as the first data point and υ_{cl} = (x-intercept) – ½. This result is identical to the result taken from the plot versus υ discussed in the Example 28.2.2. However, some authors instead use:

$$\tilde{D}_o^{ex} \cong \text{area} = ½(\text{y-intercept})(\text{x-intercept})$$

Evaluate the error in the corresponding calculation of $\tilde{D}_o^{ex}$ by showing that:

$$\tilde{D}_o^{ex} = ½\,(\text{y-intercept})(\text{x-intercept}) - ¼\,\tilde{\nu}_e^{ex} + ½\,\chi_e^{ex}\,\tilde{\nu}_e^{ex}\,\upsilon_{cl} + ¼\,\chi_e^{ex}\,\tilde{\nu}_e^{ex}$$

24. As an alternate to the Birge-Sponer plot where $\Delta\tilde{\nu}_\upsilon$ is plotted versus υ, show that a plot of $\Delta\tilde{\nu}_\upsilon$ versus $\upsilon + 1$ gives $\tilde{\nu}_e^{ex}$ directly from the intercept.

25. The ultra-violet photoelectron spectrum of HCl taken with He discharge excitation at 21.21 eV is shown below.[6,7] The doublet peaks at 12.74-12.82 and at 13.04-13.12 occur for the $^2\Pi_{3/2}$ and $^2\Pi_{½}$ states. The doublet spacing is determined by spin-orbit coupling. The peak spacings listed on the spectrum are vibrational spacings. The ground state spectroscopic constants for HCl are listed in Table 27.6.1. (a). For each band, is the molecular ion stretching frequency greater, roughly equal, or less than that of the ground state HCl? Predict the type of orbital, bonding, non-bonding, or anti-bonding, of the corresponding ionized electron. Include observations on the length of the vibrational progression of each band. (b). The molecular orbital diagram for HI is given in Figure 28.2.7. Is the molecular orbital ordering for HCl consistent with the molecular orbital ordering for HI?

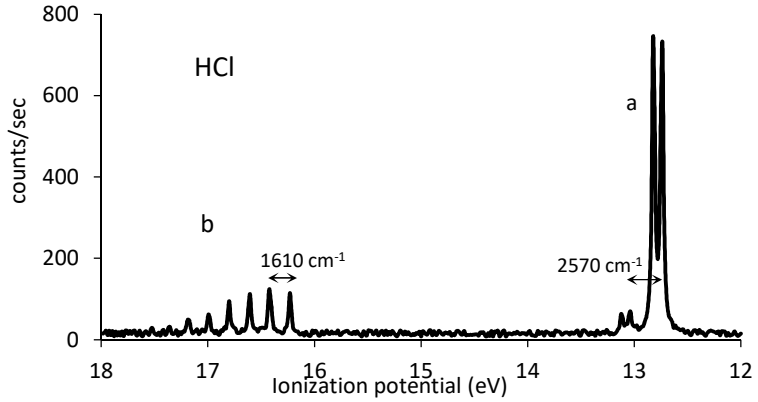

Figure 28.25.1: UPS spectrum of HCl using He discharge excitation at 21.21 eV.

26. The molecular orbital diagram for HI is given in Figure 28.2.7. (a). Sketch the four molecular orbitals. (b). Compare the molecular orbitals to the molecular orbitals for LiH, Figure 26.3.4. Suggest the reason why the 5s-orbital on the I-atom doesn't participate in the molecular orbitals to a significant extent (at least at a qualitative level). (c). The molecular orbital ordering in Figure 28.2.7 is verified using UPS. Describe the vibrational fine-structure in the UPS spectrum that is expected for HI. That is for each of the three bands, is the molecular ion stretching frequency greater, roughly equal, or less than that of the ground state HI? Also, is each vibrational progression short or long? (d). Show the "box diagrams" for the $^2P_{½}$ and $^2P_{3/2}$ states of I-atoms. (e). Find the term symbols for the excited states of HI with configuration $\sigma^2(\pi^o)^3(\sigma^*)^1$. (f). Determine the possible projections of the total angular momentum for each term: $\Omega = |\Lambda + \Sigma_s|$.

27. Determine the density of states of a one-dimensional particle in a box. Determine the density of states near the state with quantum number n = 100, for CO_2 molecules in a 10.0 cm "box". Express the units as states per wave number.

28. Determine the density of states of a linear rigid rotor. Rotational energy levels have a degeneracy of (2J + 1), which we must take into account. The degeneracy is the number of states at a given energy level. The density of states is the product of the number of states at the given energy level with the number of levels per unit energy. The rotational constant for acetonitrile, H–C≡N, is 0.307 cm^{-1}.[8] Calculate the density of states for H–C≡N.

29. The UV-visible absorption spectrum of SO_2 is given in Figure 28.1.1. The band origin of the visible transition is roughly 340 nm. The band origin corresponds to the $\upsilon' \leftarrow \upsilon''$ vibrational fine-structure transition of $0 \leftarrow 0$. Consider non-radiative energy transfer by internal conversion from this excited electronic state into the ground electronic state. The three normal modes of SO_2 in the ground electronic state are at wave numbers 1151 cm^{-1}, 518 cm^{-1}, and 1362 cm^{-1}, Figure 28.3.2. (a) Assuming all the vibrational energy is in the asymmetric stretch-ν_3, that is $\upsilon_1 = \upsilon_2 = 0$, calculate the vibrational quantum number of the ground state that is isoenergetic with the lowest energy vibrational level of the excited state. (b). Assuming the vibrational quantum numbers are all equal, that is $\upsilon_1 = \upsilon_2 = \upsilon_3$, calculate the approximate vibrational quantum numbers of the ground state that is isoenergetic with the lowest energy vibrational level of the excited state.

30. Avoided-crossings of degenerate states follow a common pattern. Consider two states represented by the wave functions Ψ_A and Ψ_B. The strength of the interaction between the two states is determined by the integral $c = \int \Psi_A \hat{o} \Psi_B \, d\tau$. Possibilities for the $\hat{o}$ operator include spin-orbit coupling for electronic interactions in intersystem crossing or $(\partial^2/\partial R^2)$ for vibronically coupled states. Vibronic coupling is important in internal conversion and pre-dissociation. We consider the interaction as a perturbation on the unperturbed wave functions Ψ_A and Ψ_B. We assume that there is no net interaction without the perturbation, giving an overlap-type integral:

$$\int \Psi_A \Psi_B \, d\tau = S_{AB} = 0$$

A zero overlap integral is often the result of orthogonality. Any two different electronic states of the same molecule are orthogonal. The unperturbed energies of the two states are:

$$a = \int \Psi_A \hat{\mathcal{H}}' \Psi_A \, d\tau \qquad \text{and} \qquad b = \int \Psi_B \hat{\mathcal{H}}' \Psi_B \, d\tau$$

with $\hat{\mathcal{H}}'$ given by the unperturbed Hamiltonian ($\hat{o}$ is not present). The energies of the two states with the interaction present are the eigenvalues of the secular equations, λ_i, as in Eq. 26.1.13:

$$\begin{vmatrix} a-\lambda & c \\ c & b-\lambda \end{vmatrix} = 0$$

with the eigenvalues given by Eq. 6.3.23. Recasting Eq. 6.3.23 into the terms used in this problem gives:

$$\lambda_i = \frac{(a+b) \pm \sqrt{(a-b)^2 + 4\,c^2}}{2} \qquad \text{P28.32.1}$$

(a). In pre-dissociation, a and b scale with the distance, with a = b at the avoided-crossing. Assume two states are nearly degenerate and have energies: a = 5.00 eV + δ and b = 5.00 ev – δ. The energy gap, δ, has units of eV. Plot the energies of the two states with the interaction present for c = 0.2 eV for δ in the range of $-0.5 < \delta < 0.5$. Determine the energy gap at $\delta = 0$.
(b). Compare the previous plot to Figure 28.2.8. How can you tell that the crossing is avoided?
(c). Decrease the interaction parameter to c = 0.01 eV. Is the crossing still avoided? RT at room temperature is 0.0257 eV. Predict the behavior of the system at room temperature at the avoided-crossing.

31. Determine the symmetry species of the following molecular orbitals of ethylene. The symmetry species are the irreducible representations. In addition, classify the molecular orbitals as σ or π, non-bonding or bonding.

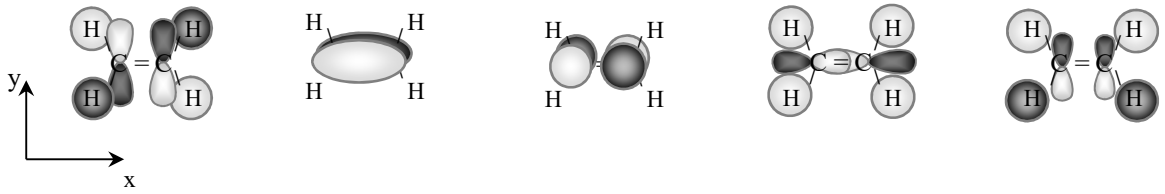

32. Use electronic selection rules to determine if the LUMO+1 ← HOMO and LUMO+2 ← HOMO transition are allowed in absorption spectra. The corresponding molecular orbital diagram for the $1b_{1g}$, $1b_{1u}$, $1b_{2g}$, a_g, and b_{2g} levels is given below.

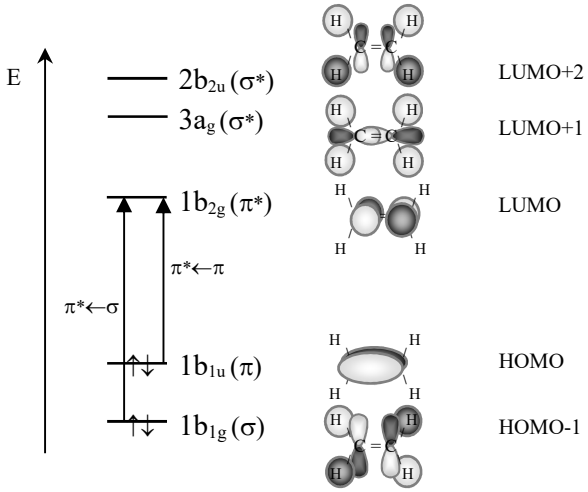

33. In Example 28.8.1 we used group theory based electronic selection rules to determine if the low energy $\pi^* \leftarrow \sigma$ and $\pi^* \leftarrow \pi$ transitions of ethylene are allowed or forbidden. Configuration interaction calculations are used to find excited states, electronic transition energies, and intensities within the Hartree-Fock formalism. Single excitations don't contribute to ground state stability, however single excitations generate many possible excited states. As a consequence configuration interaction with single excitations, CIS, is used to simulate UV-visible spectra. First, do a geometry optimization for ethylene at HF/6-311G* (equivalent to HF/6-311G(d)). Then do a CIS/6-311G* single point calculation to compare to the intensity predictions in Example 28.8.1. [Hints: To do a CIS calculation: Using the Spartan visualization environment select an Energy calculation and check "UV/Vis" and "Orbitals & Energies". Using the WebMo visualization environment for Gaussian choose the Calculation type as "Excited States and UV-Vis". Use the Basis Set "Other" option to specify 6-311G(d). Using the GaussView visualization environment for Gaussian set the Method as CIS and check "Solve for More States, N = 6".]

34. Determine the symmetry species of the following molecular orbitals of formaldehyde. The geometry is shown at bottom. The x-direction is the π-bonding direction for these plots. The HOMO has a small contribution from the $2p_y$ orbital on the C-atom. As a result the HOMO is primarily a non-bonding $2p_y$ atomic orbital on the O-atom. [Hint: Use the symmetry operations given in Figure 26.6.4. Formal group theory is not required for this problem.]

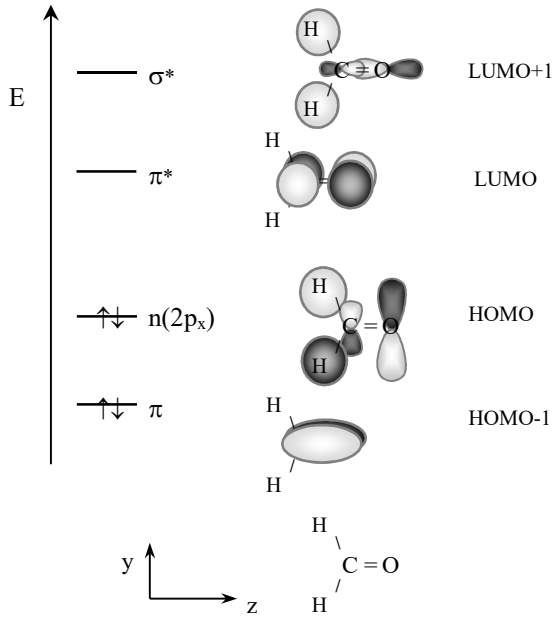

35. Use electronic selection rules to determine if the LUMO←HOMO, LUMO←HOMO-1, and LUMO+1←HOMO electronic transitions of formaldehyde are allowed or forbidden. The symmetries of the molecular orbitals are:

Orbital	7	8	9	10
MO	HOMO-1	HOMO	LUMO	LUMO+1
Symmetry	b_1	b_2	b_1	a_1
Type	π	n	π*	σ*

36. Use a configuration interaction-singles calculation to determine the predicted intensity of the LUMO←HOMO, LUMO←HOMO-1, and LUMO+1←HOMO electronic transitions of formaldehyde. First, do a geometry optimization for formaldehyde at HF/6-311G** (equivalent to HF/6-311G(d,p)). Then do a CIS/6-311G** single point calculation to compare to the intensity predictions in Problem 35. See Problem 33 for a discussion of the use of CIS calculations for predicting electronic spectra and for hints on doing the calculations.

37. K. P. Huber and G. Herzberg have produced a comprehensive reference on the spectroscopic data of diatomic molecules.[2] This reference has been transcribed by the National Institute of Standards and Technology, NIST, as an on-line database.[1] The entry for Na_2 is listed as an example below. The spectroscopic constants are presented in wave numbers and the equilibrium bond length in Å. The book tables start with a listing of the reduced mass, μ, in g mol^{-1}. Next the dissociation energy at absolute zero, D_o^o, which we have been referencing as just D_o, and the ionization energy to form the ground state of the molecular ion, I.P. The on-line version excludes μ, D_o^o, and I.P. By convention, the ground state is labeled as X, which for Na_2 is explicitly X $^1\Sigma_g^+$. Excited electronic states are labeled as states A, B, C, D … in order of increasing energy if the states have the same spin multiplicity, or a, b, c, d … if the excited states have a different multiplicity. Many literature references and many notes are included in the tables, which we have omitted in this example for brevity. For this homework problem (a) find the Na_2 reference in the book or on-line, http://webbook.nist.gov/chemistry, and (b) write a spreadsheet to plot the potential energy surfaces as a function of R for the X ground state, and A and B excited states. Use the Morse function for the potential energy surfaces. The A and B excited states dissociate to a ground and excited state Na atom: $Na_2 \rightarrow Na\ (^2S) + Na\ (^2P)$. The atomic excitation energy, ΔE_{atomic} is 16961 cm^{-1} to the $^2P_{½}$ state. From Figure 28.2.5, note that $\tilde{T}_e + \tilde{D}_e^{ex} = \tilde{D}_e + \Delta E_{atomic}$.

State (1)	T_e	ω_e	$\omega_e\chi_e$	$\omega_e y_e$	B_e (2)	α_e	D_e (3)	r_e	Trans.	ν_{oo}
$^{23}Na_2$	μ = 11.4948852		D_o^o = 0.720 eV[a]		I.P. = 4.90 eV[b]					
	Diffuse bands of Na_2 Van der Waals molecules close to the lines of principal series of Na. Several fragments of other UV emission and absorption band systems.[c]									
E ($^1\Pi_u$)	35557	106.2 [H]	0.65						E←X R	35530.6 [H]
D $^1\Pi_u$	33486.8	111.3 [H]	0.48		d				D↔X R	33462.9 [H]
$^1\Sigma_g^+$	(33000)	Fragment observed in two-photon excited Na_2 fluorescence								
C $^1\Pi_u$	29382	119.33 [H]	0.53		d				C↔X R	29362 [H]
B $^1\Pi_u$	20320.02	124.090 [Z]	0.6999		0.125277	7.237E-4	3.248E-7	3.4228	B↔X R	20302.49 [Z]
A $^1\Sigma_u^+$	14680.58	117.323 [Z]	0.3576		0.110784	5.488E-4	3.882E-7	3.6384	A↔X R	14659.80 [Z]
a $^3\Pi_\upsilon$	<14680	(145)			(0.140)					
X $^1\Sigma_g^+$	0	159.1245 [Z]	0.72547		0.154707	8.736E-4	5.811E-7	3.07887		

a. From D_o^o = 5890 ± 70 cm^{-1} based on RKR potential curve for the ground state. The thermochemical value obtained by a molecular beam technique is 0.732 eV.
b. From photoionization. A similar value is obtained by extrapolation of the Rydberg series B, C, D, E.
c. Molecular absorption cross sections 27000 – 625000 cm^{-1}.
d. Barrow, Travis, et al., 1960 report the following rotational constants for D: B_e = 0.1185, α_e = 0.001, C: B_e = 0.12815, α_e = 0.00084. Considerably different constants, however, are quoted by Richards in Rosen, 1970. D: B_e = 0.1152, α_e = 0.00110, C: B_e = 0.1185, α_e = 0.00096.

Footnotes:
1. Units: T_e, ω_e, $\omega_e\chi_e$, $\omega_e y_e$, B_e, α_e, D_e, and ν_{oo} in cm^{-1}, with $\omega_e = \tilde{\nu}_e$ and $r_e = R_e$ in Å as given in this text.
2. On-line NIST tables list the vibration-rotation interaction constant, γ_e, for the expansion: $B_\upsilon = B_e - \alpha_e(\upsilon + ½) + \gamma_e(\upsilon + ½)^2$
3. On-line NIST tables list β_e for the centrifugal distortion expansion: $D_\upsilon = D_e + \beta_e(\upsilon + ½)$.

(Table continued next page.)

Table Legend

H Data obtained from band head measurements (see Problem 3)
Z Data obtained from, or referring to, band origins (see Problem 3)
R Shaded towards longer wavelengths (appearance of the rotational fine-structure, $B'_e < B''_e$)
V Shaded towards shorter wavelengths (appearance of the rotational fine-structure, $B'_e > B''_e$)
( ) Uncertain data
[ ] Data refer to $\upsilon = 0$ or lowest observed level. T_e values in square brackets give the energy of this level relative to the minimum of the ground-state potential energy curve. Vibrational frequencies in square brackets correspond to $\Delta G(½)$ or the lowest observed interval.

38. The Huber-Herzberg tables of diatomic spectroscopic constants are introduced in the previous problem. Refer to the previous problem for interpretation and footnotes. (a) Find the $^{12}C_2$ reference in the book or on-line, http://webbook.nist.gov/chemistry, and (b) write a spreadsheet to plot the potential energy surfaces as a function of R for the X $^1\Sigma_g^+$ ground state, and a $^3\Pi_u$, b $^3\Sigma_g^-$, and A $^1\Pi_u$ excited states. Use the Morse function for the potential energy surfaces. The ground state dissociation energy is 6.21 eV. The a- and b-excited states dissociate to ground state atoms: $C_2 \rightarrow C\ (^3P) + C\ (^3P)$. The A excited state dissociates to a ground state and an excited state atom: $C_2 \rightarrow C\ (^3P) + C\ (^1D)$. The atomic excitation energy, ΔE_{atomic}, is 10192 cm^{-1} to the ^1D state. From Figure 28.2.5, note that $\tilde{T}_e + \tilde{D}_e^{ex} = \tilde{D}_e + \Delta E_{atomic}$.

39. In Chapter 27, we did not justify the vibrational selection rule that in absorption, the transition dipole moment vanishes unless the normal mode transforms according to the same representation as the x, y, or z-component of the electric dipole moment. The transition electric dipole moment is proportional to the integral given by Eqs. 27.9.13. For a diatomic molecule aligned along the x-axis, the harmonic oscillator wave functions are functions of the displacement along the x-axis, $x = R - R_o$. The electric dipole operator along the internuclear axis is also a function of the x-axis position of the nuclei and the partial charge on the atoms. The transition dipole moment is then proportional to:

$$\mu_{tr,x} \propto \int_{-\infty}^{\infty} \chi_{\upsilon'}\, x\, \chi_{\upsilon''}\ dx$$

The integrand contains three functions, the final harmonic oscillator wave function with quantum number υ', the x-operator, and the initial harmonic oscillator wave function with quantum number υ''. The x-operator is purely odd. The integral is over all space, so that the integral vanishes for an odd integrand. As a consequence the product of the three functions must be overall even for the transition moment integral to be non-zero.

For polyatomics, we must consider the x, y, and z-components of the transition dipole. The symmetry of each vibrational wave function is represented by an irreducible representation of the point group of the molecule. Consider the case for the fundamental transition $1 \leftarrow 0$. The ground state vibrational wave function, $\upsilon = 0$, always transforms according to the totally symmetric irreducible representation. As a result, to give a non-vanishing integral the product of the excited state vibrational wave function and the x-operator must contain the totally symmetric irreducible representation. The normal mode must transform according to the same representation as the x, y, or z-component of the electric dipole moment.

How can we illustrate that the ground vibrational state is totally symmetric under the operations of the point group? Consider a simple polyatomic such as CO_2 as compared to a diatomic molecule. The diatomic harmonic oscillator wave functions for $\upsilon = 0$ and 1 are shown

at left and the corresponding wave functions are illustrated for CO_2 at right, Figure P28.39.1. The ground state, $\upsilon = 0$, wave function of any normal mode necessarily retains the same sign upon any symmetry operation of the point group, since the wave function is always positive. Now, consider the action of the reflection operator on the excited state wave function. For the $\upsilon = 1$ state, the inversion operation is symmetric for the symmetric stretch and anti-symmetric for the asymmetric stretch. As a result, the symmetric stretch is IR-inactive and the asymmetric stretch is IR-active.

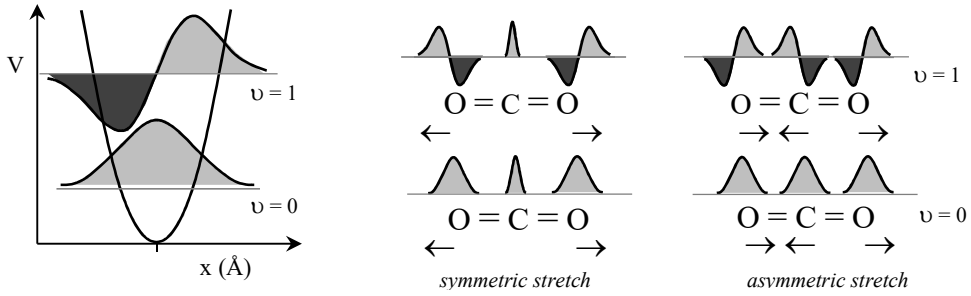

(a). Diatomic vibrational wave functions (b). Polyatomic normal modes

Figure P28.39.1: Symmetry of harmonic oscillator wave functions for (a) diatomics and (b) the symmetric and asymmetric stretch of CO_2. The CO_2 symmetric stretch is symmetric with respect to a plane perpendicular to the internuclear axis, passing through the center of mass (a σ_v-plane). The asymmetric stretch is anti-symmetric with respect to reflection.

The symmetry of bending vibrations is possibly confusing, based on displacement arrows. Please review Problem 27.38. For this problem, using depictions of the quantum mechanical wave function of the type shown in Figure P28.39.1b, determine the symmetry of the wag-bending vibration with respect to C_2-rotation and reflection across σ_v, Figure P28.39.2:

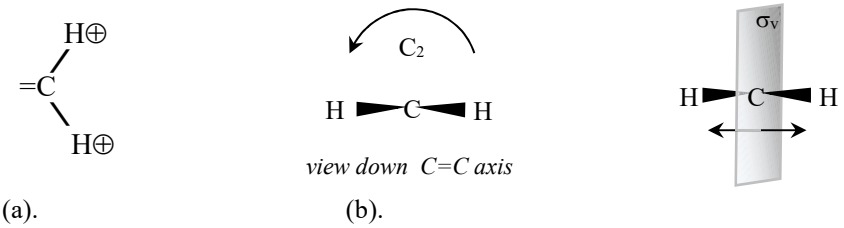

(a). (b).

Figure P28.39.2: (a). Top down view of the wag-mode of a CH_2 group. (b). End-on view, down the C=C internuclear axis, showing the C_2-rotation and σ_v-reflection operations.

Literature Cited:

1. K. P. Huber and G. Herzberg, *Constants of diatomic molecules*, (data prepared by J. W. Gallagher and R. D. Johnson, III) in NIST Chemistry WebBook, NIST Standard Reference Database Number 69, Eds. P. J. Linstrom and W. G. Mallard, National Institute of Standards and Technology, Gaithersburg MD, http://webbook.nist.gov/chemistry, (last accessed 4/2015).
2. K. P. Huber and G. Herzberg, *Molecular Spectra and Molecular Structure: IV. Constants of diatomic molecules,* Van Nostrand Reinhold, New York, NY, 1979.

3. G. Herzberg, *Molecular Spectra and Molecular Structure: Spectra of Diatomic Molecules, 2nd. Ed.*, Van Nostrand Reinhold, New York, NY, 1950. pp. 212-216, 240-243.

4. A. G. Gaydon, Dissociation Energies and Spectra of Diatomic Molecules, Dover, New York, NY, 1950.

5. E. E. Vago, R. F. Barrow, "Ultra-violet Absorption Band-Systems of SiS, SiSe, and SiTe," *Proc. Phys. Soc*., **1946**, *58*, 538-544.

6. H. J. Lempka, T. R. Passmore, W. C. Price, "The photoelectron spectra and ionized states of the halogen acids," *Proc. Roy. Soc. A*., **1968**, *304*, 53-64. Spectrum simulated from numerical data.

7. D. W. Turner, "Molecular photoelectron spectroscopy," *Phil. Trans. Roy. Soc. Lond. A*., **1970**, *268*, 7-31.

8. M. S. Lojko, Y. Beers, "A Table of Rotational Constants of Symmetric Top Molecules Giving Rise to Microwave Spectra," *J. Research National Bureau of Standards – A. Physics and Chemistry*, **1969**, *73A(2)*, 233-239. Available online at (last accessed 4/8/2015):
http://nvlpubs.nist.gov/nistpubs/jres/73A/jresv73An2p233_A1b.pdf